Republic of Iraq
Ministry of Higher Education
and Scientific Research
University of Babylon
College of Engineering
Mechanical Engineering Department

A Comparative Study of Nano Lubricated Circular and Elliptical Journal Bearings

A Thesis
Submitted to the College of Engineering/University of Babylon in Partial Fulfillment of the Requirements for the Degree of Master in Engineering/Mechanical Engineering/Applied Mechanics

By

Mohammed Oday Yasir Ali

Supervised by

Prof. Dr. Basim A. Abass ***Prof. Dr. Saba Y. Ahmed***

2023A.D ***1444A.H***

بسم الله الرحمن الرحيم

﴿وَلَقَدْ آتَيْنَا دَاوُودَ وَسُلَيْمَانَ عِلْمًا ۖ وَقَالَا الْحَمْدُ

لِلَّهِ الَّذِي فَضَّلَنَا عَلَىٰ كَثِيرٍ مِّنْ عِبَادِهِ الْمُؤْمِنِينَ﴾

صدق الله العلي العظيم

سورة النمل, آية 15

Dedication

A fountain of giving and support… (My mother)

Help and advise me throughout research study… (My supervisors)

Their assistance and encouragement… (My family)

Inspiration and motivation… (My two little heroes)

Mohammed 2023

Acknowledgment

I would like to express my most sincere thanks and gratitude to ALLAH for granting me success in completing my thesis.

I would like to express my thanks and gratitude to my supervisors, Prof. Dr. Basim A. Abass and Prof. Dr. Saba Y. Ahmed for their guidance, help, and encouragement during the preparation study.

Finally, I would like to express my heartfelt appreciation to my family and friends for their assistance and support.

Mohammed 2023

TABLE OF CONTENTS

NOMENCLATURE

Symbol	Description	Units
a_a	Radii of aggregate nanoparticles	nm
a	Radii of primary nanoparticles	nm
C	Radial clearance	mm
C_h	Horizontal clearance	mm
C_v	vertical clearance	mm
C_p	Specific heat	J/kg . °C
e	Distance between shaft and bearing centers	mm
E_p	Ellipticity ratio $E_p = \frac{C_h - C_v}{C_v}$	
f	Coefficient of friction	
F_{fr}	Friction force	N
H	Power loss	kW
h	Oil film thickness	mm
k	Thermal conductivity	W/m. °C
L	Length of the bearing	mm
L/D	Length/diameter	
M_p	mass of the nanoparticles	g
M_f	mass of the base fluid	g
N	Journal rotational speed	rpm
O_b	Bearing center	
O_j	Journal center	
P	Poise (unit of dynamic viscosity)	N.s/m^2
Q_s	side leakage flow	L/min
R_b	Bearing Radius	mm
R_j	Journal Radius	mm
U_j	journal speed	m/s
W	Load carrying capacity	N
x	Coordinates in direction of motion	
y	Coordinates perpendicular in direction of motion	
z	Coordinates through the film	

Greek Symbols		
β	viscosity–temperature index	$1/℃$
ε	Eccentricity ratio	
μ_f	Viscosity of the base fluid	$Pa.sec$
μ_{nf}	Viscosity of Nanofluid	$Pa.sec$
θ	Circumferential angle	degree
ϕ	Attitude angle	degree
ω	journal speed	rad/sec
ρ_p	density of the nanoparticles	kg/m^3
ρ_f	density of the base fluid	kg/m^3
ρ_{nf}	density of Nanofluid	kg/m^3
φ	volume fraction	
φ_m	maximum particle packing fraction	
η	intrinsic viscosity	
Subscript		
b	Bearing	
f	Base fluid	
j	Journal	
nf	Nanofluid	
p	Particle of nano	
Abbreviation		
CFD	Computational Fluid Dynamics	
DLS	Dynamic Light Scattering	
EJB	Elliptical Journal Bearing	
FDM	Finite Difference Method	
FEM	Finite Element Method	
FVM	Finite Volume Method	
$JCPDS$	Joint Committee On Powder Diffraction Standards	
SEM	Scanning Electron Microscopy	
TiO_2	Titanium dioxide	
THD	Thermo-hydrodynamic	
$TEHD$	Thermo-elasto-hydrodynamic	
TEM	Transmission Electron Microscopy	
UDF	User Defined Function	
wt	Weight concentration	
XRD	X-Ray Diffraction	
ZnO	Zinc oxide	

ABSTRACT

The current study aims to perform a comparative study of static performance for circular and elliptical journal bearings lubricated with base oil SAE 15W-40 and experimentally characterized with TiO_2 and ZnO nanoparticles at different weight concentrations of 0.5, 1, and 2 wt%.

A three-dimensional CFD model for oil film was implemented using ANSYS Fluent 19 software. The continuity, Navier Stokes, and energy equations for laminar flow fields on rigid and smooth bearing surfaces have been solved using suitable boundary conditions to determine the oil film pressure and temperature, which allows evaluating the main bearing performance parameters such as the load-carrying capacity, side leakage flow, friction force, power loss, and attitude angle. The study of such parameters has been done considering the effects of different journal speeds (3000–5000 rpm), different weight concentrations, eccentricity ratios (0.1–0.9), and ellipticity ratios (0-1). The effect of oil film temperature and nanoparticle concentration on nano-lubricant viscosity was studied using the Krieger–Dougherty viscosity model.

A validation study has been carried out to confirm the accuracy of the numerical model with different numerical and experimental studies that are in good agreement.

The obtained results showed that the oil film pressure and temperature, load-carrying capacity, side leakage flow, friction, and power loss increased when the bearing worked at higher eccentricity ratios and journal speeds for both circular and elliptical bearings. So these bearing parameters were also found to increase when the bearing was lubricated with a nano-lubricant that has higher particle concentrations, except that side leakage flow and attitude

angle decreased with increased weight concentration of particles at any eccentricity ratio.

The obtained results for the static characteristics of circular and elliptical bearings also show that circular journal bearings have higher oil film pressure, temperature, load-carrying capacity, friction force, and power loss compared with elliptical bearings.

Chapter 1

Introduction

CHAPTER ONE

INTRODUCTION

A hydrodynamic journal bearing is a machine element that handles heavy loads as a result of the wedge-shaped geometry created by the eccentricity of the journal and bearing geometric centers and the relative motion between their surfaces. It is also characterized by a good damping effect owing to the existence of an oil film with suitable viscosity. There are two types of journal bearing such as circular, and elliptical as shown in fig (1.1).

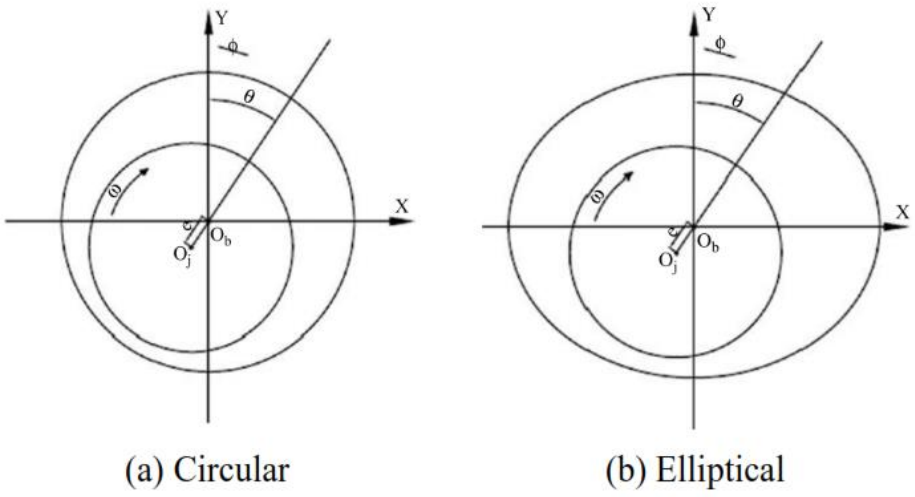

Fig(1.1) Schematic of two types of bearings

The circular journal bearing provides a larger load capacity than other forms of journal bearing of comparable size. Normally it has only one active oil film so its thermal effects are concentrated within small zone of the bearing. Therefore, the temperature in the active zone rises rapidly, resulting in decreasing of in viscosity of the lubricant and a lowering of the load capacity. However, elliptical journal bearings operating with more than one active oil film, account for the superior stiffness, damping and lessening of the maximum temperature in the oil film. Besides, elliptical journal bearings

provide higher stability, lower power losses, and lower bearing temperature owing to their geometrical features than circular ones **(Huang et al. 2014)**.

It was found that dispersing small quantities of different materials as Nano additives in pure oil caused an increase in its viscosity; hence, the load increased at the expense of a slight increase in oil film temperature. The influence of nanoparticle parameters such as size, structure, and morphology has played an important role in the lubrication mechanisms **(Lourtioz et al. 2016)**.

The main purpose of the current study is to examine the steady-state characteristics of circular and elliptical journal bearings when lubricated with nano-lubricants that have different nanoparticle concentrations and work under different working conditions such as journal speeds, eccentricity ratios, ellipticity ratios, and nanoparticle concentrations, considering thermal effects using the CFD technique.

1.1 Objectives of the Present Work

The main objectives of the current study are:

1- Examining the effect of using different weight concentrations of TiO_2 and ZnO, journal speed, eccentricity, and ellipticity ratios on thermo-hydrodynamic steady-state performance for circular and elliptical journal bearings.
2- Implementing a performance comparison between circular and elliptical journal bearings lubricated with experimentally characterized nano-lubricants based on thermo-hydrodynamic lubrication analysis.

Chapter 2

Literature Review

CHAPTER TWO

LITERATURE REVIEW

Extensive work has been implemented in the field of conventional and nonconventional hydrodynamic bearings. The previous studies focused on how various characteristics affected the effectiveness of these bearings using conventional, CFD, and experimental methods. The survey of literature performed in this chapter includes the following items:

1. Characterization of Nano-Lubricants
2. Performance of Journal Bearings with Nano-Lubricant
3. Performance of Elliptical Journal Bearings
4. CFD Analysis of Journal Bearings
5. Comparative Studies of Elliptical and Circular Bearings
6. Concluding Remarks

2.1 Characterization of Nano-lubricants

The nano-lubricant characteristics can be implemented by different methods. The quality of the prepared nano-lubricant depends on its stability and cost. Many techniques can be used to determine the nanoparticle size distribution and tribological characteristics of nano-lubricants.

Murshed et al.(2008) investigate experimentally and theoretically the effective thermal conductivity and viscosity of nanofluids including TiO_2 and Al_2O_3 nanoparticles were dispersed in deionized water, ethylene glycol, and engine oil to prepare nanofluids. Cetyl Trimethyl Ammonium Bromide (CTAB) was used as a surfactant to improve the stability and dispersion of the nanoparticles in the base fluids. Krieger-Dougherty and Nielsen's models show reasonably good agreement with the experimental results and give better predictions for the effective thermal conductivity of nanofluids. It has

been found that the viscosity and thermal conductivity of nanofluids both increase with an increased volume fraction of nanoparticles.

Kole and Dey (2011) examined the viscosity of nano-lubricants containing spherical CuO nanoparticles with a 40 nm average diameter dispersed in gear oil (IBP Haulic-68). The use of oleic acid as a dispersant helped stabilize the resulting nano-lubricant, while ultrasonic mixing was used to homogenize the resulting nano-lubricant. A Brookfield programmable rotational viscometer was used at temperatures between 10 and 80 °C to study the effect of shear rate, temperature, and nanoparticle concentration on the prepared nano-lubricant viscosity. Dynamic Light Scattering was used to measure the aggregate size of nanoparticles. The CuO volume fraction dependency of viscosity of CuO gear oil nanofluids was well predicted by the modified Krieger-Dougherty model taking aggregation into account. It was confirmed that Nano-lubricant viscosity was improved by three times in comparison with pure oil at 2.5% volume fraction. This is consistent with the fact that an increase in nanoparticle concentration in nanofluid increases the fluid's internal shear stress

Anoop et al.(2014) used a high-pressure high-temperature viscometer to examine the rheological characteristics of mineral oil (Therm Z-32, QALCO QATAR) based on a nanofluid containing 1% and 2% volume concentrations of SiO_2 nanoparticles. Nanofluid was prepared using a magnetic stirrer, an ultrasonic bath, and probe-type ultrasonication was applied to disperse SiO_2 in the base fluid. The findings indicated an increase in nano-lubricant viscosity with an increase in nanoparticle concentration and a decrease with an increase in temperature. Also, found that viscosity values of both base fluid and nanofluids increased with an increase in pressure.

Wan et al. (2015) studied the characteristics of commercial lubricating oil (SE 15W-40, Sinopec Lubricants, China) containing 0.1wt.%, 0.5wt.%, and 1.0wt.% of boron nitride (BN) nanoparticles with a diameter of 120 nm. Oleic acid was utilized as a surfactant for suspension stability. Nano-lubricants were prepared using a two-step method. The crystals of BN nanoparticles and morphology have been checked by XRD and TEM, respectively. The viscosities of these lubricating oils were measured using a rheometer at a temperature of 20-60 °C. It has been found that viscosities of the base oil and Nano lubricant oils dropped with rising temperature. Also, anti-friction and anti-wear properties of base oils could be enhanced by nanoparticle additives, and lower concentrations of nanoparticles showed higher tribological behavior.

Ali et al. (2016) used two types of nanoparticles, Al_2O_3 and TiO_2, with average particle sizes of 8–10 and 12 nm, respectively, as an additive to engine oil (Castrol 5W-30) for enhancing tribological characteristics of piston ring assembly. A magnetic stirrer was used for blending nanoparticles with the engine oil at different concentrations of 0.05, 0.1, 0.25, and 0.5 wt%. Oleic acid was used as a surface modifier to ensure proper dispersion of nanoparticles within the engine oil. The morphology of the nanostructures and pattern of nanoparticles has been investigated by field emission scanning electron microscopes (FE-SEM) and XRD. It has been found that 0.25 wt.% of nanoparticles is the optimum concentration. In addition, the friction coefficient, frictional power losses, and wear rate of piston ring were reduced as compared with use of engine oil without nanoparticles. The surface morphology of piston ring indicated that use of nano-lubricant additives produced smoother worn surfaces.

Mousavi et al. (2020) made a comparative study of tribological and thermal properties of oil by adding ZnO and MoS_2 to SAE-40 monograde diesel oil at various concentrations (0.1, 0.4, and 0.7 wt.%). Triton X-100 was used as a surfactant to disperse nanoparticles in a base oil. Thermo-physical parameters like viscosity, flash point, pour point, friction factor, and viscosity index were studied and compared to pure oil. SEM and XRD are used to examine surface morphologies and patterns of nanoparticles respectively. It has been found that the viscosity of MoS_2 and ZnO nano lubricants with 0.7 wt% of nanoparticles at 100 °C increased by about 9.58% and 10.14%, respectively. Furthermore, it was discovered that increasing the concentration of nanoparticles improved thermo-physical parameters while decreasing the pour point and applying ZnO nanoparticles to pure oil improved its thermo-physical characteristics better than MoS_2 nanoparticles.

Parvar et al. (2020) investigate the effect of temperature and ZnO nanoparticle concentration on the thermal conductivity and dynamic viscosity of transformer oil at volume fractions of 0.05%, 0.125%, 0.25%, 0.5%, and 1%. Pure transformer oil was mixed with ZnO by using a magnetic stirrer for 2 hours and an ultrasonic homogenizer for 15 minutes to break down the agglomerated particles. DLS was used to ensure the dispersion of these samples and measure the aggregate size of nanoparticles. The viscosity and thermal conductivity of the nanofluids were measured by a Brookfield viscometer and KD2 Pro device, respectively. The results reveal a decrease in the oil viscosity at an increasing shear rate in all concentrations, which ensures the non-Newtonian behavior of that lubricant. However, the dynamic viscosity of lubricant decreases with an increase in temperature at a given nanoparticle volume fraction. Moreover, dynamic viscosity improved with higher nanoparticle concentrations. The results also

revealed that the thermal conductivity of the nanofluids was higher than that of the pure transformer oil at a constant temperature of 25 °C.

Gupta et al. (2021) investigate the characterization and rheological behavior of five types of nano-lubricants. The nano lubricants used are SnO_2, TiO_2, Fe_3O_4, CuO, and ZnO at a volume concentration of 1% mixed with a base oil grade 5W-30. The nanoparticles were magnetically stirred and sonicated in the base oil to ensure the uniform dispersion of nanoparticles in the base oil. The viscosity of samples was measured using a rotational rheometer at varying temperatures of 30-80°C. XRD and photoluminescence spectroscopy were used to characterize and identify the nanoparticles. DLS technique is used to measure the average particle size of each sample. The Newtonian behavior of these nano-lubricants was confirmed since the results show that the viscosity was independent of the shear rate. Also, viscosity decrease with increased temperatures at a constant shear rate.

2.2 Performance of Journal Bearings with Nano-lubricant

Many researchers looked at how adding nanoparticles of various materials to pure oil affected the journal bearing's performance. It was found the existence of such nano additives enhances load-carrying capacity and side leakage of the lubricant from its ends with a slight rise in the oil film temperature.

Nair et al. (2011) examined static performance characteristics of thermo-hydrodynamic journal bearing operating with Veedol SAE 15W-40 multi-grade engine oil and nanoparticles of CuO, CeO_2, and Al_2O_3. Pressure and temperature distribution are calculated by solving modified Reynolds and energy equations simultaneously by using FEM and MATLAB. The static performance parameters such as load capacity, attitude angle, end

leakage, and friction force are examined in the case of iso-viscous and thermo-viscous conditions at varying weight concentrations of nanoparticles (0.1, 0.25, and 0.5 wt%) and eccentricity ratios (0.1-0.9). It was found that bearing performance characteristics are not affected when bearing works at low eccentricity values with increased concentration of the nanoparticles in the iso-viscous case, while a significant effect was observed at higher values of eccentricity in the case of thermo-viscous condition. Additionally, it was found that higher concentrations of nanoparticles enhance load capacity and friction force of bearing with a decrease in the end leakage and attitude angle for both iso- and thermo-viscous cases at any eccentricity ratio.

Shenoy et al. (2012) examined the effect of CuO, TiO_2, and Nano-Diamond nanoparticle additives in API-SF engine oil and base oil (SAE30 LB51163-11) on the static characteristics of an externally adjustable fluid-film bearing at different eccentricity ratios. The static characteristics in terms of load-carrying capacity, attitude angle, friction, and end leakage has been evaluated from pressure distribution. The results showed that adding nanoparticles increased bearing load capacity and friction force with reduced end leakage compared to API-SF engine oil and base oil without nanoparticle additives.

Binu et al. (2014b) examined the static characteristics of a journal bearing operating with nano lubricant based on TiO_2 blended with SAE 30 engine oil at weight concentration ranging from 0.05% to 2.5% and different eccentricity ratios. Lubricant viscosity was evaluated using a modified Krieger–Dougherty model, which was validated using data obtained experimentally with good agreement. The results reveal that the pressure distribution of the lubricant film increases with higher volume fractions of TiO_2 nanoparticle additives. It has been found that there is a significant increase in load-carrying capacity and friction force with increasing volume

fractions of TiO_2 and eccentricity ratio. It was also discovered that as volume fractions of TiO_2 increased, attitude angle and side leakage decreased.

Babu et al. (2014) studied the performance characteristics of circular journal bearings lubricated with SAE 15W-40 engine oil dispersed with Al_2O_3 and ZnO nanoparticles. The static performance characteristics in terms of load capacity, friction force, end leakage, and attitude angle are computed for different values of eccentricity ratios and weight concentration of nanoparticles for non-thermoviscous and thermoviscous cases. The results reveal that an increase in the weight concentration of nanoparticles has a slight effect on the load capacity and friction force of the bearing in the non-thermoviscous case, but it has a significant effect in the thermoviscous case, particularly with a high eccentricity ratio. End leakage and attitude angle were also found to decrease with increasing nanoparticle concentration in both non-thermoviscous and thermoviscous cases at any eccentricity ratio.

Binu et al. (2014a) investigated the effect of a lubricant additive containing TiO_2 nanoparticles on the load-carrying capacity of a journal bearing. A modified Krieger-Dougherty viscosity model is used to represent an increase in lubricant viscosity due to the presence of TiO_2 nanoparticle additives at volume fractions ranging from 0.005 to 0.025. To measure pressure distribution and load-carrying capacity theoretically, a modified Reynolds equation at different TiO_2 concentrations and aggregate sizes is evaluated. The particle size distribution of TiO_2 nanoparticle dispersion in engine oil is studied using DLS. It has been obtained that the load-carrying capacity of journal bearings improved with increased volume fractions of nanoparticles with compare to plain engine oil without nanoparticle additives. Also, the load-carrying capacity increases with higher nanoparticle aggregate packing ratios.

Nicoletti (2014) examined the static behavior of journal bearings lubricated with oil ISO VG68 and different nanoparticles of Si, SiO_2, Al, Al_2O_3, Cu, and CuO. The finite difference method is used for solving the energy and Reynolds equations. Nanoparticle additives increase the viscosity of lubricants and change the thermal properties of lubricants. The increase in volumetric heat capacity and viscosity due to the addition of nanoparticles caused an increase in the bearing load capacity to 10%. The generation temperature in the bearing gap has decreased due to the higher volumetric heat capacity of the lubricant.

Patil and Deshmukh (2016) examined experimentally the thermal behavior of Journal bearings lubricated with SAE 15W-50 oil containing hybrid nanoparticle additives for evaluating the load-carrying capacity of journal bearings. The viscosity of lubricating oil had a significant effect on the load-carrying capacity of journal bearings. The heat generated in the bearing decreased viscosity of oil and its load-carrying capacity. It has been discovered that adding nanoparticles to base lubricants can increase viscosity, thereby enhancing load-carrying capacity of bearing.

Suryawanshi and Pattiwar (2019) studied the tribological performance (anti-friction and anti-wear properties) of commercial Mobil grade lubricants (DTE 24, DTE 25, and DTE 26) used in a journal bearing of a system in a power plant. Nanolubricants prepared by blending 0.5 wt% of TiO_2 have an average diameter of 40 nm in a base oil. Oleic acid is used as a surfactant to enhance solubility. Lubricant viscosity is measured using a viscosity model (modified Krieger-Dougherty). SEM, ultraviolet spectrophotometer, and XRD are used to examine the morphology of TiO_2 nanoparticles. This research shows that adding TiO_2 to lubricants improves their anti-friction and anti-wear properties. It has also improved the thermo-physical characteristics of the lubricant.

Ramaganesh et al. (2020) used COMSOL multi-physics approach to evaluate the oil film pressure generated in journal bearings lubricated with different types of lubricants and make a comparison with experimental results at a speed of 3000 rpm and a load of 10 kN. The lubricant contains SAE 20W-40 as a base oil with 0.5 wt% of CuO, TiO_2, and WS_2. It has been found that the results of COMSOL model were successfully validated with those obtained experimentally.

Singh et al. (2020) examined experimentally the effect of different volume fractions of TiO_2 additive (0.075%, 0.1%, and 0.15%) in lubricant oil SAE30 on the performance of hydrodynamic journal bearings. Experimental analysis has been carried out using a test rig at a journal speed of 1400 rpm and a varying load of 600–1000 N. The performance of hydrodynamic journal bearings in terms of coefficient of friction, pressure distribution, temperature increase, eccentricity ratio, attitude angle, and minimum film thickness have been examined. It has been found that the addition of TiO_2 nanoparticles improves performance, minimizes the friction coefficient, and drops maximum temperature rise of journal bearings.

Gundarneeya and Vakharia (2021) examined experimentally the characteristics of journal bearings operated with nano-lubricants by adding nanoparticles of TiO_2, CuO, and Al_2O_3 to Veedol Avalon grade 46 oil at various volume fractions (0.25%, 0.5%, 1%, and 2%). Oleic acid is used as a surfactant to minimize the aggregation of nanoparticles. The pressure distribution and load of the journal bearing have been evaluated by a test rig (TR-60) at journal speeds of 250 and 500 rpm and loads of 300 and 450 N, respectively. The findings show that adding nanoparticles to the base oil enhances the maximum pressure and load-carrying capacity.

Dang et al. (2021) examined the static thermal performance of circular journal bearings at varying weight concentrations (0.5%, 1%, and 2%) of CuO(40nm) and TiO_2(40nm) nanoparticles, journal speeds (2000, 3000, 4000, and 5000 rpm), and eccentricity ratios of (0.4-0.7). The viscosity of nano-lubricants has been calculated using the modified Krieger-Dougherty method. Reynolds equation and Energy equation are solved by finite difference method. MATLAB model was used to calculate hydrodynamic pressure and oil film temperature. The results reveal that oil film pressure, power loss, and load capacity significantly improve with a slight increase in oil temperature with increased concentration of nanoparticles, journal speed, and eccentricity ratio.

2.3 Performance of Elliptical Journal Bearings

The increase in journal bearing speed leads to the problem of instability, which was found to be treated by using nonconventional (noncircular) bearings. One of the most important types used in this field is the elliptical journal bearing. It was found that this type of bearing has a lower oil temperature due to its higher clearance. Several studies have been implemented to discuss the performance of such bearings under different working conditions.

Mishra (2007) examined numerically isothermal and thermal performance under the adiabatic boundary condition of an elliptical bearing at different eccentricity and non-circularity ratios (Ellipticity ratios). The bearing performance parameters like bearing load, friction force, coefficient of friction, flow in the bearing, and side leakage have been studied. It has been found that oil film thickness increases with an increase in the non-circularity ratio, causing a decrease in oil film pressure and temperature. The pressure of the oil film obtained under isothermal conditions is higher than that obtained under thermal conditions. Also, the friction coefficient and side

leakage decreased with an increase in the non-circularity ratio (ellipticity ratio).

Chauhan and Sharma (2010) evaluated thermo-hydrodynamic behavior for elliptical bearings using three different grades of oil. The pressure and temperature distributions were obtained numerically by solving the Reynolds and energy equations with finite difference method. The temperature in the oil film is calculated using the parabolic temperature profile estimation method. It appeared that the oil film temperature and thermal pressures of the bearing increased as the speed and eccentricity ratio increased. However, it has been found that the temperature and pressure decrease as the elliptical ratio of the bearing increases.

Sehgal (2010) examined the thermal behavior of an elliptical journal bearing lubricated with different grades of oil experimentally by using a suitable test rig at three different speeds (3000, 3500, and 4000 rpm), varying loads(200,400, and 500) and constant oil pressure of 0.3 MPa. The FUNGILAB Digital Readout Viscometer Model "VISCOBASIC L" is used to measure the viscosity of lubricating oil. It has been found that thermal behavior of journal bearings is affected by rotational speed, loads, and type of oil used. It was also found that flow rate increased with speed and applied load.

Singla and Chauhan (2016) made experimental investigations of the oil film pressure and temperature in the center plane of an elliptical journal bearing lubricated with several HYDROL oil grades (32, 68, and 150). The data has been obtained through a test rig with applied loads of 500–2000 N and varying speeds of 2000–5000 rpm. Investigations have demonstrated that an increase in speed causes to raise in the temperature of the lubricating oil. It has been also observed that oil film pressure and temperature increase with increased load, speed, and viscosity of lubricating oil.

Ebrahimi et al. (2020) studied the effect of the geometrical parameters of elliptical journal bearing on load capacity, friction force, pressure, and oil temperature. Vogel equation was used to investigate the effect of temperature on viscosity. Reynolds and energy equations are solved simultaneously under an adiabatic boundary condition by using finite element method. The results have been obtained at different eccentricity ratios and non-circularity values (Ellipticity ratio). Results show that an increase in non-circularity causes a decrease in maximum oil film pressure, temperature, and friction force while these parameters increase at higher eccentricity ratios.

Dang et al. (2020) used MATLAB model to examine the effect of TiO_2 and CuO nanoparticles on the thermal behavior of elliptical bearings. Bearing performance parameters have been investigated for bearings lubricated with nano-lubricant based on TiO_2(40nm) and CuO(40nm) at weight concentrations of 0.5, 1, and 2 wt% mixed with three different grades of mineral oils at varying speeds and eccentricity ratios. Reynolds equation and Energy equation are solved with finite difference method. The effect of oil film temperature and nanoparticle concentration on lubricant viscosity was evaluated using a modified Krieger-Dougherty model. It has been found that maximum values of pressure, load, temperature, and power losses increased at higher nanoparticle concentrations, viscosity-grade lubricants, speeds, and eccentricity ratios.

Kumar et al. (2021) examined the effect of geometrical parameters on elliptical journal bearing lubricated with Newtonian fluid. The analysis has been done in MATLAB to examine the geometrical analysis of elliptical journal bearings. Pressure profile, load-bearing capacity, and variation of film thickness have been investigated at varying eccentricity and non-circularity ratios. The result shows that the film thickness is reduced with a

decreasing value of the non-circularity ratio at a constant eccentricity ratio. The pressure increases with an increase in eccentricity ratio, while it decreases with an increase in non-circularity ratio. It has been also observed that load-bearing capacity increased with the increased eccentricity ratio.

2.4 CFD Analysis of Journal Bearings

Computational fluid dynamics is an important technique widely applied to evaluate the flow model between the journal and the bearing spatially in bearings with complex geometry. It allows using three-dimensional modeling to analyze such machine elements reliably.

Gertzos et al. (2008) used a 3-D CFD model to investigate the performance characteristics of a hydrodynamic journal bearing lubricated with a Bingham fluid. The FLUENT software was used to solve Navier-Stokes equations. The results of generated CFD model were compared with theoretical and experimental findings from previous studies for both Newtonian and Bingham lubricants, and it was observed that they were in very good agreement. It has also been observed that a Bingham fluid has a greater load-bearing capacity, film pressure, and frictional force than a Newtonian fluid.

Chauhan (2014) studied the influence of speed on pressure and temperature distribution in a circular journal bearing at isothermal and thermo-hydrodynamic analyses. CFD ANSYS Fluent Software has been used to solve 3-D Navier Stokes and energy equation. The analysis has been carried out at an eccentricity ratio of 0.8 and speeds ranging from 2500 to 5500 rpm. Pressure and temperature at isothermal have been found to be higher than those determined by thermo-hydrodynamic analysis at all journal speeds.It was also found that pressure, temperature, and oil force increased as the journal speed increased at both cases.

Chauhan et al. (2014) studied THD analysis of a circular journal bearing operated at an eccentricity ratio of 0.6 and 2500 rpm of journal speed. Performance parameters of bearing in terms of lubricant pressure and temperature have been determined by using the CFD software ANSYS Fluent to solve three-dimensional Navier-Stokes and energy equations. It has been discovered that maximum pressure and temperature in the lubricant are higher at constant viscosity than at varying viscosity.

Solghar (2015) performed CFD technique to investigate THD of journal bearing that has a single groove operating with two types of lubricant: pure oil and base oil blended with a 5% volume fraction of Al_2O_3 nanoparticles. The cavitation effects and lubricant recirculation mixing are considered. The set of governing equations for continuity, momentum and energy inside the lubricant and energy within the solid bush are simultaneously solved by using finite volume method. It was revealed an increase in coefficients of friction and load-carrying capacity (17.7% at an eccentricity ratio of 0.9) with an increased concentration of nanoparticle additives, while the lubricant flow rate was decreased in comparison to pure oil.

Susilowati et al. (2016) used a 3-D CFD technique to examine the hydrodynamic behavior of a journal bearing operated with a thin oil film working at laminar and turbulent regimes at different speeds of 3000, 5000, and 10000 rpm. The numerical simulation shows that hydrodynamic pressure is significantly influenced by the journal speed. It was observed that both laminar and turbulent regimes have similar results in the distribution of static hydrodynamic pressure. Additionally, it is discovered that the static pressure is low at the start of the contact, gradually increases to its maximum, and then suddenly decreases.

Jamalabadi et al. (2019) used CFD technique to investigate THD performance of plain journal bearings, including the effect of TiO_2 nanoparticles with varying volume fractions (0%, 5%, and 10%), lubricant type (DTE 24, DTE 25, and DTE 26), and rotational speeds (500, 1000, and 1500 rpm). The Reynolds equation was used to determine the pressure distribution for journal bearings. The results show that increasing rotational speed and nanoparticle volume fraction increases the dissipation power, average shear stress, and temperature rise for all lubricant types.

Susilowati et al. (2019) used the CFD approach to study the influence of eccentricity ratio on performance of journal bearings including the multi-phase flow cavitation effect. Navier-Stokes, continuity, and cavitation models have been computed using the finite volume method. The friction force, load support, and hydrodynamic pressure are the main estimated bearing performance parameters. According to the results obtained, operating a bearing at a high value of eccentricity ratio caused a larger maximum hydrodynamic pressure and a higher load carried by the bearing.

Sadabadi and Nezhad (2020) used CFD approach to evaluate the application of WS_2 nano-lubricant on the load-carrying capacity of high-load journal bearings. Nano-lubricant based on synthetic industrial oil with different weight fractions of WS_2 (50 nm). The average aggregate size of nanoparticles is measured by images from SEM. The modified Krieger–Dougherty model was used to measure viscosity of nano-lubricant taking into account aggregation effect. The pressure profile of the hydrodynamic lubrication has been studied at different weight fractions to evaluate load capacity of bearing. The results showed that 5 wt% of WS_2 additive improved load-carrying capacity of journal bearings by 20%.

Ahmed et al. (2021) used the CFD technique to investigate THD performance in journal bearings lubricated with nano-lubricants based on TiO_2 and Al_2O_3 nanoparticles at different volume fractions of (0.5 %, 1 %, 2 %, and 3 %). Modified Krieger- Dougherty model has been evaluated to measure the viscosity of nano-lubricants. It has been observed that increasing the concentration of the nanoparticles causes an increase in the maximum oil film pressure, oil film temperature, and load-carrying capacity. Also, the best performance parameters have been obtained when using TiO_2 nanoparticles rather than Al_2O_3 nanoparticles.

2.5 Comparative Studies of Elliptical and Circular Bearings

Hussain et al. (1996) analyzed distribution temperature in elliptical, two-lobe, and orthogonally bearings (noncircular), as well as the conventional circular bearing. It has been discovered that the load is greatest for two-lobe bearings and decreases for elliptical and orthogonal bearings. The load capacity of circular bearings is more sensitive to variations in the eccentricity ratio in comparison with noncircular bearings, while it is influenced by the ellipticity ratio in the case of noncircular bearings. Walther equation is used to analyze the variation of viscosity with temperature. It was also found that the position of the groove has a significant effect on the temperature rise, and the increase in temperature is greatest for two-lobe bearings, followed by elliptical and orthogonal journal bearings.

Mishra et al. (2007) examined the effect of non-circularity (Ellipticity ratio) on performance parameters of the elliptical journal bearing and make a comparative study with a circular case. The numerical solution of the Reynolds equation and the energy equation was analyzed to show the temperature profile at a varying value of non-circularity. It was found that

pressure decreases as non-circularity increases and the rise in temperature is less with a higher non-circularity value of a journal bearing.

Huang et al. (2014) studied the influences of elliptical ratio on the lubricant performance of elliptical, two-lobe, and circular journal bearings. THD model has been evaluated by finite difference method to solve the Reynolds equation and energy equation. Viscosity variation with temperature is examined using the Walther equation. It has been found that a circular bearing has the highest value of oil film pressure, followed by a two-lobe and elliptical bearing, which has the lowest value. The first peak pressure and the oil temperature at the midplane of the two-lobe and elliptical bearings decrease with the increase in the elliptical ratio.

Pawar et al. (2014) used the CFD ANSYS 14.5 software package to execute a comparison study between a two-lobe and a circular hydrodynamic journal bearing. The variation pressure of a two-lobe and a circular journal bearing was tested at a speed of 3000 RPM and a constant eccentricity ratio of 0.7 with varying elliptical ratios of (0.5, 1, 2, and 3). It was found that the maximum pressure of a two-lobe journal bearing is less than that of a circular bearing, which indicates that a two-lobe journal bearing is more stable than a circular. Furthermore, the maximum pressure decreases with increasing the elliptical ratio. It has also been discovered that the load-carrying capacity of a circular journal bearing is greater than that of a two-lobe bearing at different speeds.

Suryawanshi and Pattiwar (2018) executed experimentally the performance of plain and elliptical journals containing 0.5 wt% of TiO_2 nanoparticles (40 nm) blended with three different lubricants. The tests were performed on a four-ball tester at speeds ranging from 500 to 1000 rpm with a constant load of 1000 N. The Krieger-Dougherty viscosity model is for evaluating viscosity. The effect of TiO_2 on the performance characteristics

in terms of pressure distribution, temperature rise, load carrying capacity, attitude angle, power loss, oil flow rate, side leakage, and frictional force have been investigated. Elliptical bearing lubricated with TiO_2 nanoparticles gives best performance than circular bearing at the same concentration.

Wang et al. (2021) used CFD ANSYS Fluent to investigate the effect of ellipticity ratio on the performance of elliptical journal bearings using the mixture two-phase flow model. The obtained results show that as ellipticity increased, the maximum positive pressure of the upper and lower bushes increased. It was also discovered that elliptical bearings have two temperature rise regions while circular bearings only have one. The maximum temperature rise of the circular bearing is higher than that of the elliptical bearing, proving that the heat dissipation of the elliptical bearing is better than that of the circular bearing.

2.6 Concluding Remarks

Thermo-hydrodynamic analysis of journal bearing is important due to the increase in the rotational speed limits of the machines. The governing equations including continuity, Navier Stokes, and energy equations required to be solved simultaneously to obtain the pressure and temperature distribution through the oil film of the bearing. The literature survey on the performance of journal bearings done in the present work shows that thermo-hydrodynamic analysis for journal bearings was used to investigate the enhancing effect of using different types of nano-lubricants on the oil film pressure and temperature of such bearings. The same procedure was used to prepare nano lubricants to measure the viscosity and aggregate ratio by **Gundarneeya and Vakharia (2021)** in their doctoral thesis. The effect of nanoparticles concentration, eccentricity ratios, and journal speed on the performance of journal bearing has been studied such as **Dang et al.(2021).** However, little work was observed to be done in the field of using the CFD

technique to analyze the performance of the circular and elliptical types of journal bearings lubricated with nano-lubricants and compared them, which is the main goal of the present work.

Chapter 3

Mathematical and Numerical Model

CHAPTER THREE

MATHEMATICAL AND NUMERICAL MODEL

The mathematical model for conventional circular as well as elliptical bearings lubricated with nano-lubricants based on TiO_2 and ZnO is presented here. The effect of different parameters such as the ellipticity ratios, the journal speed, particle concentrations, and eccentricity ratios on the performance of such bearings with different boundary conditions have been discussed. A comparative study for these types of bearings has been also implemented. This chapter is divided into different subsections as follows:

3.1 Bearing Geometry and Coordinate Axis

The circular and elliptical journal bearings with the geometries and coordinates systems shown in figure 3.1(a-b) have been analyzed.

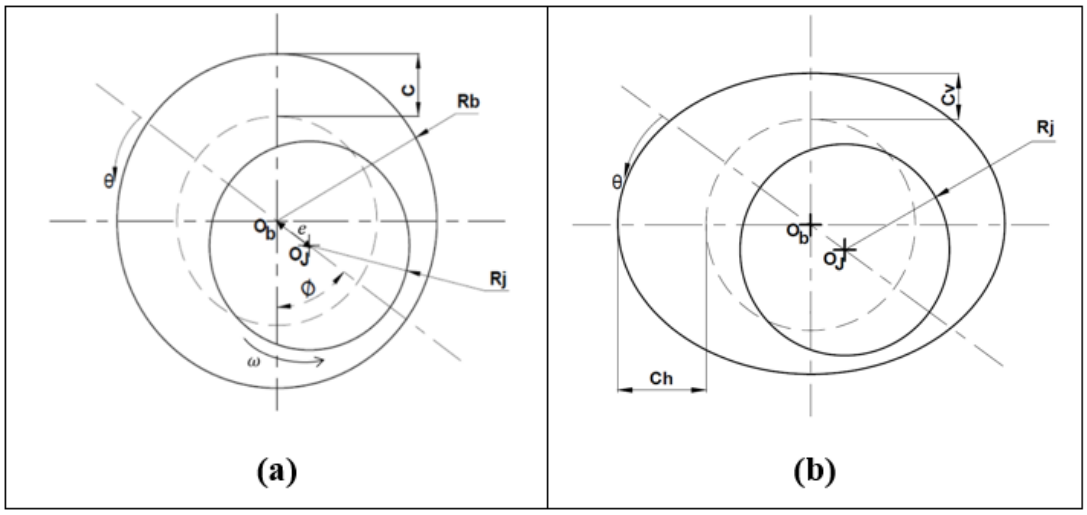

Fig(3.1) Geometry and coordinate axis of the bearings studied in the present work (a) circular Journal bearing,(b) elliptical Journal bearing

This figure shows that both bearings consist of a fixed bearing and rotating journal with rotational speed ω; the nomenclature of such bearings can be presented as:

O_b Bearing center

O_j Journal center

e Distance between shaft and bearing centers

C Radial clearance at circular journal bearing

C_v Vertical clearance of the elliptical bearing

C_h Horizontal clearance of the elliptical bearing

θ Coordinates in the circumferential direction

ϕ Attitude angle

R_b Bearing Radius

R_j Journal Radius

The main bearing's geometrical characteristics with the lubricant's physical and thermal properties are presented in table (3.1).

Table (3.1) Geometrical and operational characteristics of journal bearing**(Dang et al., 2020)**

Parameter	**Value**	**Unit**	**Parameter**	**Value**	**Unit**
L/D	1		Viscosity(μ)	0.0985	Pa. sec
R_j	50	mm	β	0.034	1/°C
C_v	0.1	mm	Density(ρ)	877	kg/m^3
Major Axis	100.4	mm	Specific heat(C_p)	2000	J/kg °C
Minor Axis	100.2	mm	Thermal conductivity (k)	0.13	W/m. °C
ε	0.1-0.9		wt.%	0.5,1,2	
E_p	0-1		ϕ	45	degree
N	3000-5000	RPM			

3.2 Basic Assumptions

The following assumptions are considered throughout the study:

1. The flow is laminar.
2. The lubricant is incompressible.
3. Steady-state condition.
4. Bearing surfaces are smooth (neglecting the roughness effect).
5. Newtonian lubricant.
6. The shaft and bearing materials are rigid.
7. The viscosity of oil was considered as a function of temperature only.
8. There is no slip at the boundaries (coherent boundary conditions)

3.3 Governing Equations

The main governing equations, including continuity, momentum ,and energy equations, required to obtain the pressure and temperature of an oil film are discussed in this section. The three-dimensional Navier-Stokes and continuity equations are used to obtain the velocity of flow field required to evaluate the oil film pressure of a journal bearing operated with a thin oil film. Since the oil film thickness is much smaller than the length and width of the bearing, these equations can be written in Cartesian coordinates.

The commercial CFD software ANSYS FLUENT 19 used a finite volume method (FVM) to solve Navier-Stokes equations over the fluid domain in three dimensions (x, y, and z).

3.3.1 Conservation Equations

The pressure distribution of oil film inside the fluid domain of hydrodynamic journal bearings has been evaluated by solving the following three-dimensional continuity of flow for incompressible fluid **(Versteeg and Malalasekera, 2007)**

$$\frac{\partial u}{\partial x}+\frac{\partial v}{\partial y}+\frac{\partial w}{\partial z}=0 \tag{3.1}$$

Momentum Equation

The velocities of lubricant flow obtained from equation (3.1) are used in the following momentum equations to obtain the oil film pressure distribution.

Momentum equation in X -direction

$$\rho\frac{Du}{Dt}=-\frac{\partial p}{\partial x}+\frac{\partial}{\partial x}\left[2\mu\frac{\partial u}{\partial x}+\lambda\mathrm{div\,u}\right]+\frac{\partial}{\partial y}\left[\mu\left(\frac{\partial u}{\partial y}+\frac{\partial v}{\partial x}\right)\right]+\frac{\partial}{\partial z}\left[\mu\left(\frac{\partial u}{\partial z}+\frac{\partial w}{\partial x}\right)\right]+S_{Mx} \tag{3.2}$$

Momentum equation in Y -direction

$$\rho\frac{Dv}{Dt}=-\frac{\partial p}{\partial y}+\frac{\partial}{\partial x}\left[\mu\left(\frac{\partial u}{\partial y}+\frac{\partial v}{\partial x}\right)\right]+\frac{\partial}{\partial y}\left[2\mu\frac{\partial v}{\partial y}+\lambda\mathrm{div\,u}\right]+\frac{\partial}{\partial z}\left[\mu\left(\frac{\partial v}{\partial z}+\frac{\partial w}{\partial y}\right)\right]+S_{My} \tag{3.3}$$

Momentum equation in Z-direction

$$\rho\frac{Dw}{Dt}=-\frac{\partial p}{\partial z}+\frac{\partial}{\partial x}\left[\mu\left(\frac{\partial u}{\partial z}+\frac{\partial w}{\partial x}\right)\right]+\frac{\partial}{\partial y}\left[\mu\left(\frac{\partial v}{\partial z}+\frac{\partial w}{\partial y}\right)\right]+\frac{\partial}{\partial z}\left[2\mu\frac{\partial w}{\partial z}+\lambda\mathrm{div\,u}\right]+S_{Mz} \tag{3.4}$$

The **Navier–Stokes equations** can be written in the most useful form for the development of the finite volume method:

$$\rho\frac{Du}{Dt}=-\frac{\partial p}{\partial x}+\mathrm{div}(\mu\,\mathrm{grad}\,u)+S_{Mx} \tag{3.5}$$

$$\rho\frac{Dv}{Dt}=-\frac{\partial p}{\partial y}+\mathrm{div}(\mu\,\mathrm{grad}\,v)+S_{My} \tag{3.6}$$

$$\rho\frac{Dw}{Dt}=-\frac{\partial p}{\partial z}+\mathrm{div}(\mu\,\mathrm{grad}\,w)+S_{Mz} \tag{3.7}$$

Where:

' u ', $'v'$, and ' w ' in equations (3.1 - 3.4) are velocity surface components in *x*, *y*, and *z* directions, respectively.

μ lubricant viscosity (Pa. s)

p lubricant pressure(N/m^2)

ρ lubricant density(kg/m^3)

t time (s)

The terms of S_{Mx},S_{My}, and S_{Mz} in equations (3.5 - 3.7) represent components resulting from body forces in x, y, and z respectively.

Where;

$$S_{Mx} = \left[\frac{\partial}{\partial x}\left(\mu\frac{\partial u}{\partial x}\right) + \frac{\partial}{\partial y}\left(\mu\frac{\partial v}{\partial x}\right) + \frac{\partial}{\partial z}\left(\mu\frac{\partial w}{\partial x}\right) + \frac{\partial}{\partial x}(\lambda \mathrm{div\ u})\right]$$

$$S_{My} = \left[\frac{\partial}{\partial y}\left(\mu\frac{\partial u}{\partial x}\right) + \frac{\partial}{\partial y}\left(\mu\frac{\partial v}{\partial x}\right) + \frac{\partial}{\partial z}\left(\mu\frac{\partial w}{\partial x}\right) + \frac{\partial}{\partial y}(\lambda \mathrm{div\ u})\right]$$

$$S_{Mz} = \left[\frac{\partial}{\partial z}\left(\mu\frac{\partial u}{\partial x}\right) + \frac{\partial}{\partial y}\left(\mu\frac{\partial v}{\partial x}\right) + \frac{\partial}{\partial z}\left(\mu\frac{\partial w}{\partial x}\right) + \frac{\partial}{\partial z}(\lambda \mathrm{div\ u})\right]$$

3.3.2 Energy Equation

The bearing oil film temperature was determined using the below three-dimensional energy equation **(Versteeg and Malalasekera, 2007)**

$$\rho C_p\left(\frac{\partial T}{\partial t} + u\frac{\partial T}{\partial x} + v\frac{\partial T}{\partial y} + w\frac{\partial T}{\partial z}\right) = \frac{\partial}{\partial y}\left(k\frac{\partial T}{\partial y}\right) + \mu\left[\left(\frac{\partial u}{\partial y}\right)^2 + \left(\frac{\partial w}{\partial y}\right)^2\right] \quad (3.8)$$

Where;

k and C_p Represent thermal conductivity and specific heat of lubricant respectively.

T temperature of oil film (^{o}C)

Convectional heat transfer is represented by the term on the left equation (3.8), while viscous heat transfer and conduction are represented by a term on the right of the same equation.

3.4 Physical and Rheological Characteristics of Nano-Lubricant

The main physical and rheological properties of the nano-lubricant as density, viscosity, specific heat, thermal conductivity, etc. presented in this section.

3.4.1 Model of Krieger-Dougherty

A modified Krieger-Dougherty model as a function of volume fractions calculated the viscosity of nano-lubricants.

$$\mu_{nf} = \mu\left[1 - \frac{\varphi}{\varphi_m}\right]^{-[\eta]\varphi_m} \tag{3.9}$$

Where:

μ: Base oil viscosity

μ_{nf}: Viscosity of nano lubricant at different nano-particles volume fraction

φ: Volume fraction of nanoparticles.

φ_m: maximum fraction of particles packed; η is viscosity intrinsic have been chosen as 0.605 and 2.5 respectively **(Krieger and Dougherty, 1959)**

Equation (3.9) can be modified as follows by using values of η:

$$\mu_{nf} = \mu\left(1 - \frac{\varphi_a}{\varphi_m}\right)^{-2.5\varphi_m} \tag{3.10}$$

Where;

$$\varphi_a = \varphi\left(\frac{a_a}{a}\right)^{3-D} \tag{3.11}$$

Where;

a_a Radius of aggregate nanoparticles (nm)

a Radius of primary nanoparticles (nm)

D is the fractal factor of nanofluids and has 1.8 as a specific value

$\frac{a_a}{a}$ is a ratio of nanoparticles in aggregation

According to the temperature and volume fraction of nanoparticles, the lubricant's viscosity may be represented as follows:

$$\mu = \mu_{nf} \exp[-\beta(T - T_i)] \quad (3.12)$$

Where;

β is a viscosity-temperature factor for lubricants with a value of $0.034C^{-1}$

T_i is the inlet oil film temperature.

The volume fraction of the nanoparticles that were used in the present study was calculated by using the below equation for converting their weight fraction **Azmi et al. (2013)**:

$$\varphi = \left[\frac{(\frac{M_p}{\rho_p})}{\left(\frac{M_p}{\rho_p} + \frac{M_f}{\rho_f}\right)} \right] \times 100 \quad (3.13)$$

Where;

φ Volume fraction of the nanoparticles

M_p Mass of nanoparticles

M_f Mass of pure oil

ρ_p, and ρ_f are the density of the nanoparticles and the pure oil

Weight fractions of nanoparticles and their corresponding volume fractions utilized in current work are presented in table (3.2)

Table (3.2) Volume fractions corresponding to the weight fraction

Weight fraction %	0.5	1	2
Volume fraction % (TiO_2)	0.104	0.2089	0.4213
Volume fraction % (ZnO)	0.07863	0.1579	0.3185

3.4.2 Nano-Lubricant Density

The nano-lubricant density is determined as a function of the volume fraction of nanoparticles **(Maneshian and Nassab, 2009)**

$$\rho_{nf} = (1-\varphi)\rho_f + \varphi\rho_p \quad (3.14)$$

Where;

ρ_f Density of pure oil

ρ_p Density of nanoparticles

ρ_{nf} Nano lubricant density

3.4.3 Specific Heat

The specific heat of nano-lubricants as a function of nanoparticle volume fractions can be calculated **(Maneshian and Nassab, 2009)**

$$\rho_{nf}C_{p,nf} = (1-\varphi)\left(\rho C_p\right)_f + \varphi\left(\rho C_p\right)_p \quad (3.15)$$

Where $\left(C_p\right)_p$, $\left(C_p\right)_f$ and $C_{p,nf}$ represent the specific heats of nanoparticles, pure oil, and nano-lubricants, respectively.

3.4.4 Thermal Conductivity

Using the Maxwell model, the Nano lubricant's thermal conductivity was determined. **(J.C. Maxwell 2010)**

$$k_{nf} = k_f \left[\frac{\left(k_p + 2k_f\right) - 2\varphi\left(k_f - k_p\right)}{\left(k_p + 2k_f\right) + \varphi\left(k_f - k_p\right)}\right] \quad (3.16)$$

Where k_p , k_f, and k_{nf} the thermal conductivities of nanoparticles, pure oil, and nanofluid, respectively.

3.5 Performance Parameters for Bearings

The major bearing performance indicators are as follows:

3.5.1 Load-Carrying Capacity

It is possible to present the component of bearing load in a vertical direction as:

$$\mathrm{W}_y = \iint_{A_i} P_j \cdot \cos\theta \cdot \left(dA_j\right) = -W \quad (3.17)$$

The load component can also be identified in the horizontal direction as:

$$\mathrm{W}_x = \iint_{A_j} P_j \cdot \sin\theta . \left(dA_j\right) = 0 \quad (3.18)$$

The total bearing load has been determined as:

$$W = \sqrt{W_x^2 + W_y^2} \quad (3.19)$$

The equilibrium point of the journal center can be achieved when the vertical component of the bearing load capacity (W_y) is equal to the external load (W) ($W_x \approx 0$).

3.5.2 Attitude Angle

It is possible to determine the attitude angle of bearing as follows:

$$\phi = \tan^{-1}\left(\frac{W_y}{W_x}\right) \quad (3.20)$$

3.5.3 Friction Force

The friction force at the surfaces of the bearing can be evaluated as:

$$F_{fr} = \iint \tau \cdot (dA) \quad (3.21)$$

Where τ represent the shear stress

The friction coefficient can be presented as:

$$f = \frac{F_{fr}}{W} \quad (3.22)$$

3.5.4 Power Loss

The frictional force that causes the power loss as heat is dissipated from the bearing surfaces as a result of induced friction at the bearing surfaces can be determined as follows:

$$H = f\, W U_j \quad (3.23)$$

3.5.5 Side Flow Leakage

The side leakage flow can be presented as:

$$Q_s = \int_{\theta_1}^{\theta_2} \frac{h^3}{12\mu}\left(\frac{\partial P}{\partial z}\right)_{z=0 and\ L} d\theta \quad (3.24)$$

Where:

h is the oil film thickness of circular journal bearing **(Dang et al., 2021)** can be expressed:

$$h = c + e\cos\theta \quad (3.25)$$

Where:

c is the clearance radial of bearing

e is the eccentricity of the bearing center from the journal center

The oil film thickness of the elliptical journal bearing **(Dang et al., 2020)** can be expressed as:

$$h = C_v\left(1 + \varepsilon\cos\theta + E_p\sin^2(\theta + \phi)\right) \quad (3.26)$$

Where:

$\varepsilon = \dfrac{e}{C_v}$ is the eccentricity ratio

E_p is the ellipticity ratio which can be defined as

$$E_p = \frac{C_h - C_v}{C_v}$$

3.6 Method of Solution

In this section, the required steps for creating and solving the CFD models of circular and elliptical journal bearings are presented in figure (3.2). The mesh generation procedure, the computation procedure, and the algorithm of the solution will be investigated in the following articles. Ansys Fluent 19 has been used to solve the mathematical model of the current study.

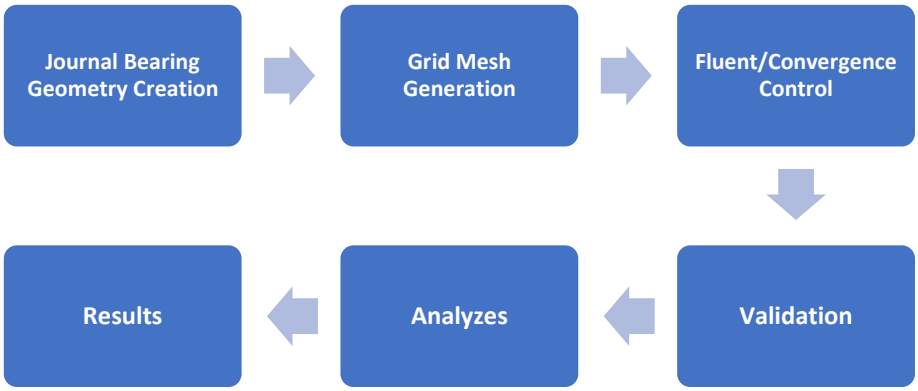

Fig(3.2) Steps required to solve the CFD model

3.7 Mesh Generation

The oil film of the bearing was discretized into a number of elements in three directions ($\theta, y, and\ z$). It is well known that the accuracy of the numerical analysis is greatly influenced by the simulation's mesh quality. Hence, the shape and the number of elements are chosen according to a suitable convergence test. Independent mesh has been examined in the simulation analysis before beginning a case study to ensure response accuracy. At a journal speed of 5000 rpm, an eccentricity ratio of 0.7, and pure oil (oil with 0 wt% of nanoparticles), the study was carried out for a bearing. The maximum oil film pressure for such a bearing was tested for a different number of elements, and the results are presented in figure (3.3).

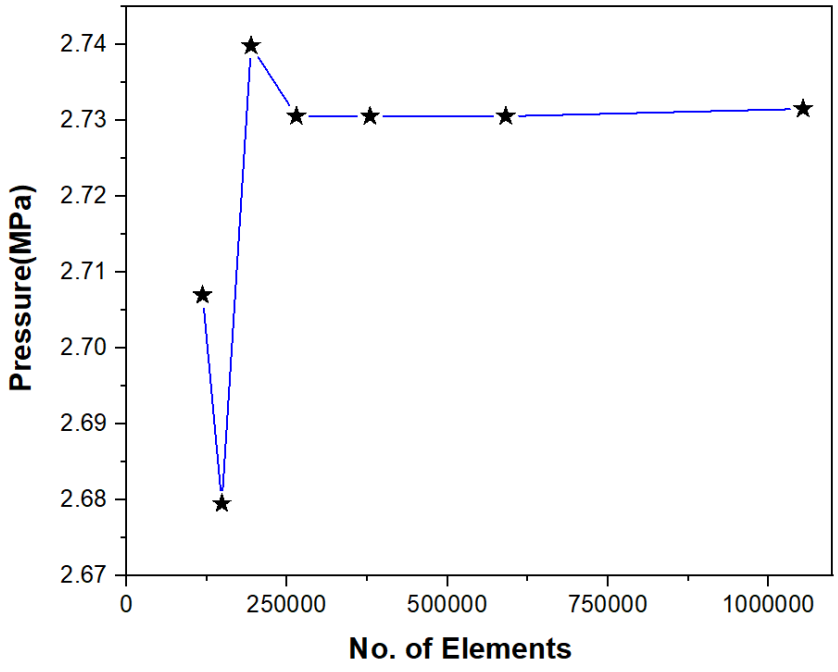

Fig(3.3) Grid Independences at N=5000 rpm,ε=0.7

This figure demonstrated that a stable solution is attained when the oil film is divided into three layers in a radial direction of bearing and mesh elements number 379200 (hexahedral) with an element size of 0.5 mm. Stable results with an aspect ratio of 17.083 have been obtained, which ensures good mesh quality.

3.8 CFD Model and Computational Procedure

A computational fluid dynamics (CFD) ANSYS FLUENT 19 program solved governing equations (continuity, Navier Stokes ,and energy), which required obtaining oil film pressure and temperature distributions. The fluid flow was considered Newtonian, laminar, moving on smooth and rigid bearing surfaces with coherent boundary conditions.

The governing equations have been solved at a steady-state condition and the inlet pressure was fixed as atmospheric pressure (101325 Pa). The bearing was assumed to be constructed of a stationary wall (for the bearing surface), rotating walls with an absolute rotational speed of the journal surface, and two sides of the bearing referred to as pressure outlets, as shown in figure (3.4). The two main inputs are eccentricity value and attitude angle, which provide the origin of the shaft's rotation necessary to define the shaft axis' location.

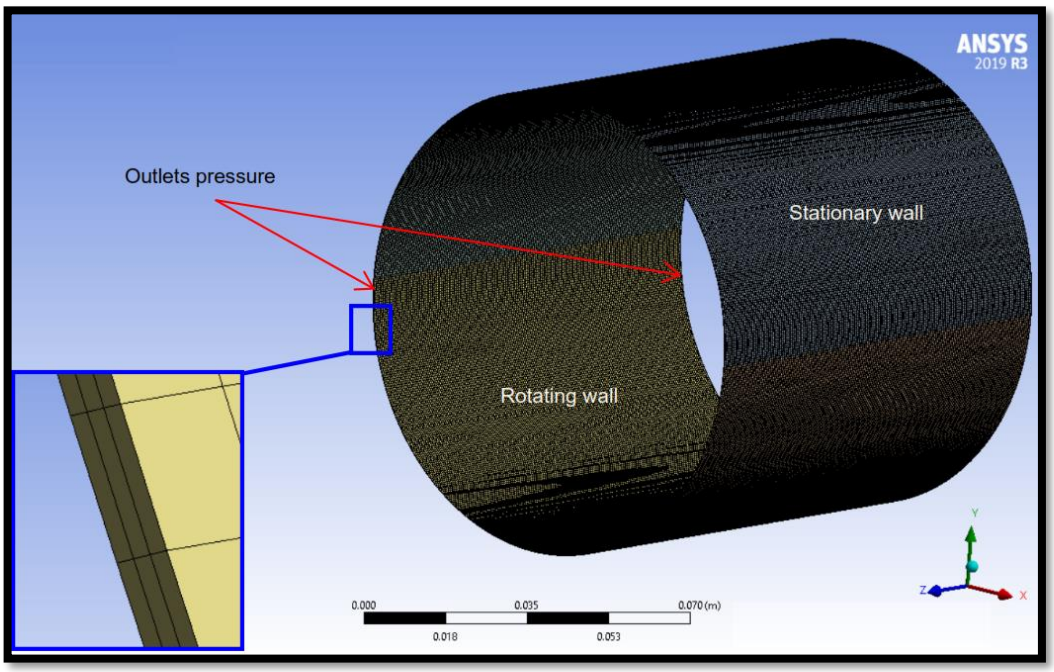

Fig(3.4) Grid and boundary of fluid domain

3.9 Solution Procedure

The present study uses computational fluid dynamics to achieve a thermo-hydrodynamic analysis of the circular and elliptical journal bearings. The main steps followed to obtain the CFD solution in this study are as follows:

1. The model with the specified dimensions of a journal bearing has been drawn by the design modeler geometry.
2. The model has been meshed to ensure the accuracy of the response during the simulation process.
3. Input variables are defined in the setup of fluid flow Fluent by using modeling sets.
4. The geometry of the bearing has been imported into the ANSYS Fluent software.
5. The FLUENT software is used to discretize the fluid film of the bearing into finite volume cells, and the bearing shell is discretized into finite elements.
6. The viscosity of base oil has been enhanced by adding nanoparticles to base oil, so the viscosity changed with temperature and was calculated by the modified Krieger-Dougherty equation, which is written in the C++ language in a user-defined function (UDF).
7. A steady-state solution is activated with double precision.
8. The boundary conditions used in this model have been mentioned in figure (3.4)
9. The energy equation is activated for thermo-hydrodynamics analysis (THD).
10. The velocity pressure coupling equation is solved using a SIMPLEC technique.

11. A first-order upwind method is applied to solve the energy and momentum equations, while the PRESTO (super-pressure option) is used to determine the pressure.
12. Flux reports definition is used to determine the mass flow rate over the pressure outlet from both ends of the bearing.
13. The surface report definition's custom field functions are used to determine the X-pressure force and Y-pressure force on the shaft.
14. All residual terms are given a convergence tolerance of 10 E-4 to enhance accuracy.

Chapter 4

Experimental Work

CHAPTER FOUR

EXPERIMENTAL WORK

This chapter describes the materials, experimental methods, and different instruments used in preparing and testing the morphological and physical properties of different nano-lubricants used in the present work.

4.1 Materials

TiO_2 and ZnO nanoparticles purchased from Sky-spring Nano-materials, Inc. were used in preparing the nano-lubricants. The physical properties of the nanoparticles are presented in table (4.1). The base oil used in the experiments of the present work is SAE 15W-40. The specifications of the base oil are presented in table (4.2) as labeled by the producer.

Table (4.1) Physical characteristics of nanoparticles

Nanoparticles	**TiO_2**	**ZnO**
Color	White	White to light yellow
Form	Powder	Powder
Average particle size(APS)	30 nm	30 nm
Purity	99.50%	99.80%
Morphology	Spherical	Nearly spherical
C_P(J/kg. K)	690	544
K(W/m. K)	8.3	19
ρ (Kg/m^3)	4230	5606

Table (4.2) Characteristics of base oil

Base Oil	**Physical properties**	**Value**	**Unit**
SAE 15W-40	Viscosity @ 40 ºC.	113	mm^2/s
	Viscosity @ 100 ºC.	15	mm^2/s
	Density	877	Kg/m^3
	Viscosity Index	137	
	Pour Point	-45	ºC
	Flash Point	232	ºC

4.2 Experimental Method

The experimental method of the current study involves the following steps:

1. Surface Morphology and Structure Characterization of Nanoparticles
2. Preparation of Nano lubricants
3. Viscosity Measurement Test
4. Particle Size Analysis Test

4.2.1 Surface Morphology and Structure Characterizations of Nanoparticles

The structural and morphological properties of the nanoparticles used in the current study are implemented by SEM and XRD.

4.2.1.1 Scanning Electron Microscopy (SEM)

An SEM device type (TESCAN) shown in figure (4.1) is used to define the morphological properties of the nanoparticles used in the present experimental work.

Fig(4.1) Scanning electron microscopy

The morphology of these nanoparticles (composition, size, and shape) can be revealed by focusing an electron beam with high energy on the surface of a specimen to generate signals and these signals give us information about morphology.

4.2.1.2 X-Ray Diffraction (XRD)

The XRD test is one of the techniques extensively used for the classification of nanoparticles. This test was used to determine the crystalline grain size of TiO_2 and ZnO nanoparticles, lattice parameters, and crystalline structure of the phases. It has been implemented by using the XRD Lab 6000 Shimadzu type, as shown in figure (4.2) in the XRD lab at the College of Material Engineering, University of Babylon. The diffraction patterns resulting from the waves of electromagnetic radiation reflecting from a regular array of scatters may be compared with the reference JCPDS card database.

Fig(4.2) X-Ray Diffraction device

4.2.2 Preparation of Nano lubricants

In the current work, a two-step process is used to produce nano-lubricants. ZnO and TiO_2 nanoparticles are mixed with SAE 15W-40 base oil as shown in figure (4.3) at concentrations of 0.5, 1, and 2 wt% at the Material engineering college/polymeric materials lab, University of Babylon.

A digital weighing scale, as shown in figure (4.4) with a resolution of 1 mg is used for weighing the required quantity of the nanoparticles. The TiO_2 and ZnO nanopowder are dispersed in the pure oil using the magnetic stirrer as shown in figure (4.5) for 1 hour and then subjected to ultrasonic homogenization type (MTI) as shown in figure (4.6) with 40 kHz for 15 minutes to break down the expected agglomerated nanoparticles. Both processes have been done at room temperature and under laboratory environmental conditions.

Oleic acid, shown in figure (4.7) is utilized as a surfactant to make sure that the nanoparticles are homogeneously distributed in pure oil due to the physical adsorption of the surfactant in the solution through electrostatic repelling forces between the particles and hydrophobic surface forces. It was recommended by many researchers in this field, such as **Gundarneeya and Vakharia, (2021)**. Figures (4.8) and (4.9) show the prepared samples of the nano-lubricants with the nanoparticle concentrations mentioned above.

Fig(4.3) Base oil

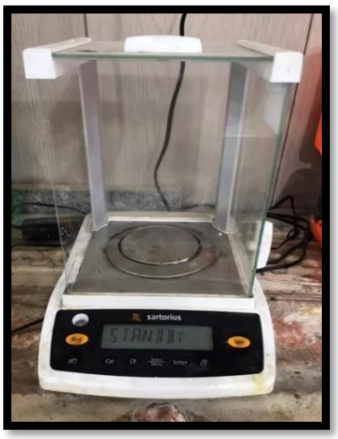

Fig(4.4) Digital Balance

Fig(4.5) Magnetic stirrer

Fig(4.6) Ultrasonic homogenizer

Fig(4.7) Oleic Acid

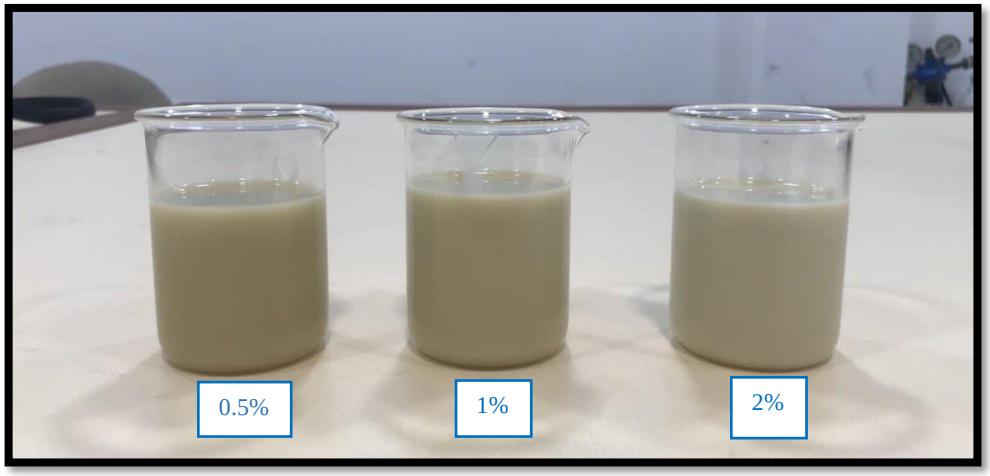

Fig(4.8) Samples of TiO_2 nano lubricants

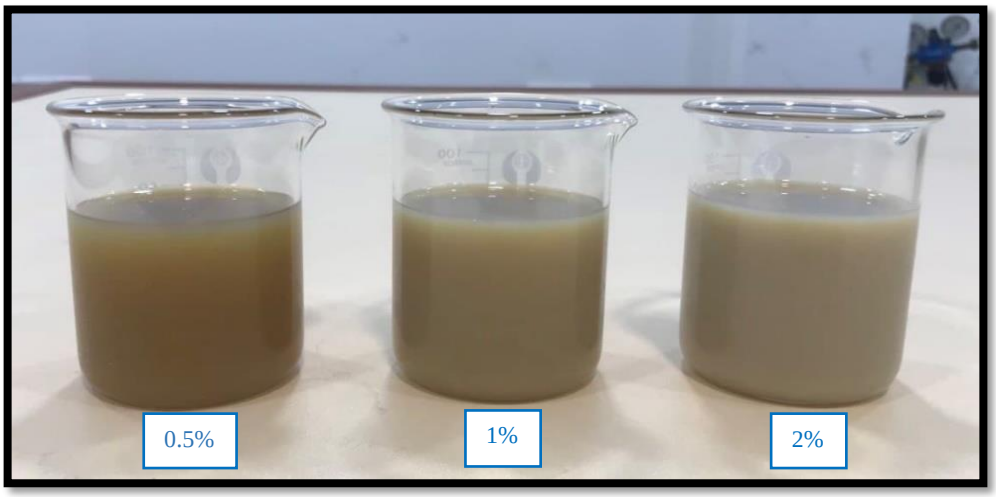

Fig(4.9) Samples of ZnO nano lubricants

4.2.3 Viscosity Measurement Test

Viscosity measurement for each nano-lubricant sample is performed using a rotational Brookfield Rheometer as shown in Figure (4.10). The tests have been implemented at the Material engineering college/polymeric materials lab, University of Babylon.

Fig(4.10) Brookfield DV-III+ Viscometer

The viscosity of nano-lubricant samples with different ZnO and TiO_2 nanoparticle concentrations is calculated at varying temperatures (10 °C to 50 °C) by using a suitably controlled hot water bath. All tests are carried out at a shear rate of 10 s^{-1} by using the spindle CP-41. The volume of each test sample is 1 mL and the test sample's temperature is monitored by a sensor temperature placed into a bath of water.

4.2.4 Particle Size Analysis Test

The dispersion of nanoparticles has been analyzed by using dynamic light scattering (DLS) type Brookhaven 90 Plus at Nano Center, University of technology as shown in figure (4.11). The aggregate size of nanoparticles in terms of the Z-average value is calculated, which is important to evaluate the agglomerated nanoparticles required in evaluating the nano-lubricant viscosities using the Krieger-Dougherty viscosity model.

Fig(4.11) Particle Size Analyzer

Chapter 5

Results and Discussion

CHAPTER FIVE

RESULTS AND DISCUSSION

In this chapter, the results obtained from the experimental work and solution of CFD models for circular as well as elliptical journal bearings will be presented and discussed extensively. The effect of different parameters, such as ellipticity ratio, journal speed, eccentricity ratio, and the percentage by weight of the nanoparticles on the static behavior of such bearings, has been extensively studied. A validation study has been implemented to confirm the suitability of the mathematical models used in this work.

5.1 Experimental Results

5.1.1 Scanning Electron Microscopy (SEM)

The shape of ZnO nanoparticles is nearly spherical with a maximum average size of 66.22 nm, as shown in figure (5.1), While figure (5.2) shows that the shape of TiO_2 nanoparticles is spherical in crystallographic structure with a maximum average diameter of 91.3 nm.

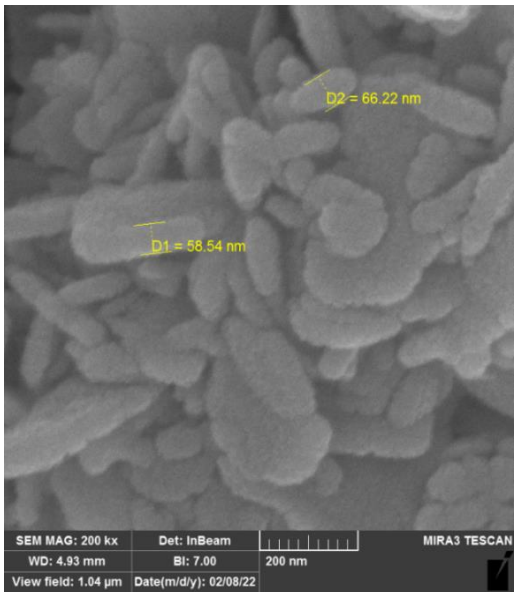

Fig(5.1) SEM images of ZnO

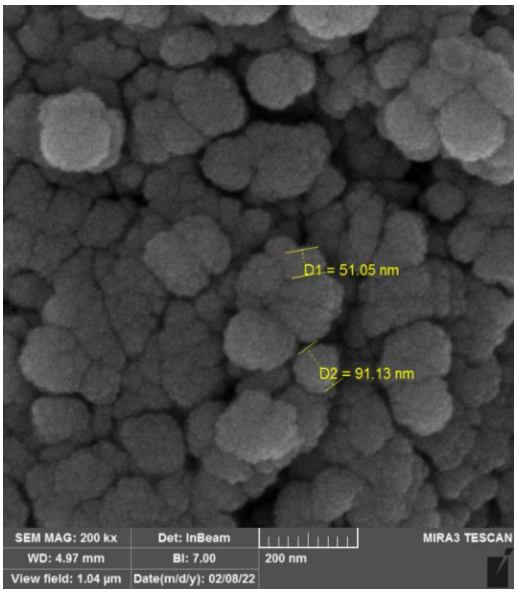

Fig(5.2) SEM images of TiO_2

However, the average sizes of both types of nanoparticles are less than 100 nm, which confirms the nanoscale dimension of such particles. The higher averaged sizes measured for both nanoparticles are due to the agglomeration of particles that are received as a powder.

5.1.2 X-Ray Diffraction (XRD)

The obtained XRD spectrum of ZnO nanoparticles is shown in figure (5.3). It was recorded in a range of 2θ (30°–70°), with peak diffraction at 2θ = 31.8°,34.5°,36.4°,47.7°,56.7°,62.9°,66.8°,68.3°, and 69.1°, corresponding to planes (100), (002), (101), (102), (110), (103), (200), (112), and (201).This pattern was compared with the standard diffraction spectrum, and it was found that all peaks were in good agreement with (JCPDS card numbers 36–1451) from the standard card **Chen et al. (2008)**, This is related to the hexagonal structure of several crystal planes in ZnO nanoparticles.

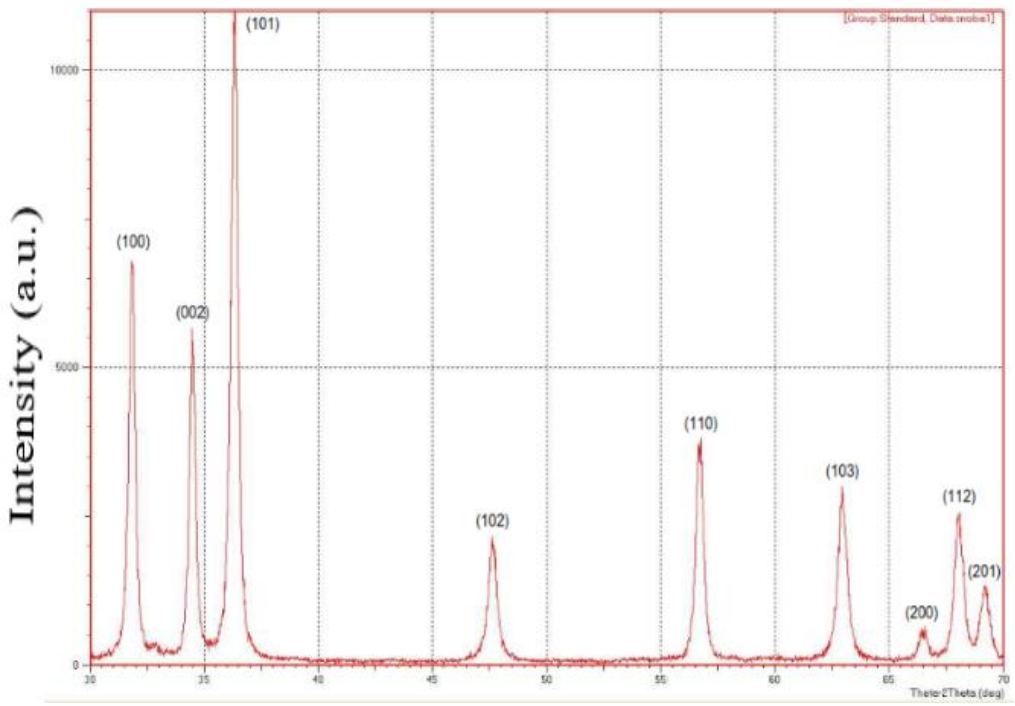

Fig(5.3) XRD patterns of ZnO nanoparticles

Figure (5.4) shows the X-ray diffraction of TiO_2 nanoparticles. It was recorded in the range of 2θ (20°–60°), with diffraction peaks at 2θ = 25.2°, 36.9°, 48°, 55°, and 62° corresponding to the planes (101), (004), (200), (105), and (211), which indicate spherical structure. It was observed that all peaks are in good agreement with (JCPDS card numbers 84-1286) from the standard card **Thamaphat et al. (2008).**

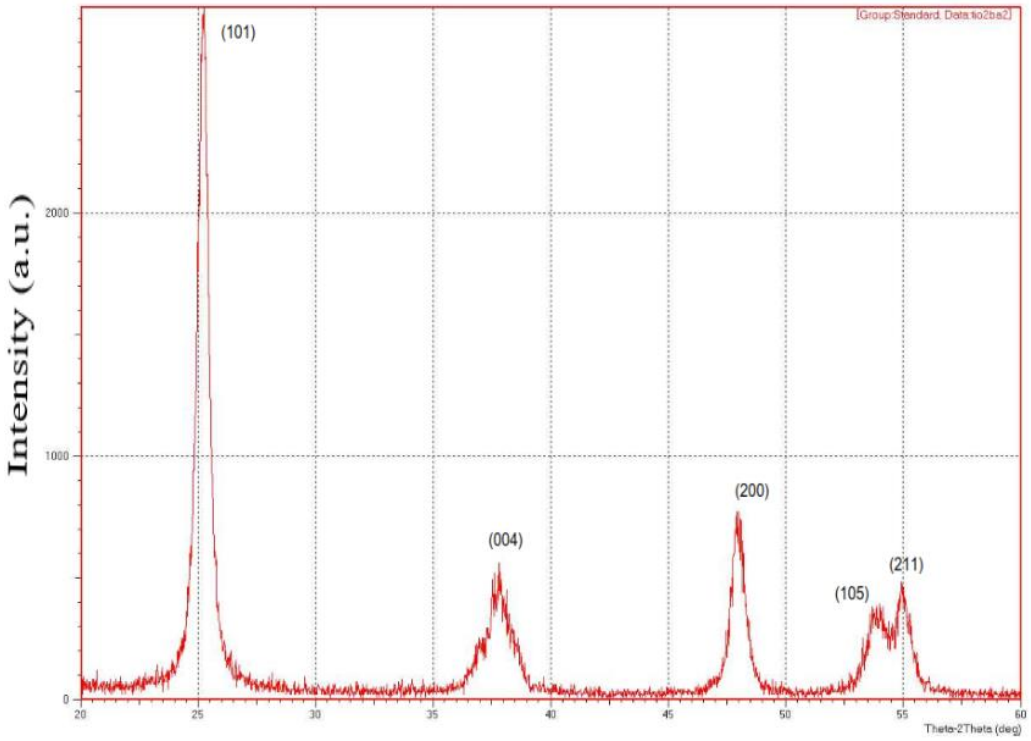

Fig(5.4) XRD patterns of TiO_2 nanoparticles

5.1.3 Viscosity Measurement

Figures (5.5) and (5.6) show viscosity variation with temperature for ZnO and TiO_2 nano-lubricants containing different weight concentrations of the nanoparticles. These figures pointed out that the nano-lubricant viscosity drops at high temperatures due to a reduction in the intermolecular cohesive force of such lubricants at higher temperatures.

However, these figures also show that the nano-lubricant viscosities increased for the lubricant with a higher weight percentage of the

nanoparticles in comparison with that of pure oil. This is due to the fact that nanoparticle concentration increases internal shear stress between layers of oil film. This is identical to the results reported by **Sepyani et al. (2017).**

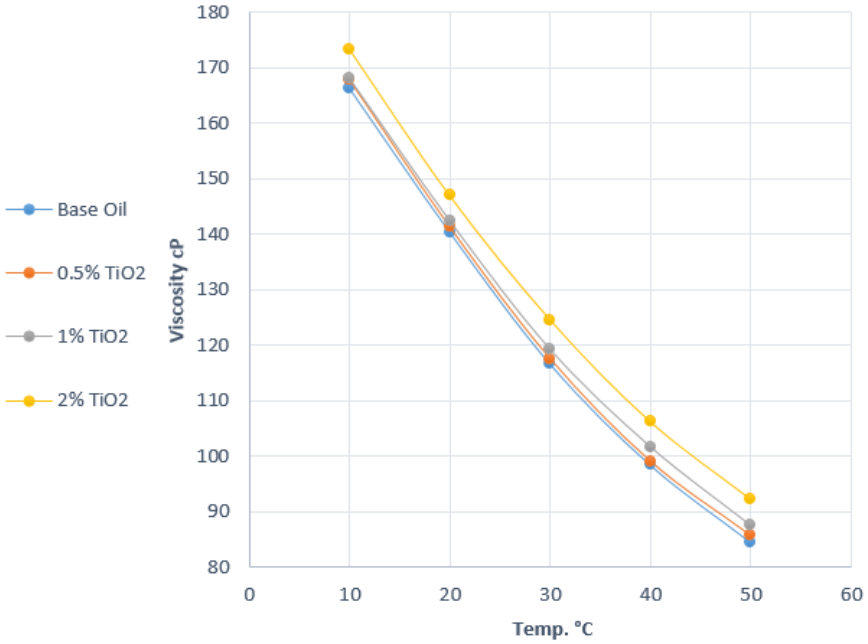

Fig(5.5) Viscosity Variation as a function of temperature for TiO_2

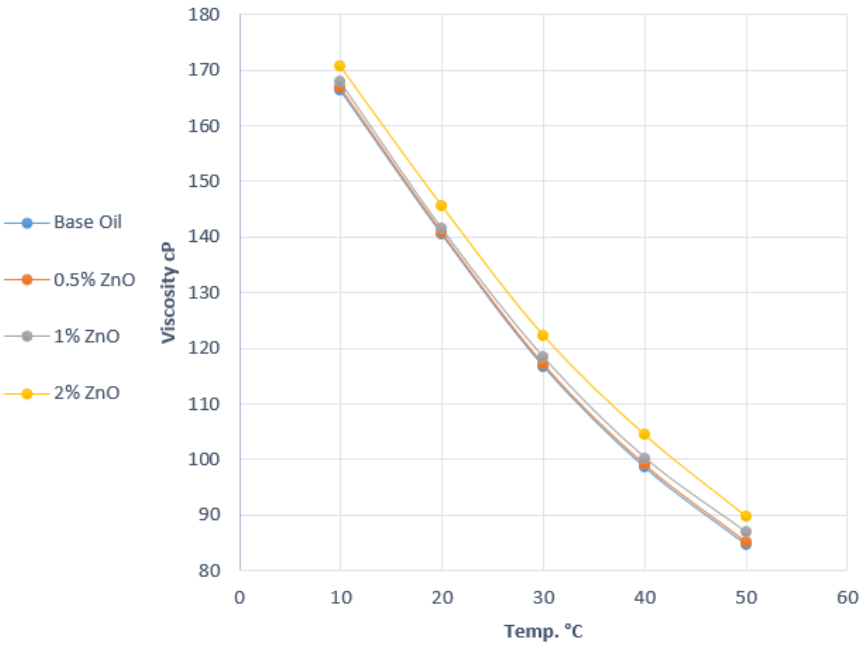

Fig(5.6) Viscosity Variation as a function of temperature for ZnO

5.1.4 Particle Size Analysis

Figure (5.7) shows the particle size distribution resulting from the DLS test for TiO_2 and ZnO nanoparticles. The effective diameters of the nano-particles aggregate have been calculated and found to be 63 nm and 72 nm respectively, which are greater than the previously described main diameters of each particle (30 nm for ZnO and TiO_2). The aggregate ratio for the nanoparticles of TiO_2 and ZnO nano-lubricats has been calculated and found to be 2.4 and 2.1 respectively. This is the effect of strong forces of Van der Wall, which resulted in a small aggregation of nanoparticles at base oil. All readings are recorded at an ambient temperature of 25 °C.

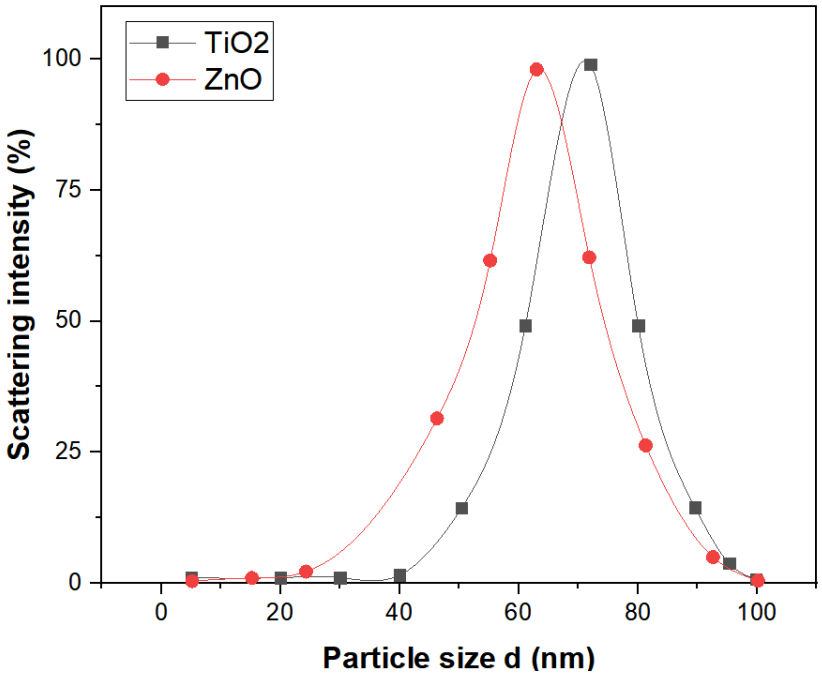

Fig(5.7) Nanoparticle size distribution

Figure (5.8) illustrates a comparison between experimentally measured nano-lubricant viscosity and the Krieger-Dougherty model's result. This figure shows that the modified Krieger-Dougherty viscosity model predicts viscosities that closely match experimentally measured viscosities.

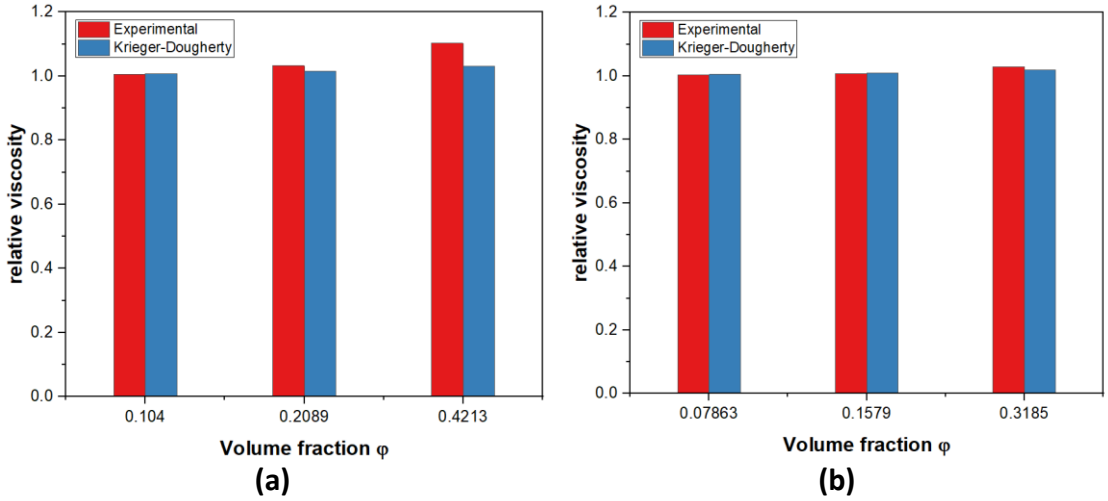

Fig(5.8) Comparison of experimentally measured viscosity with that obtained using Krieger-Dougherty (a) TiO_2 Nano-lubricant, (b) ZnO Nano-lubricant

5.2 Validation Study

Different case studies have been implemented for circular and elliptical journal bearings lubricated with both pure and nano-lubricants. The obtained results from these cases are compared with those published by other authors to validate the CFD model of the current study, as follows:

5.2.1 Circular Journal Bearing

A circular journal bearing with different geometrical properties proposed by different workers has been used to validate the CFD model of such a bearing operated with nano and without nano additives.

Figures (5.9) and (5.10) show the circumferential thermal pressure and temperature distribution in the present work and that obtained by **Ferron et al. (1983)**. The investigation was carried out for a circular journal bearing working at an eccentricity ratio of 0.5 with a journal speed of 4000 rpm lubricated with pure oil and an inlet pressure of 70,000 Pa. These figures show that the results were well validated, with a maximum deviation that does not exceed 4% and 1% for pressure and temperature, respectively.

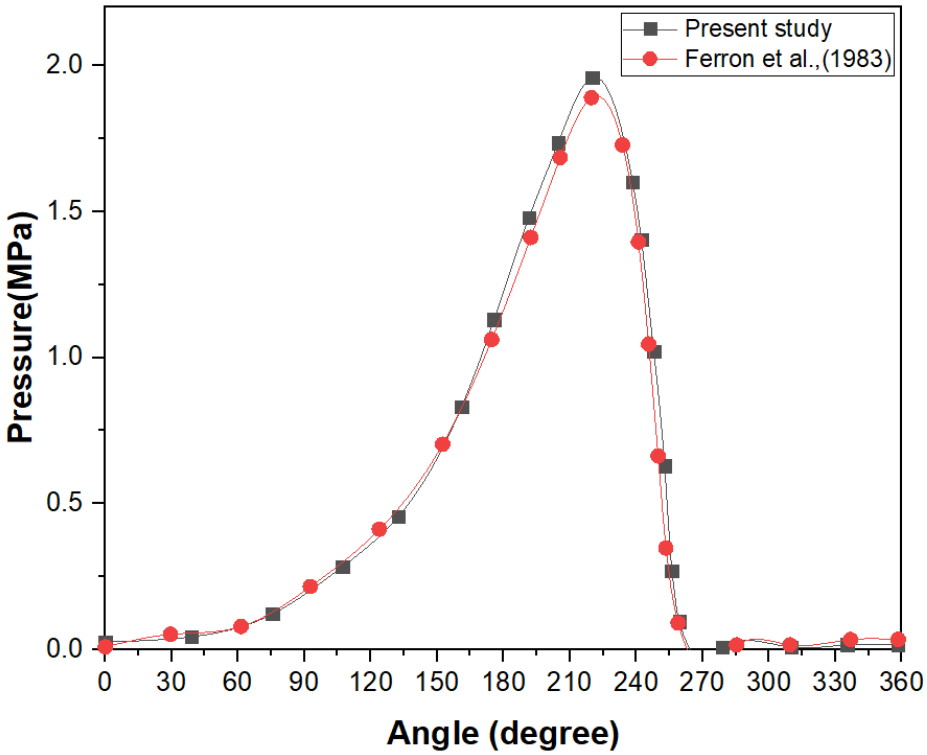

Fig (5.9) Validation of oil film pressure between present work and obtained by **Ferron et al. (1983)**

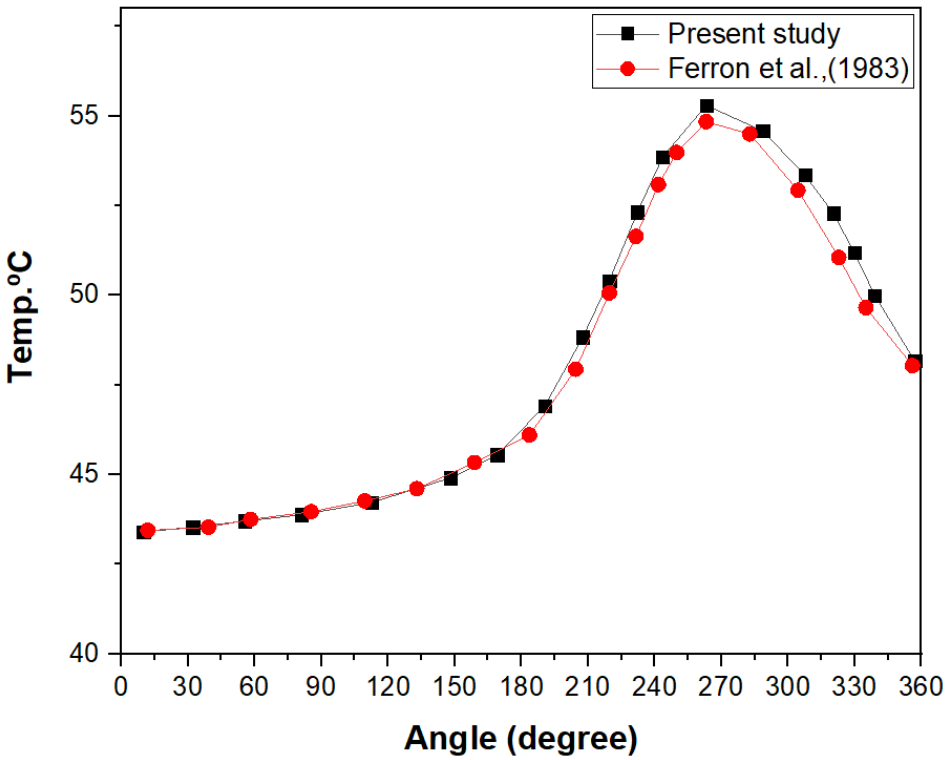

Fig (5.10) Validation of oil film temperature between present work and obtained by **Ferron et al. (1983)**

Figures (5.11) and (5.12) show the oil film pressure and temperature distributions for a bearing operating at a journal speed of 3000 rpm with an eccentricity ratio of 0.8 and an inlet pressure of 0.2 MPa. The obtained results clearly show a good agreement with those obtained by **Li et al. (2019)** with a maximum deviation of 3.92% and 0.82% for pressure and temperature, respectively.

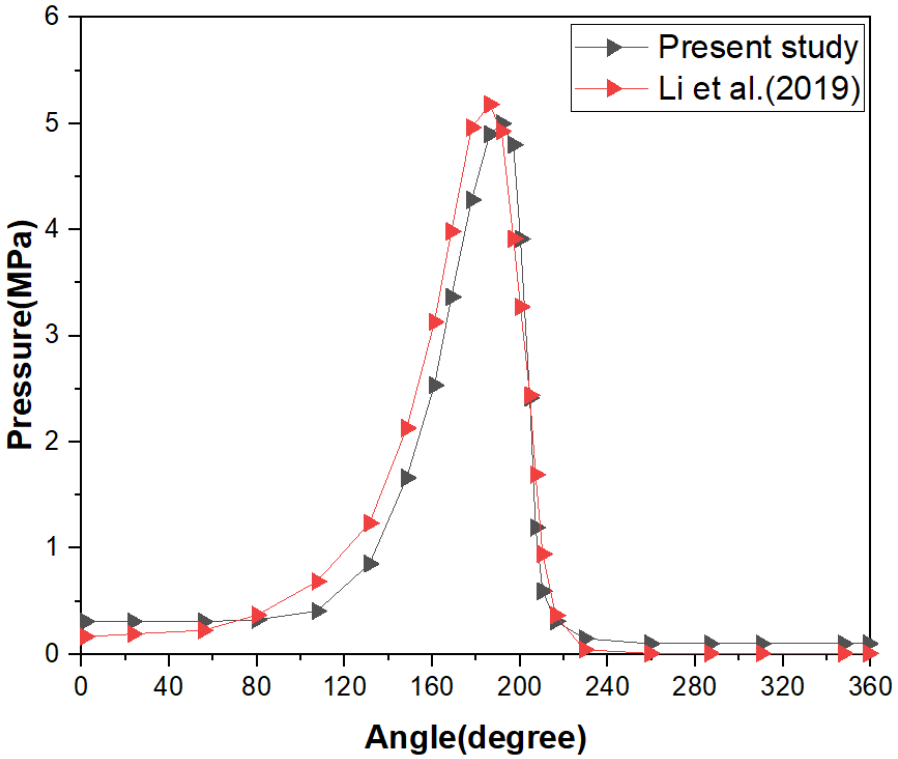

Fig(5.11) Comparison of oil film pressure between the present study and obtained by **Li et al. (2019)**

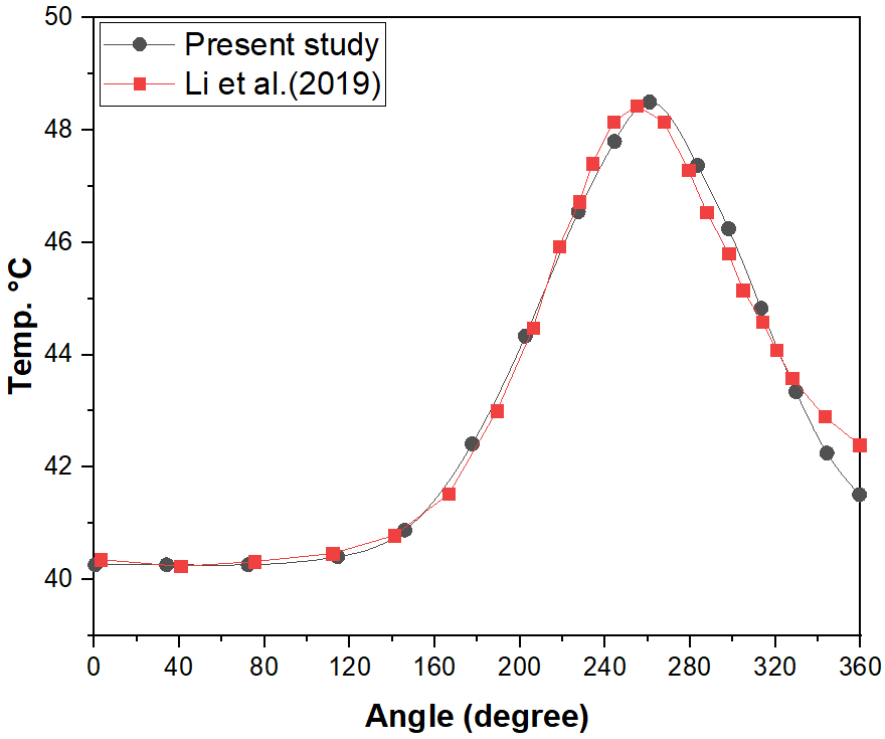

Fig(5.12) Comparison of the oil film temperature between the present study and obtained by **Li et al. (2019)**

Figures 5.13(a-b) show the pressure distribution obtained in this study and that determined by **Dang et al. (2021)** for a bearing lubricated with a base oil (AW68) blended with different weight concentrations of TiO_2 at an eccentricity ratio of 0.6 and 2000 RPM. The results obtained show a good agreement with a maximum deviation of 3.59%, 4.24%, 5.36%, and 5.42% for bearings lubricated with pure oil, 0.5%, 1%, and 2 wt% of TiO_2, respectively.

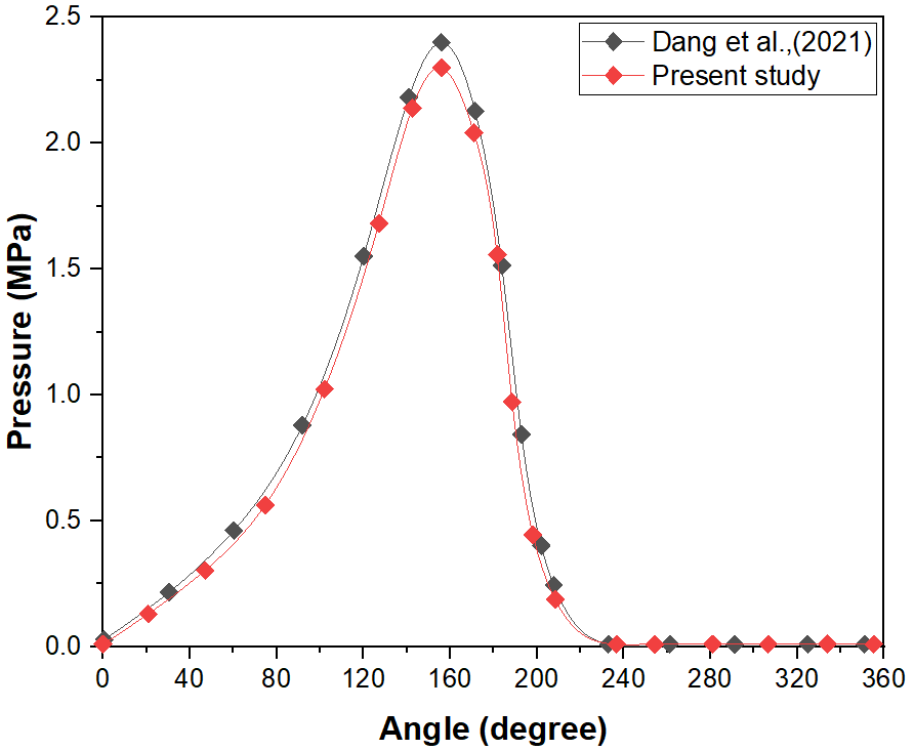

(a)

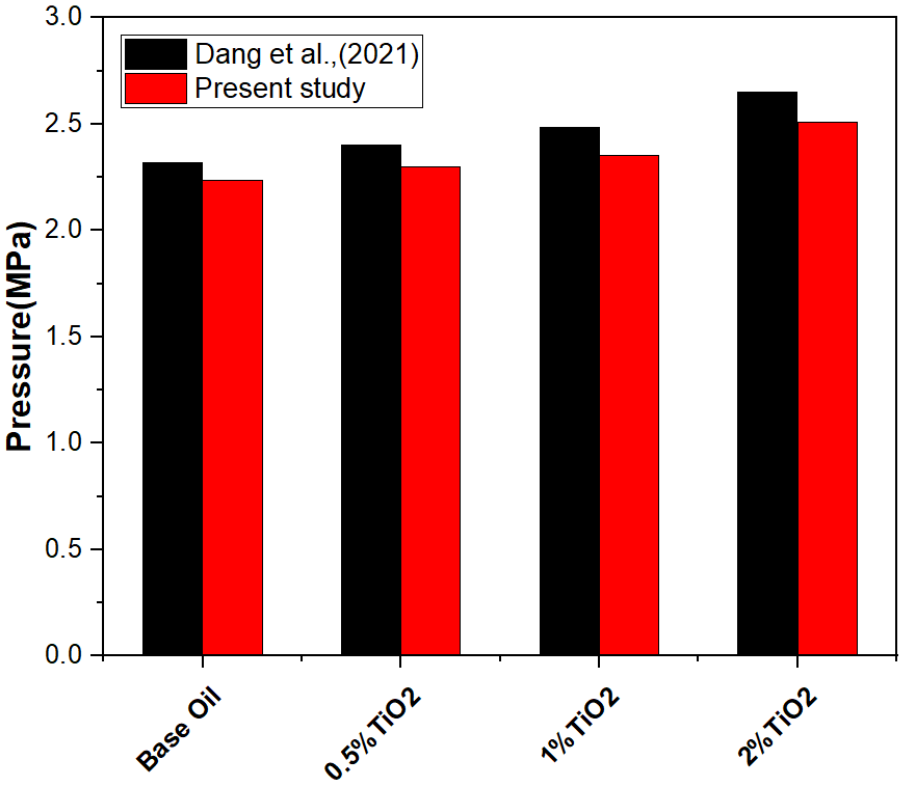

(b)

Fig(5.13) Verification of the present work results with that obtained by **Dang et al. (2021)** (a)Oil film pressure (b) maximum oil film pressure

5.2.2 Elliptical Journal Bearing

Figures 5.14(a-b) illustrate a good agreement between the pressure distribution obtained in the present work and that obtained by **Dang et al. (2020)** for an elliptical journal bearing lubricated with a pure oil (AW32) mixed with various weight concentrations of TiO_2. The bearing works at a rotational speed of 5000 RPM with eccentricity and ellipticity ratios of 0.7 and 0.5, respectively. It has been found that the maximum deviation of the pressure distribution for a bearing lubricated with pure oil was 1.03%, while it became 2.7%, 1.17%, and 2.02% for the maximum pressure of the bearing lubricated with 0.5% TiO_2, 1% TiO_2, and 2 wt% of TiO_2, respectively.

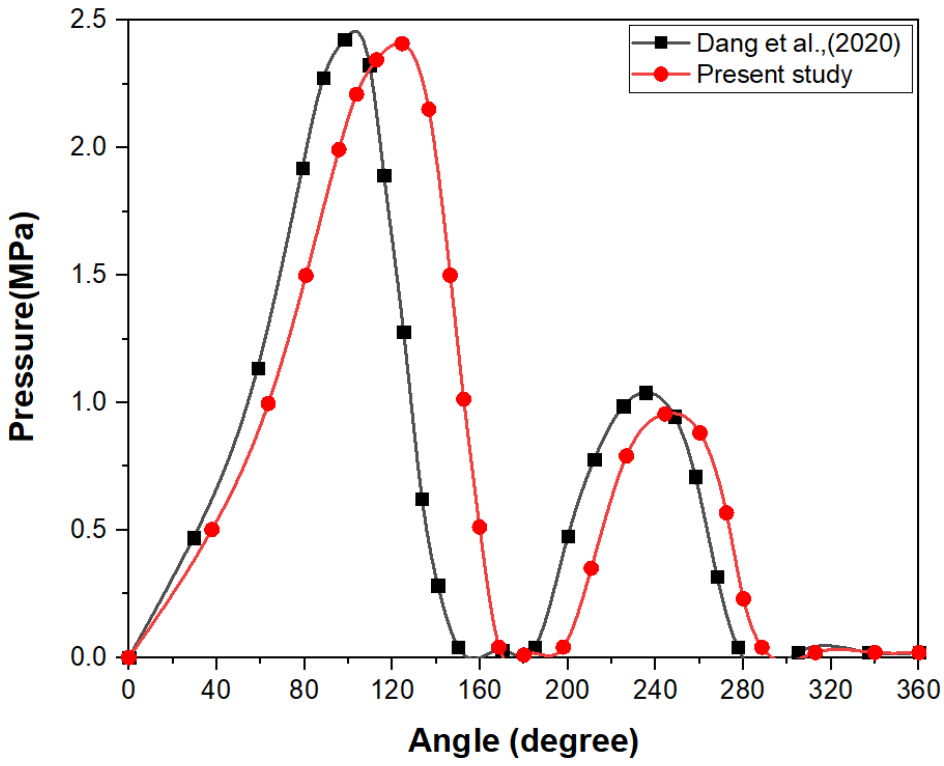

(a)

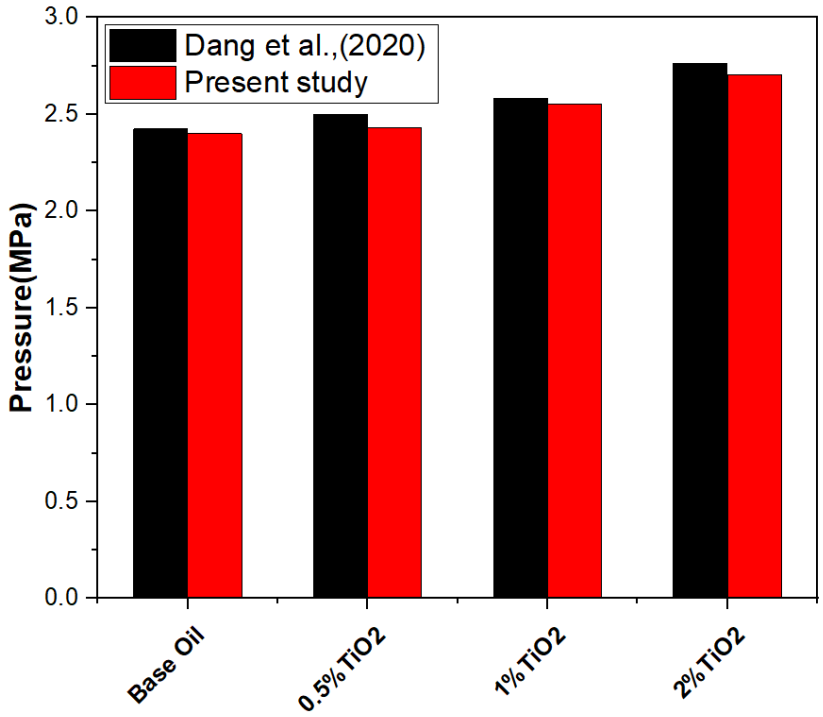

(b)

Fig(5.14) Verification of the present work results with that obtained by **Dang et al. (2020)**(a) Oil film pressure at pure oil (b) maximum oil film pressure

Figures 5.15(a-b) illustrate a good agreement between oil film pressure and temperature distributions for an elliptical bearing that has an ellipticity ratio of 0.5 operating with pure oil at an inlet pressure of 0.1 MPa and a journal speed of 3000 RPM, compared with that obtained by **Wang et al. (2021). A** good agreement between the results has been noticed with a maximum deviation of 1.38% and 1.47% for pressure and temperature, respectively.

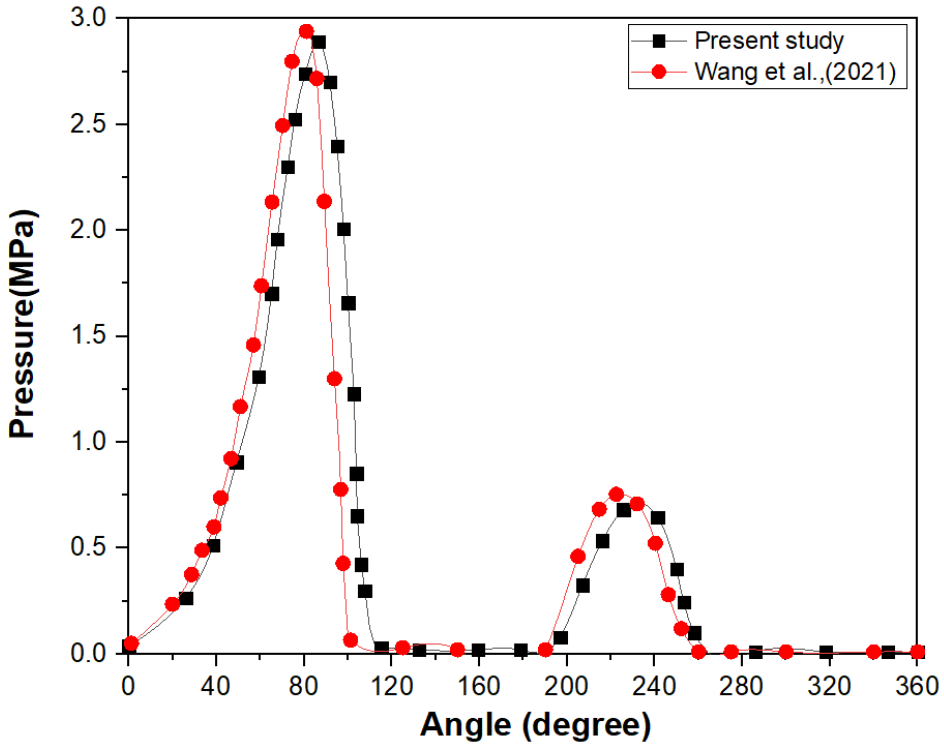

(a)

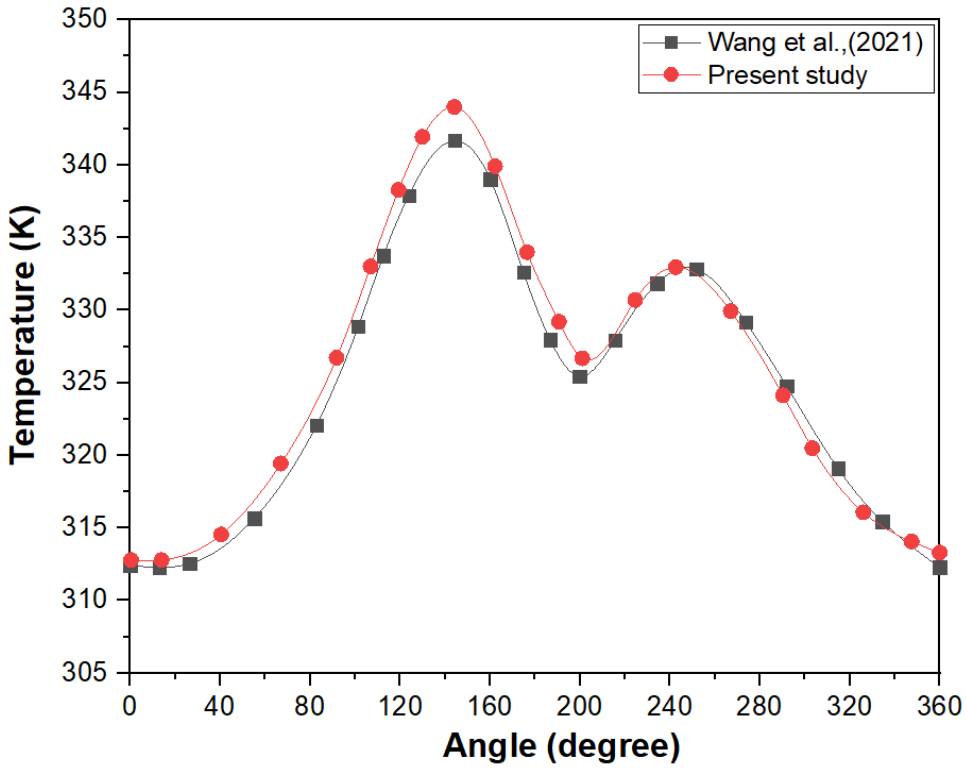

(b)

Fig (5.15) Verification of the results obtained in the present work and obtained by **Wang et al. (2021)**(a) pressure distribution (b) Oil film temperature for EJB

It can be concluded from the above verification study that CFD models constructed to analyze the performance of circular and elliptical journal bearings lubricated with pure and nano-lubricants can be used with high confidence levels.

5.3 Performance of Elliptical Journal Bearing (EJB)

An elliptical journal bearing is a non-circular journal bearing characterized by a lower oil film temperature and vibration at higher journal speeds in comparison with a conventional circular journal bearing. The most important parameters affecting the performance of elliptical journal bearings lubricated with nano-lubricants based on TiO_2 and ZnO will be presented and discussed. The lubricant was assumed Newtonian in laminar flow on smooth bearing surfaces with the viscosity as a function of temperature and nanoparticles concentration. The effects of the ellipticity ratio, speed of journal, nanoparticle concentrations, and eccentricity ratios on the performance of such bearings are considered as follows:

5.3.1 Effect of Ellipticity Ratio (E_p)

An extensive study of the effect of ellipticity ratio on the main performance parameters of EJB will be illustrated. For this purpose, the bearing eccentricity ratio and the journal speed were fixed at 0.7 and 5000 rpm, respectively.

Figure (5.16) shows the circumferential variation film thickness of EJB with the ellipticity ratio for bearing lubricated with pure oil. It can be seen from this figure that oil film thickness increases for the bearing with higher ellipticity ratios. It can also be seen that the oil film thickness at the upper lobe of the bearing is higher than that in the lower lobe due to the increase value of the horizontal clearance and the smaller vertical clearance of such

a bearing, as reported by **Mishra (2007)**. This behavior will affect the performance characteristics of the elliptical bearing, as can be shown later.

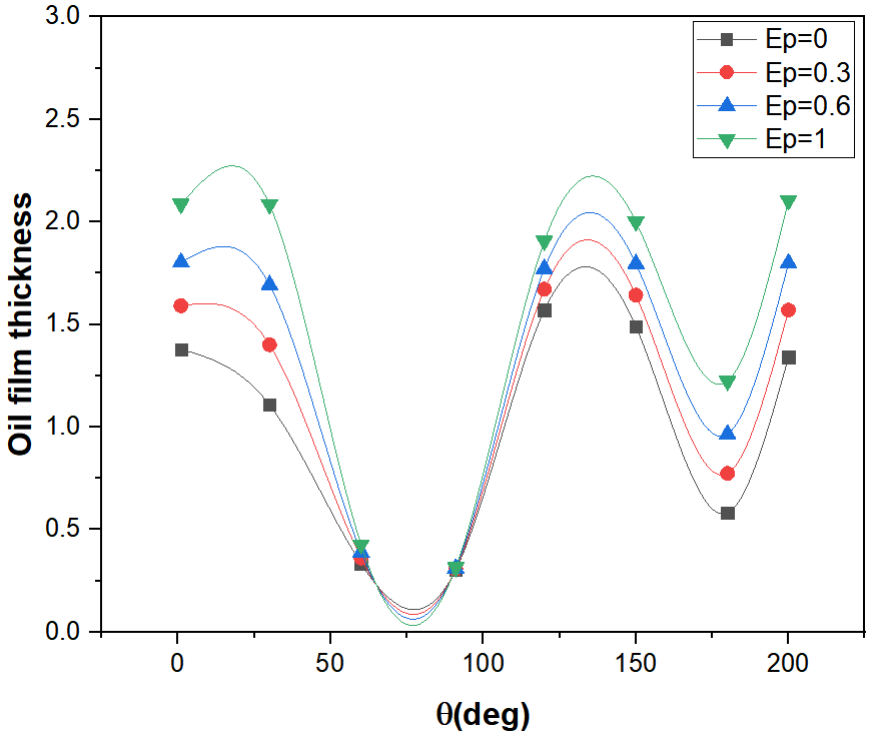

Fig(5.16) Effect of ellipticity ratio on the oil film thickness of EJB

Figure (5.17) shows the effect of the ellipticity ratio on the thermal circumferential oil film pressure of an elliptical journal bearing lubricated with pure oil. This figure also shows that the oil film pressure of bearing decreased with higher ellipticity ratios. This can be attributed to the increase in oil film thickness with increasing ellipticity ratios discussed above. It can also be seen from this figure that the pressure on the lower lobe of the bearing increases as the ellipticity ratio increases until it becomes 0.35 MPa for the bearing operating with an E_p=1 due to the decrease in the vertical clearance of the bearing.

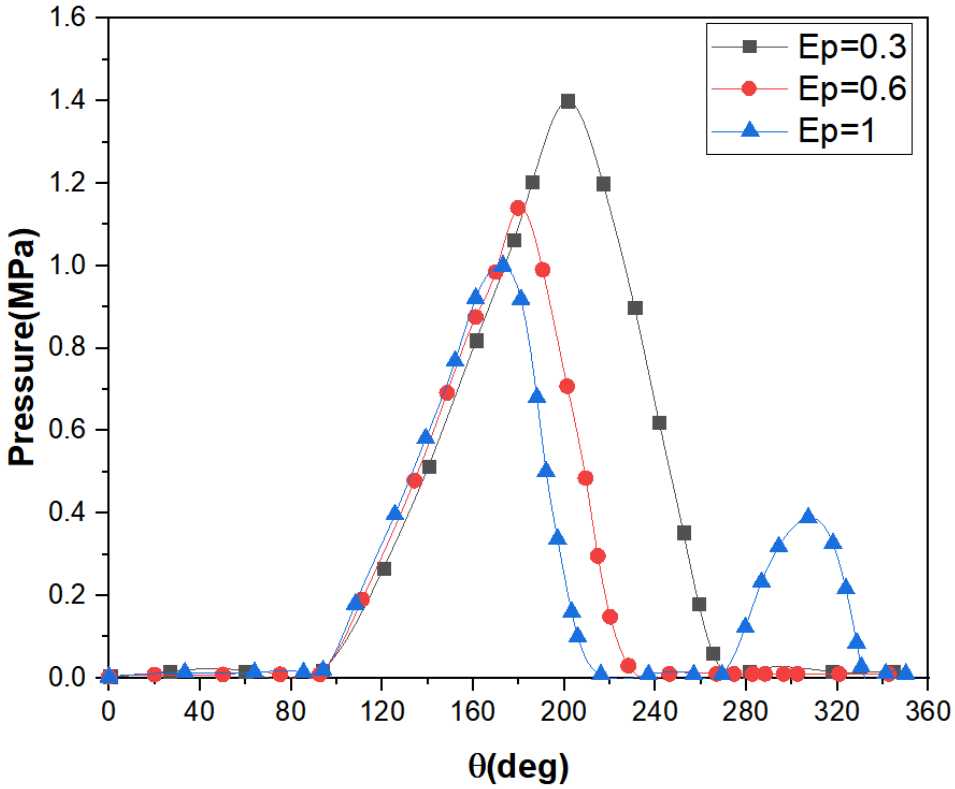

Fig(5.17) Effect of ellipticity ratio on the oil film pressure of EJB

Figures 5.18(a-c) show that the oil film pressure moves toward the inlet of the bearing as the ellipticity ratio increases, as can be shown from the movement of the red color contour.

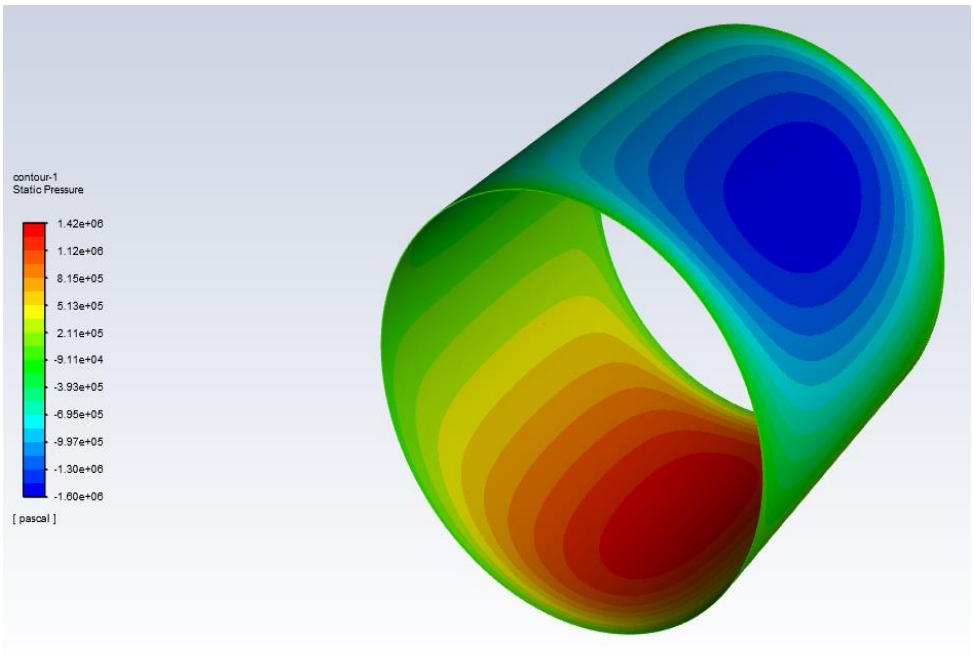

(a)

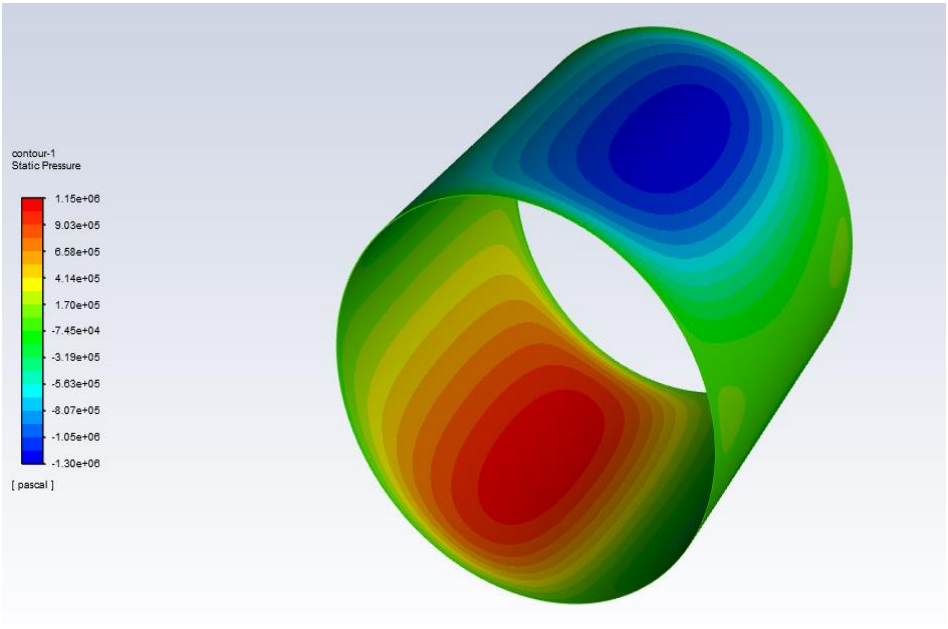

(b)

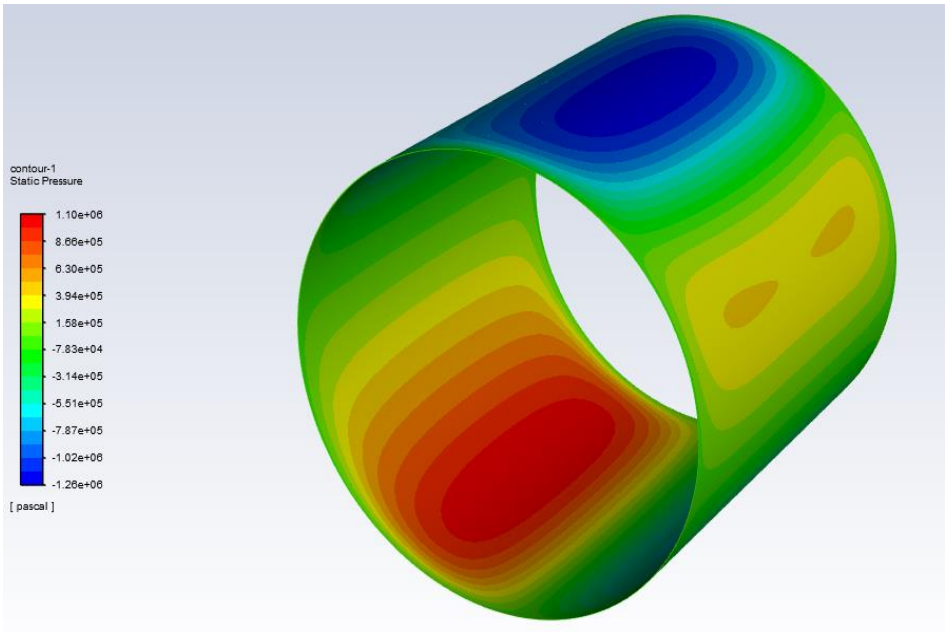

(c)

Fig(5.18) Pressure contours of EJB with different ellipticity ratios (a) E_p=0.3, (b) E_p=0.6, (c) E_p=1

Figure (5.19) shows variations of oil film temperature with ellipticity ratio for an elliptical bearing lubricated with pure oil. This figure shows that the oil film temperature decreased for a bearing with an increase in ellipticity ratio due to an increase in oil film thickness, which causes a decrease in the shear rate of the oil film and hence a decrease in induced friction force at the bearing surface, which is the main cause of decreasing the oil film temperature.

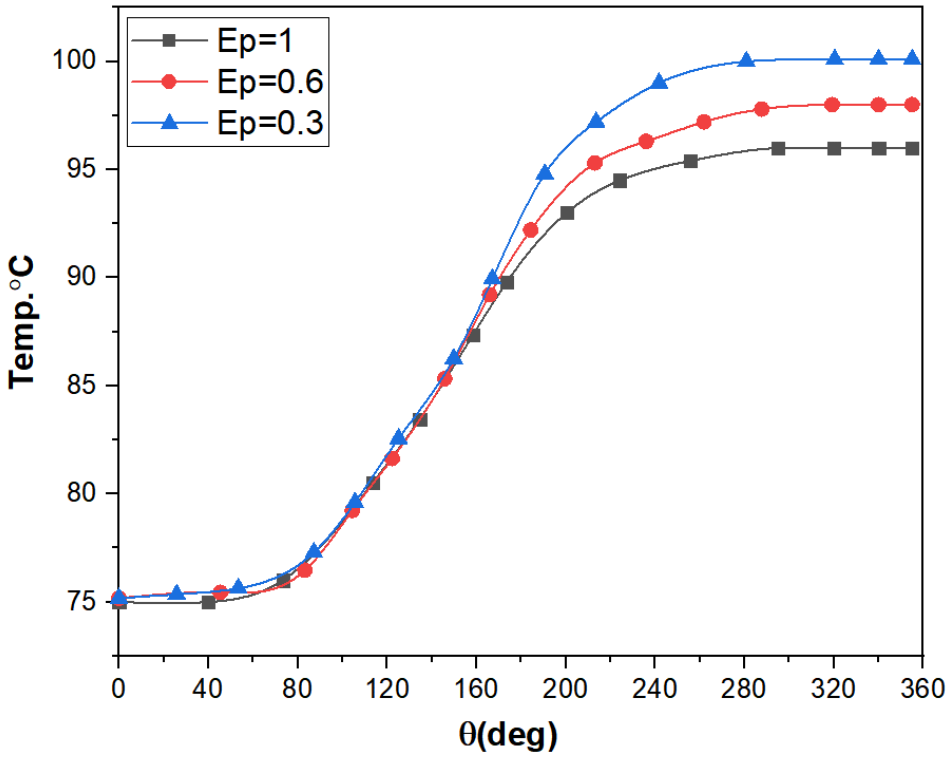

Fig(5.19) Effect of ellipticity ratio on the oil film temperature of EJB

Figure (5.20) shows the combined effect of TiO_2 and ZnO nanoparticle concentration and ellipticity ratio on the maximum oil film pressure generated in an elliptical journal bearing. This figure depicts that the maximum oil film pressure increases when the bearing is lubricated with nano-lubricant and the increase becomes higher as more nanoparticles of TiO_2 and ZnO are blended with the base oil. This can be explained by the increase in oil viscosity due to the addition of nanoparticles of such materials to the base oil. However, maximum oil film pressure decreases for elliptical

journal bearings with a higher ellipticity ratio due to an increase in the gap between the bearing and journal surfaces (higher oil film thickness). It is commonly known that changes in the oil film thickness have a significant effect on the oil film pressure.

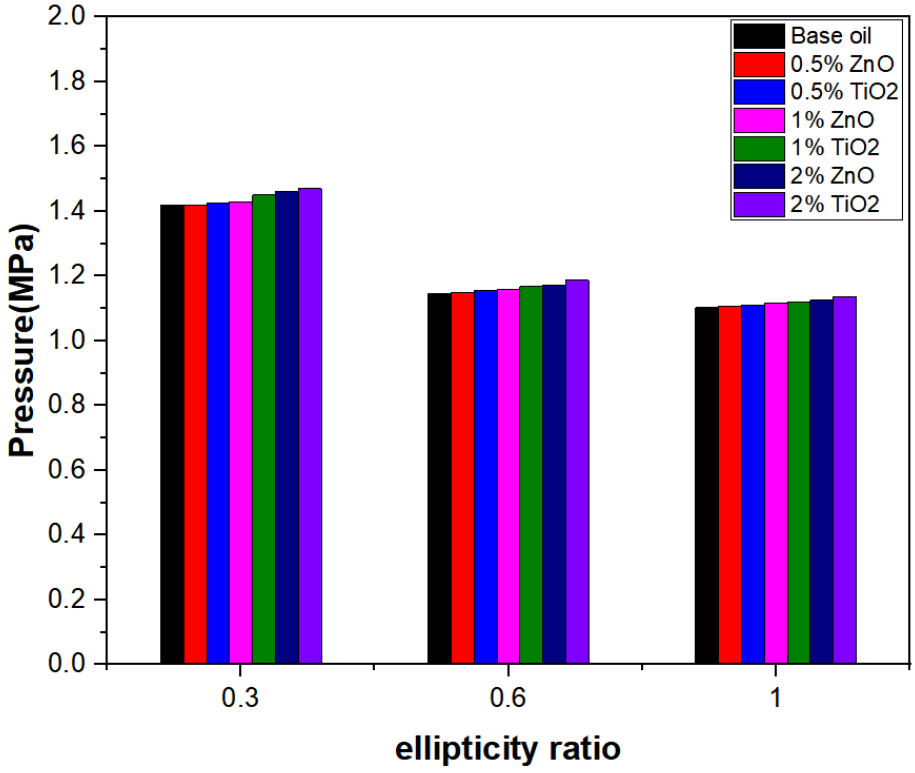

Fig(5.20) Effect of weight concentration and ellipticity ratio on the maximum oil film pressure

Figure (5.21) illustrates both effects of ellipticity ratios and weight concentrations of nano additives on the maximum temperature of the oil film for EJB. This figure recognized that maximum oil film temperature decreases for the bearing with higher ellipticity ratios. This can be attributed to the low shear rate of the oil due to the increase in the oil film. This figure also shows that the addition of the nanoparticles to base oil has a slight effect on the maximum oil film temperature.

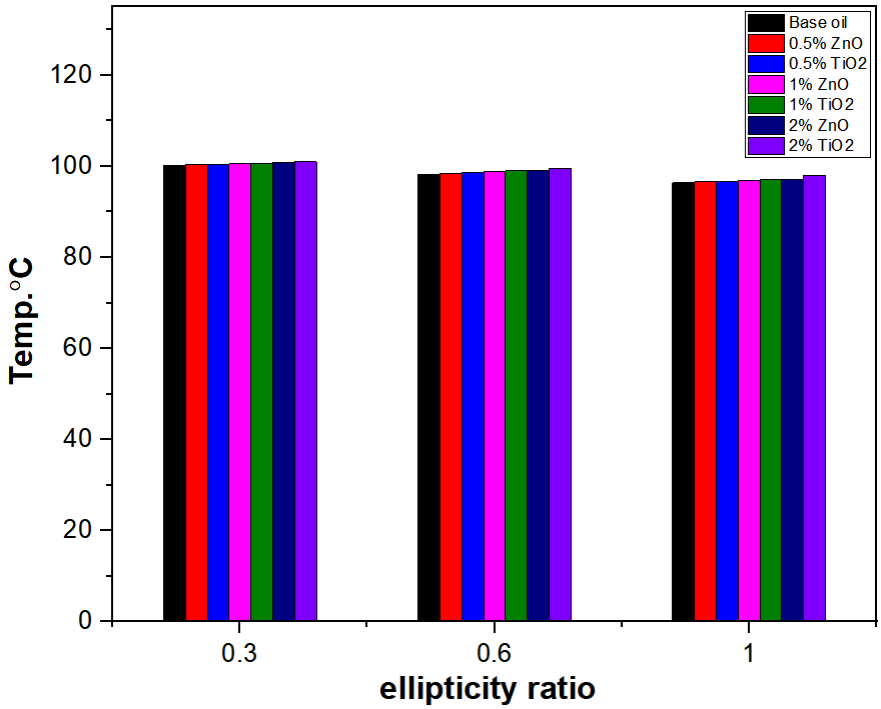

Fig(5.21) Effect of weight concentration and ellipticity ratio on the oil film temperature

Figure (5.22) shows the variation of the load carried by EJB that has a wide range of ellipticity ratios when it is lubricated with a base oil blended with different concentrations of nanoparticles. A decrease in the load-carrying capacity of the bearing with the increase of the bearing ellipticity ratios can be seen in this figure, which is associated with the increase in the oil film thickness of the bearing in this case. On the other hand, it can also be observed that the load carried by the bearing was enhanced with the addition of different weight fractions of TiO_2 and ZnO nanoparticles associated with the increase in oil viscosity in this case.

Figure (5.23) shows a decrease in friction force with increasing ellipticity ratios of EJB lubricated with varying weight concentrations of TiO_2 and ZnO nanoparticles associated with the increase in oil film thickness. It can be seen from the figure that friction force increases with increasing concentration of nanoparticles due to an increase in the viscosity

of the nano-lubricants, which causes an increase in the shear stress of the oil film.

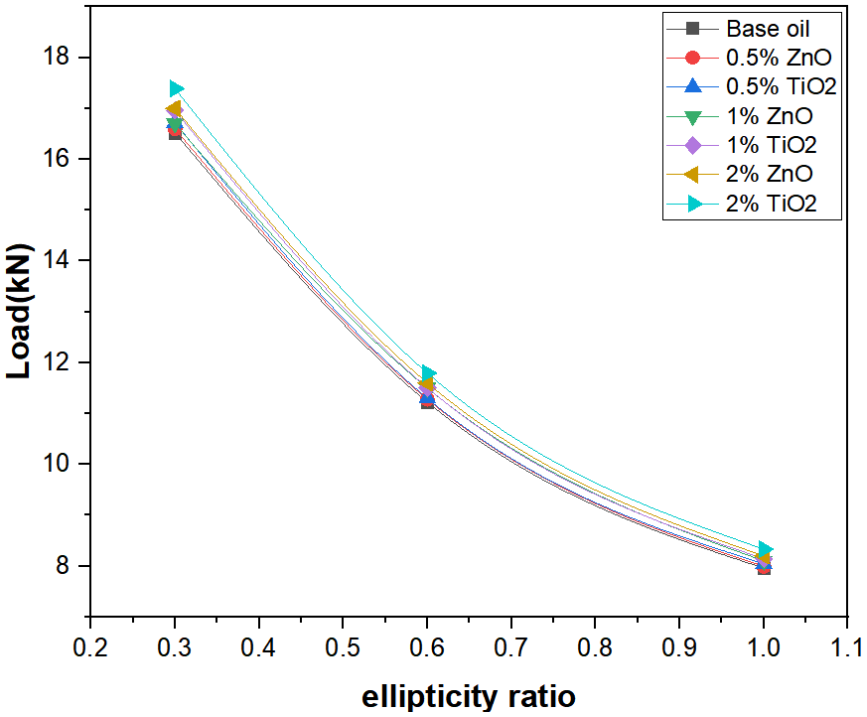

Fig(5.22) Effect of weight concentration and ellipticity ratio on the bearing load

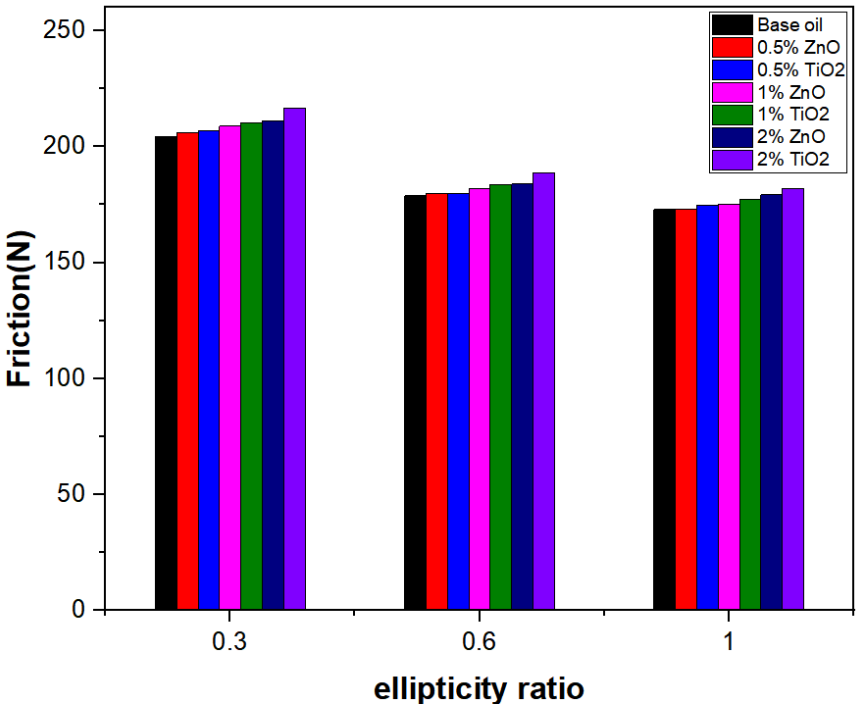

Fig(5.23) Effect of weight concentration and ellipticity ratio on the friction force

Figure (5.24) shows the decrease in side leakage flow from the ends of the bearing with increasing ellipticity ratios of the nano-lubricated EJB with varying weight concentrations of TiO_2 and ZnO nanoparticles due to an increase in oil film thickness, which causes a decrease in generated oil film pressure at the bearing ends and hence decreased in the lubricant side flow. In addition, it can be seen from this figure that side leakage flow decreases with increasing nanoparticle concentration, which affects the flow of the lubricant due to increase in the viscosity of nano-lubricant.

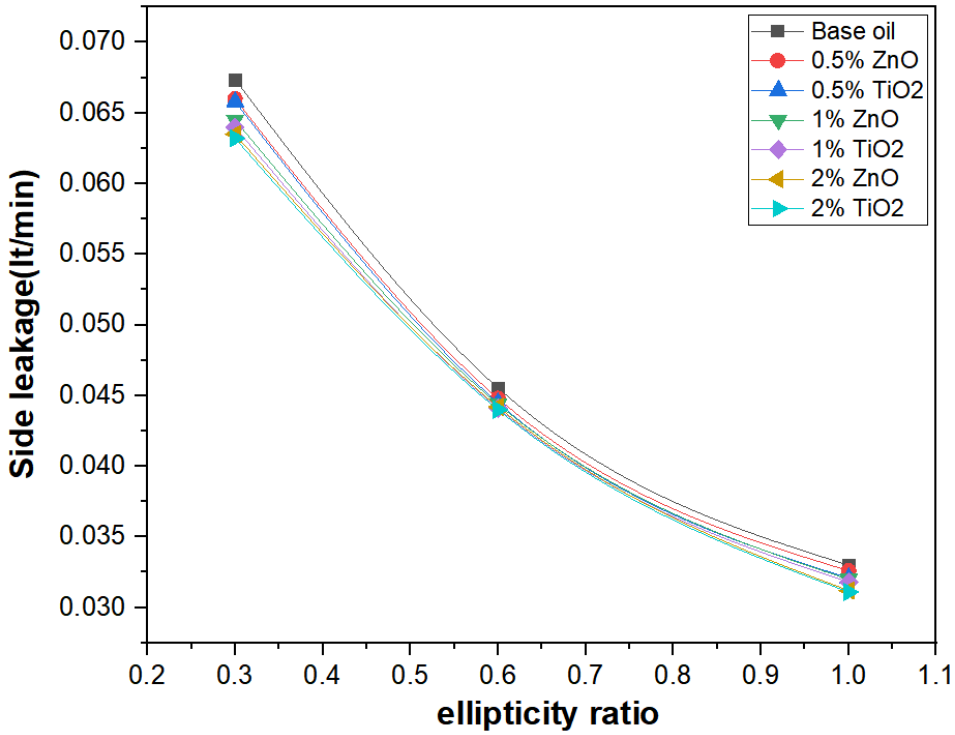

Fig(5.24) Effect of weight concentration and ellipticity ratio on the side leakage flow of EJB

5.3.2 Effect of Journal Speed

The effect of journal speed on the performance of EJB lubricated with a base oil as well as the nano-lubricants with different concentrations of nanoparticles was studied and presented here for a bearing with ellipticity and eccentricity ratios of 0.6 and 0.7, respectively.

Figures 5.25(a-c) illustrate the contours for the variation of the oil film pressure of a bearing lubricated with base oil working at different journal speeds (3000–5000 rpm). This figure depicts that oil film pressure increases at a higher journal speed of the bearing. It can be noticed from this figure that the maximum oil film pressure increases from 1.04 MPa when the journal speed is 3000 rpm to 1.1 and 1.15 MPa when the journal speed is 4000 rpm and 5000 rpm, respectively, with a percentage increase of 6.53% to 10.8% at journal speeds of 4000 and 5000 rpm, respectively, compared to 3000 rpm.

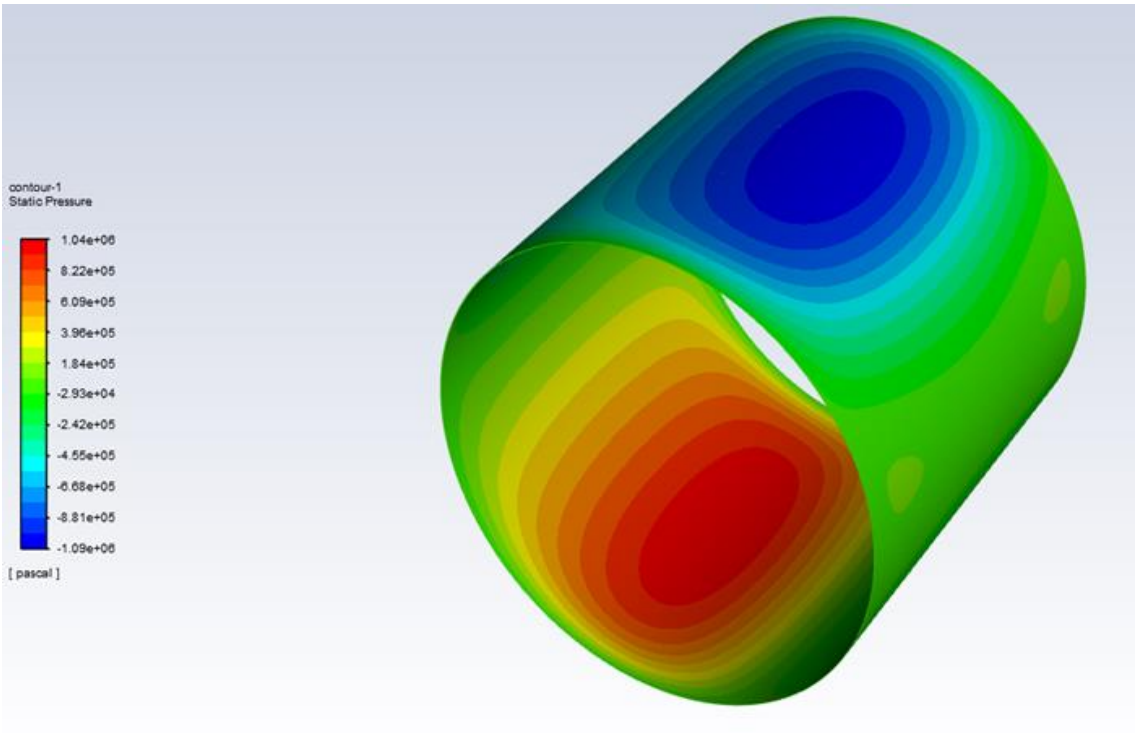

(a)N=3000 rpm

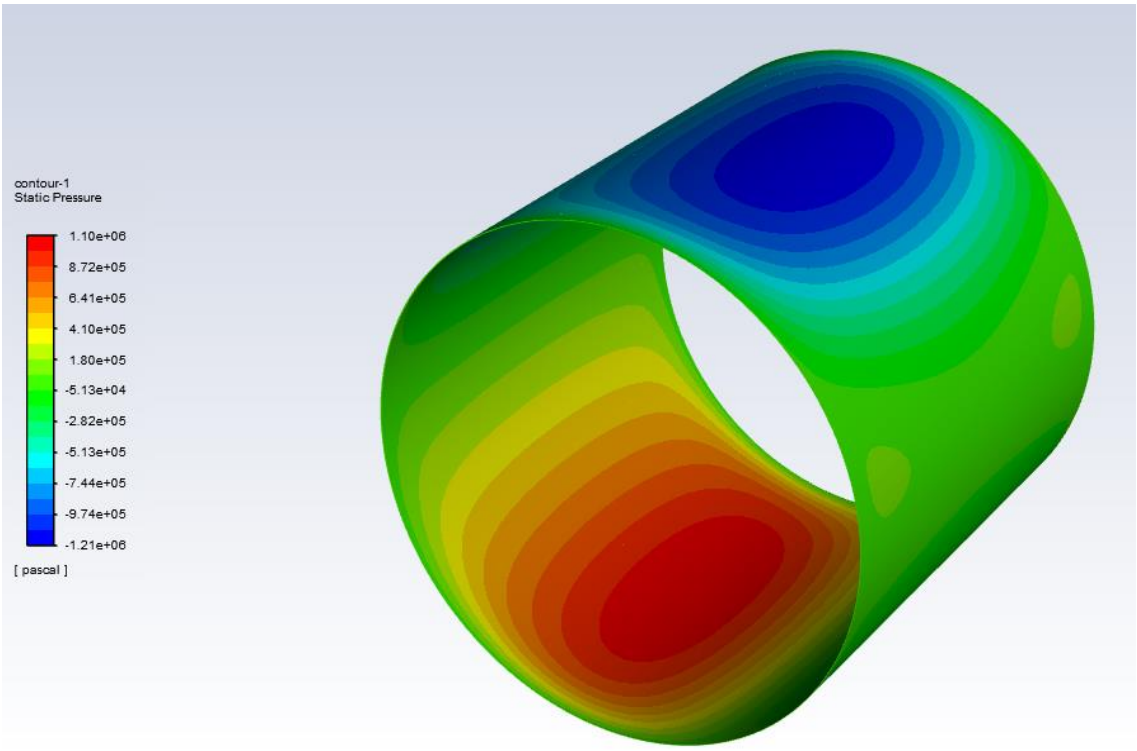

(b)N=4000 rpm

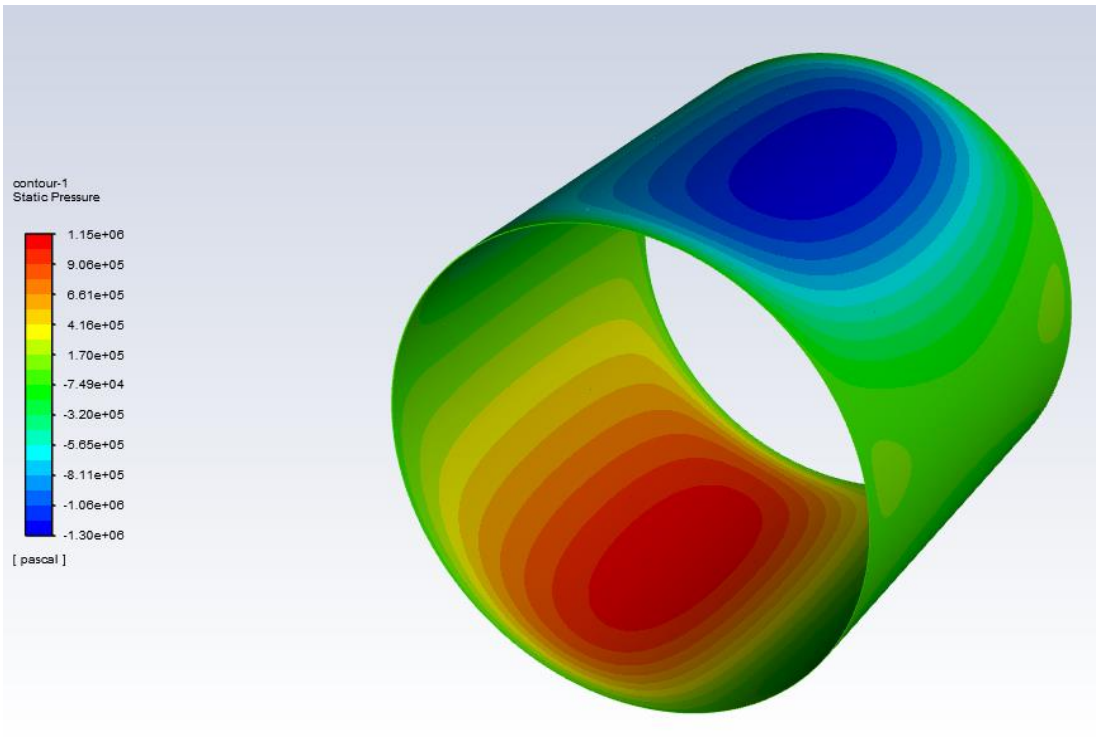

(c)N=5000 rpm

Fig(5.25) Effect of journal speed on the pressure contours at E_p=0.7, ε =0.6 (a) N=3000rpm, (b)N=4000rpm, (c) N=5000rpm

Figure (5.26) indicates both effects of journal speed and concentrations of nanoparticles on the maximum oil film pressure of EJB. It is well illustrated in this figure that the maximum oil film pressure of the bearing has a slight increase with journal speed. It has also been observed that the maximum oil film pressure increased with the addition of nanoparticles to the base oil, due to increase in the viscosity of nano-lubricant.

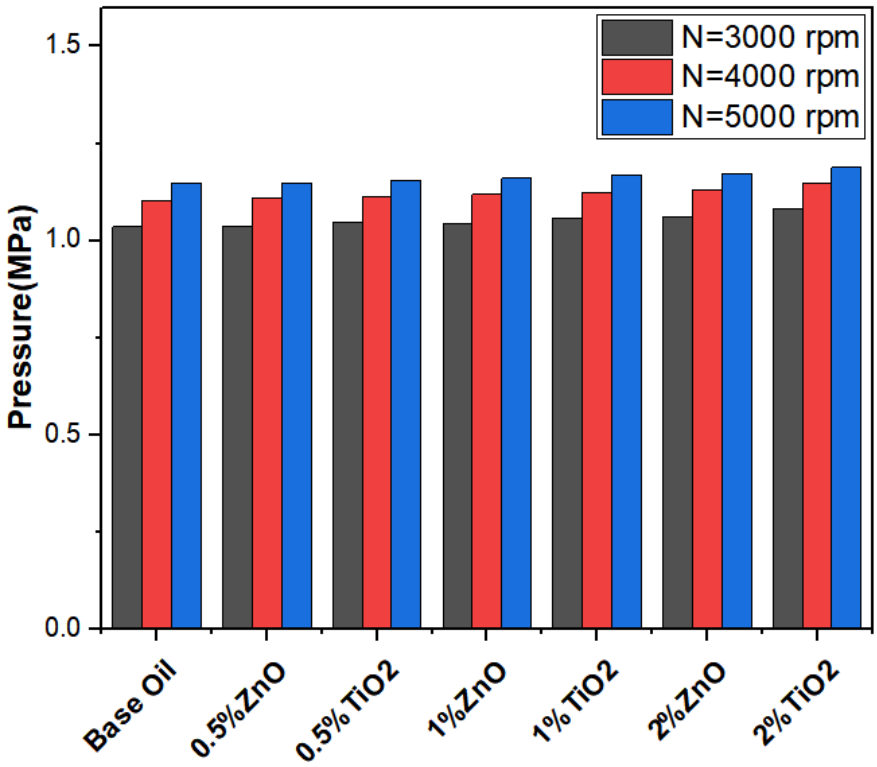

Fig(5.26) Effect of weight concentration and journal speed on the maximum pressure

Figure (5.27) shows that the addition of nanoparticles to the base oil causes a slight increase in the maximum oil film temperature of a bearing working at different journal speeds. This figure also shows that the oil film temperature increases by 9.45% and 14.58% when journal speed increases to 4000 and 5000 rpm, respectively, in comparison with 3000 rpm. This can be referenced to the increase in the shearing rate of the oil film at higher journal speeds, which leads to higher shear stress and friction force. It is well

known that the friction force at the bearing surfaces is the main cause of bearing heat generation.

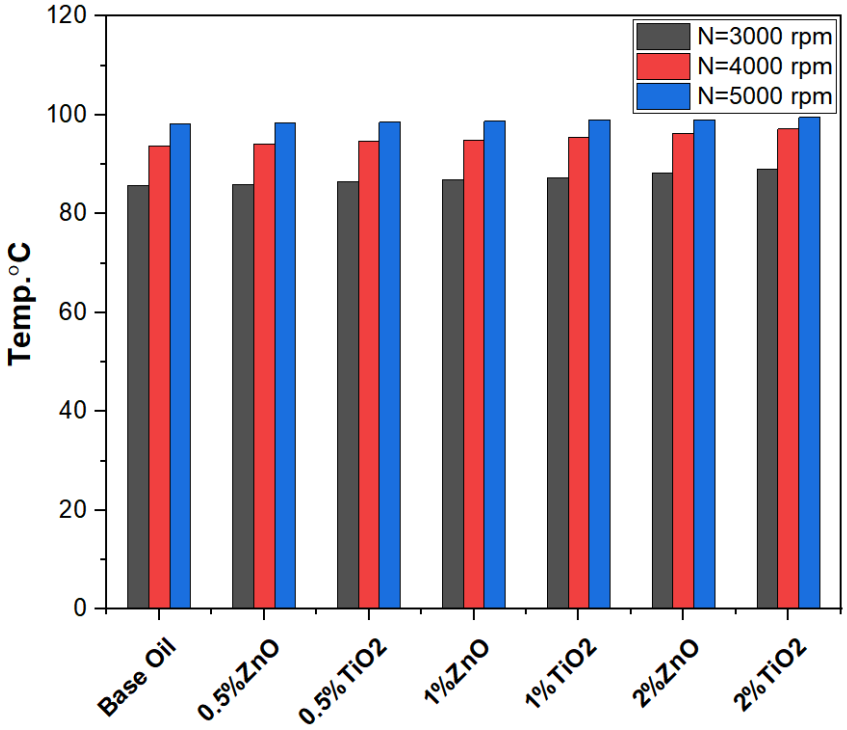

Fig(5.27) Effect of weight concentration and journal speed on the maximum temperature

Figure (5.28) shows both effects of journal speeds and the concentration of nanoparticles on the load-carrying capacity of EJB. The trend of this figure shows that the load-carrying capacity increases with an increase in journal speed while keeping the ellipticity ratio of 0.6 and the eccentricity ratio of 0.7 at base oil. It has been found that the load-carrying capacity of the bearing increases by 10% and 17.45% when the journal speed of the bearing increases from 3000 to 4000 and 5000 rpm, respectively, due to the increase in the wedge action of the bearing. It is also clearly noticed from this figure that the nanoparticles blended with the pure oil caused an increase in load carrying capacity of the bearing that related to the increase in the nano-lubricant viscosity.

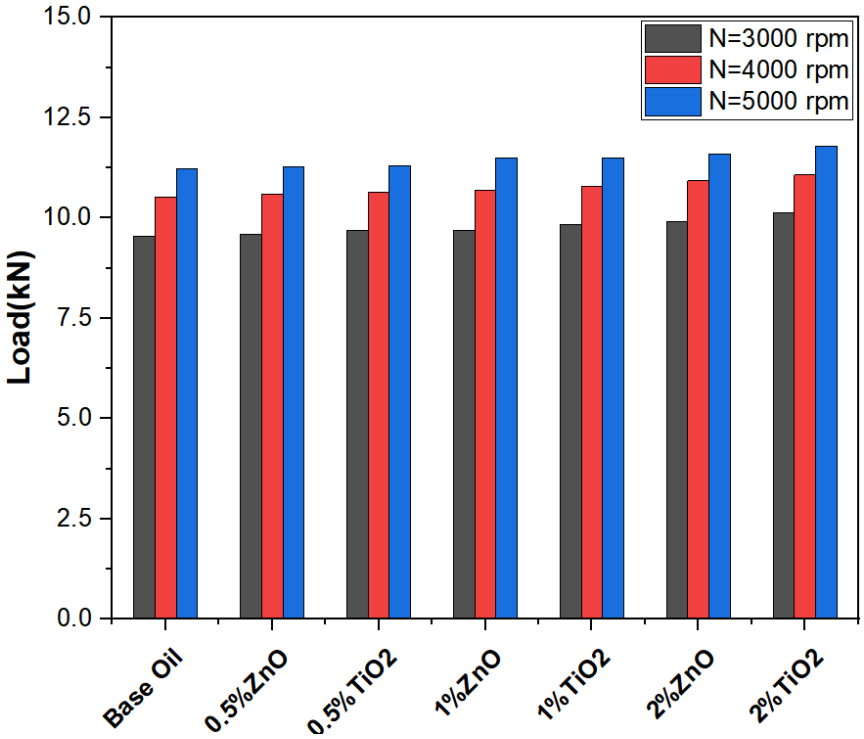

Fig(5.28) Effect of weight concentration and journal speed on the load-carrying capacity

5.3.3 Effect of Eccentricity Ratio

The effect of the eccentricity ratio on the performance of EJB was studied by fixing the bearing ellipticity ratio to 0.6 and the journal speed to 5000 rpm.

Figure (5.29) depicts the values of maximum pressure obtained for pure oil with three weight concentrations of TiO_2 and ZnO at different eccentricity ratios. Hydrodynamic pressure increases with an increase in eccentricity ratio for each type of lubricant due to the closeness between the journal surface and the bearing, which causes a thinner oil film thickness and then generates higher oil film pressure. Further, an increase in the concentration of nanoparticles increases the hydrodynamic pressure as a result of an increase in oil viscosity.

The percentage increase in the maximum oil film pressure when the bearing is lubricated with both types of nano-lubricants at an eccentricity ratio of 0.5 has been calculated and presented in figure (5.30). This figure shows that the maximum increase in oil film pressure reaches 4% when the bearing is lubricated with 2wt% of TiO_2 and 2.52% when it is lubricated with 2wt% of ZnO in comparison with that of the base oil. This can be attributed to the higher viscosity of TiO_2 as a result of the higher aggregate ratio, which opposes the lubricant flow and hence increases the lubricant viscosity.

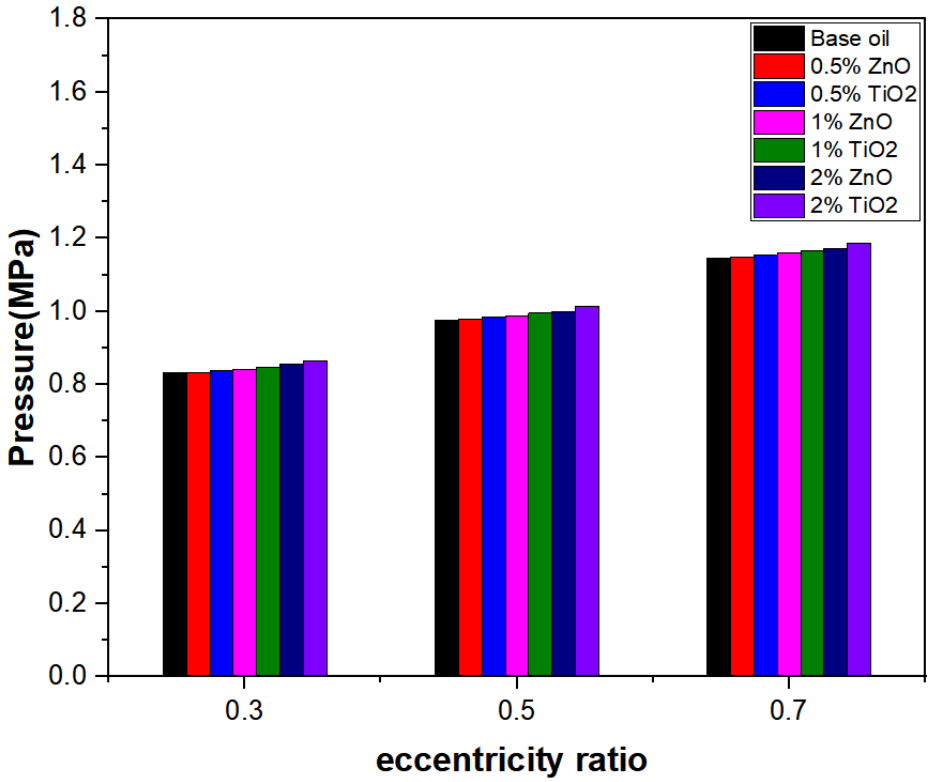

Fig(5.29) Effect of weight concentration and eccentricity ratio on the oil film pressure

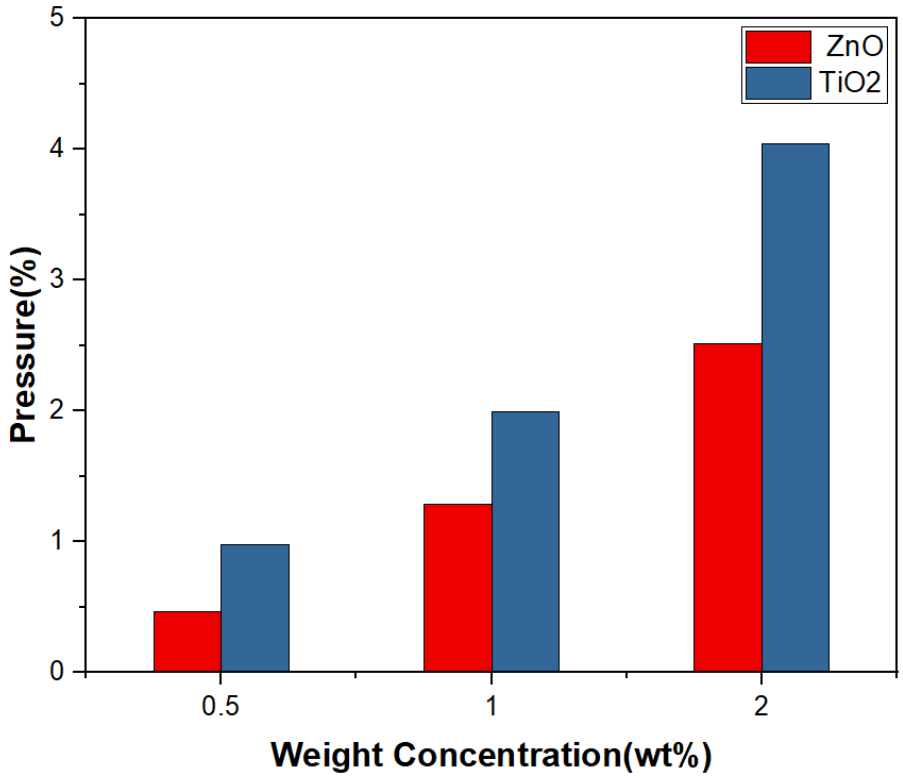

Fig(5.30) Percentage increase in maximum oil film pressure with a different weight percentage of nanoparticles

Figure (5.31) depicts the variation in maximum temperature for an EJB working at varying eccentricity ratios and lubricated with nano-lubricants based on TiO_2 and ZnO with different weight concentrations of nanoparticles. It has been observed that there is a slight increase in the maximum oil film temperature of oil due to the addition of nanoparticles in base oil and when the bearing works at different eccentricity ratios.

The percentage increase in maximum oil film temperature at an eccentricity ratio of 0.5 has been calculated and presented in figure (5.32). This figure reports that the maximum oil film temperature increases by 3.55% for the bearing lubricated with 2 wt% of TiO_2, while it increases by about 2.82% when the bearing is lubricated with 2 wt% of ZnO. This can be attributed to the lower viscosity of ZnO compared to TiO_2 at an increased concentration of nanoparticles.

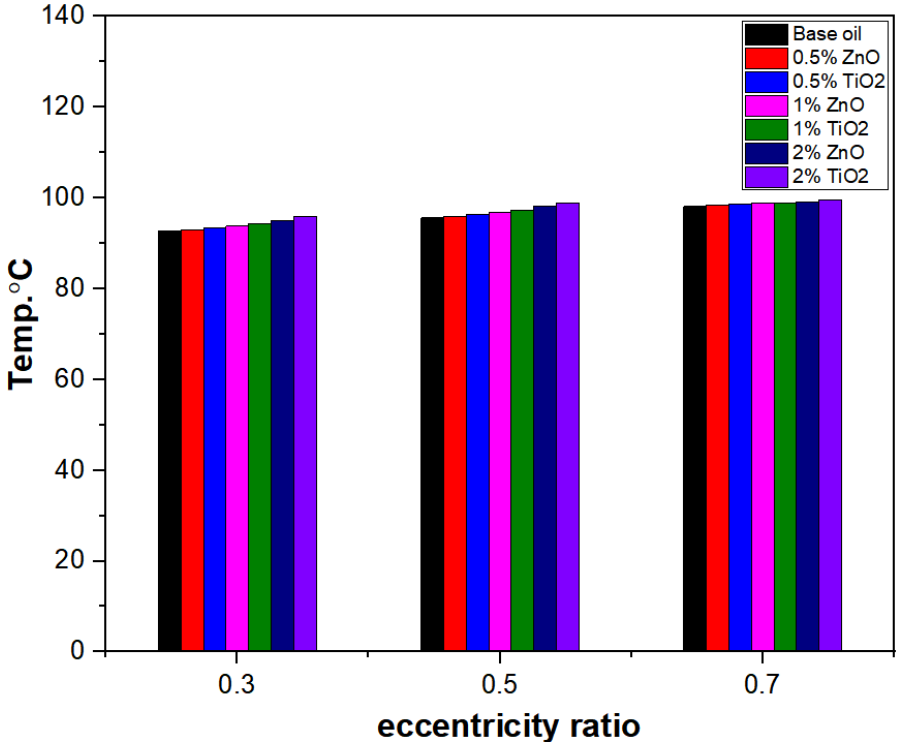

Fig(5.31) Effect of weight concentration and eccentricity ratio on the oil film temperature

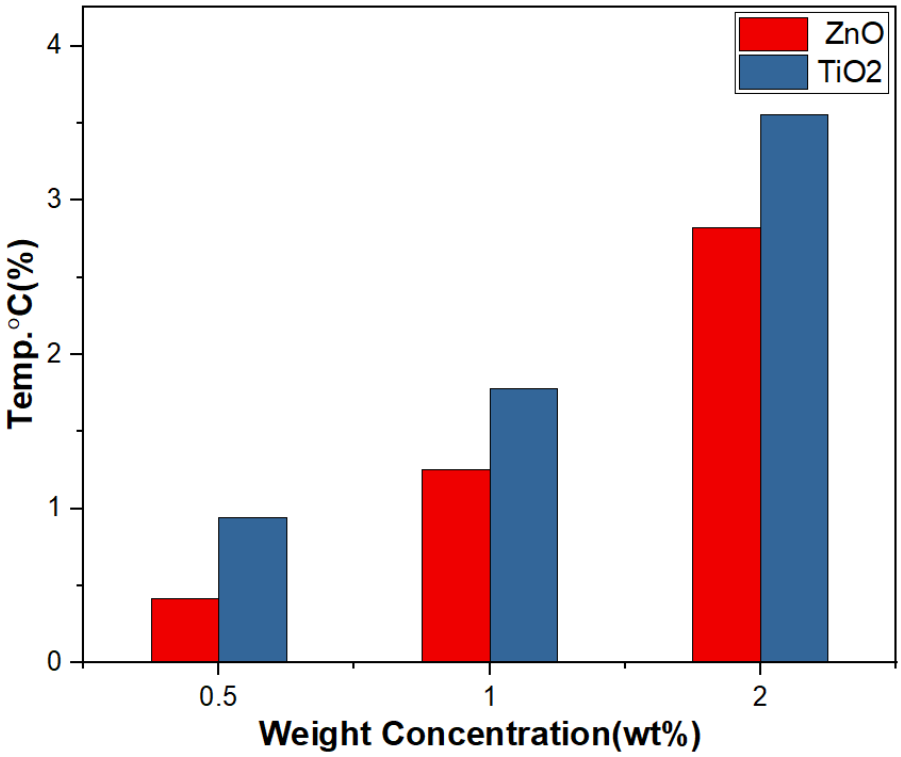

Fig(5.32) Percentage increase in maximum temperature of oil film with a different weight percentage of nanoparticles

Figure (5.33) illustrates the effect of eccentricity ratio and nanoparticle concentrations on the load-carrying capacity of EJB. This figure illustrates that when the bearing operates at high eccentricity ratios, the load carried by the bearing increases as a result of the increased oil film pressure as a result of the closeness of the journal and bearing surfaces.

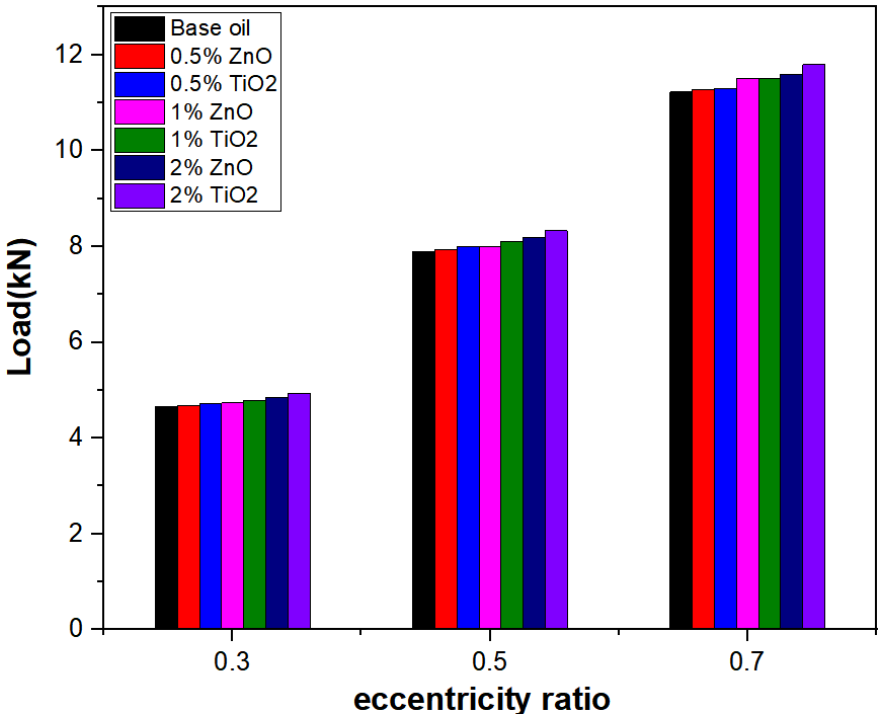

Fig(5.33) Effect of weight concentration and eccentricity ratio on the load carrying capacity

The percentage increase in the load-carrying capacity of such a bearing at an eccentricity ratio of 0.5 becomes 5.52% when the bearing is lubricated with 2 wt% of TiO_2, while it becomes about 3.93% when it is lubricated with 2 wt% of ZnO as presented in figure (5.34). The results also revealed that the increase in the concentration of nanoparticles blended in the base oil has a positive effect on the load-carrying capacity, and the increase is found to be greater when using TiO_2 rather than ZnO nanoparticles as a result of a higher aggregate ratio of the former than that of the latter, which affects the nano-lubricant viscosity.

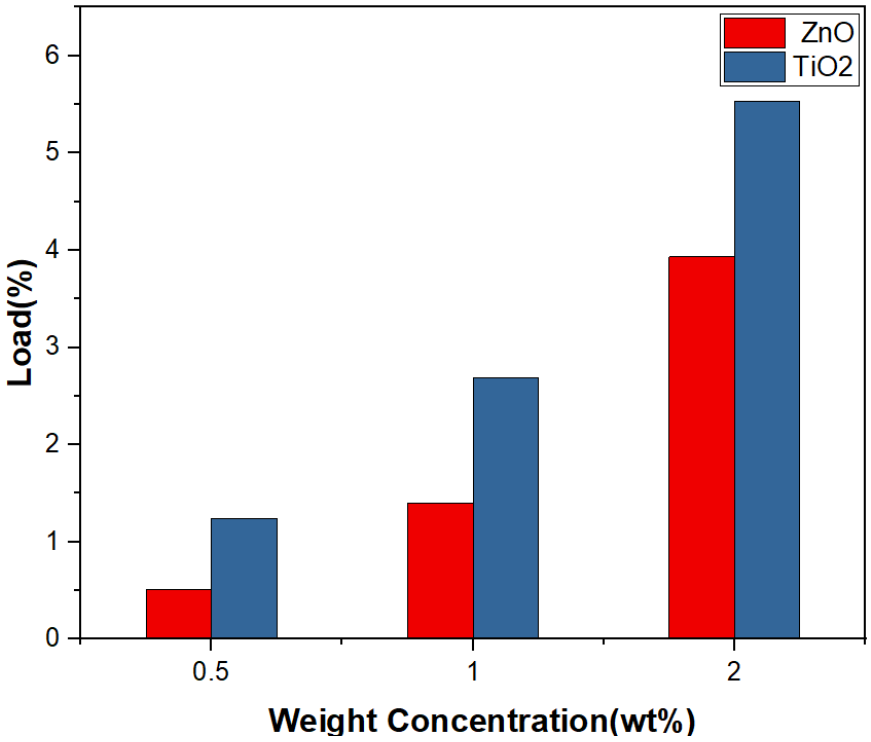

Fig(5.34) Percentage increase in load carrying capacity with a different weight percentage of nanoparticles

Figure (5.35) shows the slight increase in friction force when the EJB works at higher eccentricity ratios. This can be attributed to the closeness surface of the journal to the bearing when the bearing works at a higher eccentricity ratio. The existence of TiO_2 and ZnO nanoparticles in the base oil with different weight fractions also causes an increase in the friction force due to the higher viscosity of the lubricant in this case. This can be attributed to an increase in lubricant shear stress induced at the bearing surfaces.

The percentage increase in friction force was calculated at an eccentricity ratio of 0.5 and presented in figure (5.36). This figure shows that the maximum increase in friction force becomes 5.7% when the bearing is lubricated with 2 wt% of TiO_2, while this rate is about 3.65% when the bearing is lubricated with 2wt% of ZnO.

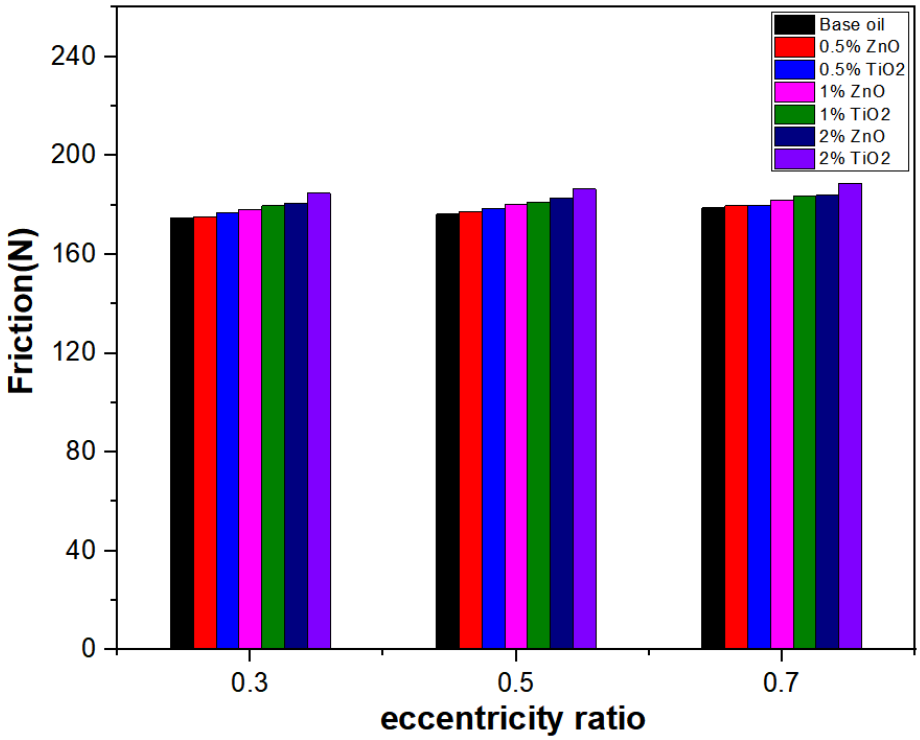

Fig(5.35) Effect of weight concentration and eccentricity ratio on the friction force of bearing

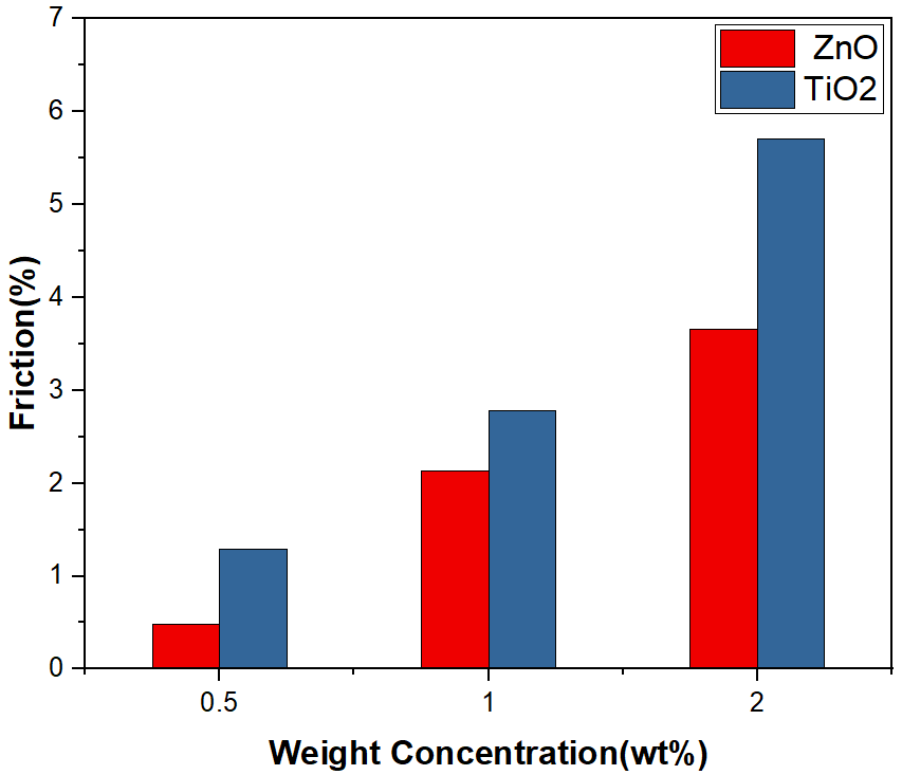

Fig(5.36) Percentage increase in friction force with a different weight percentage of nanoparticles

The variation of the side leakage flow from the ends of the bearing with the bearing eccentricity ratios when lubricated with nano-lubricant based on TiO_2 and ZnO that has different weight concentrations of nanoparticles is illustrated in figure (5.37). The findings showed that the side leakage of the oil increases when the bearing operates at a higher eccentricity ratio, as a result of increasing the oil film pressure at both ends of the bearing. However, the leakage flow decreases when the bearing is lubricated with Nano-lubricant in comparison with pure oil. This can be attributed to the higher viscosity of the lubricant, which reduces the flow velocity of the lubricant.

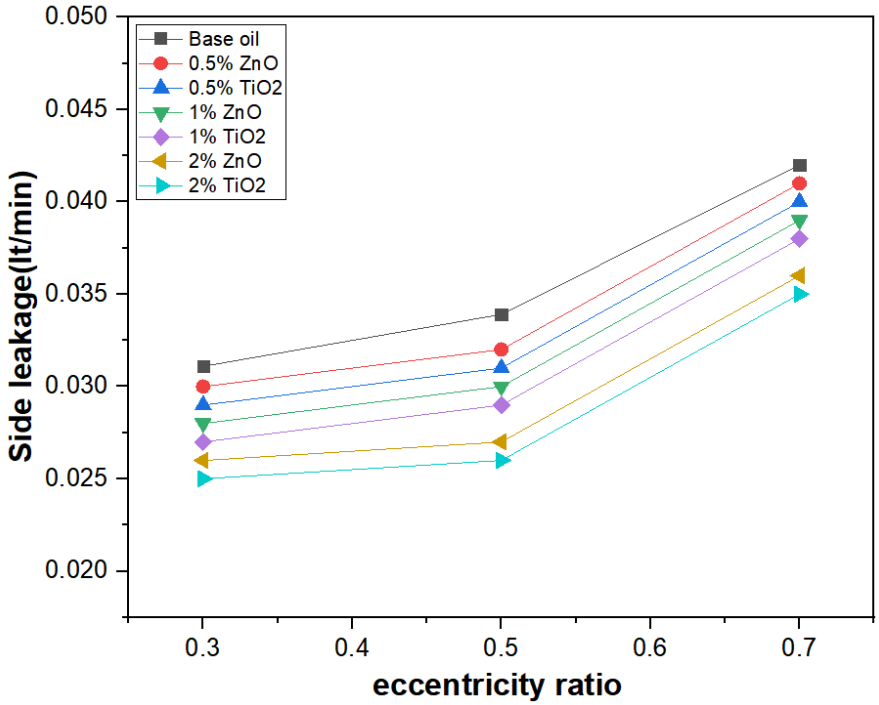

Fig(5.37) Effect of weight concentration and eccentricity ratio on the side leakage flow

It has been found that the maximum decrease in side leakage at an eccentricity ratio of 0.5 becomes 24.4% when the bearing is lubricated with 2 wt% of TiO_2, and it becomes 9% when it is operated with 0.5 wt% of TiO_2 nano-lubricant, while these percentages become 4.5% and 18.5% when the bearing is lubricated with 0.5 wt% and 2 wt% of ZnO, respectively, because

the increasing concentration of nanoparticles decreases lubricant flow, as illustrated in figure (5.38).

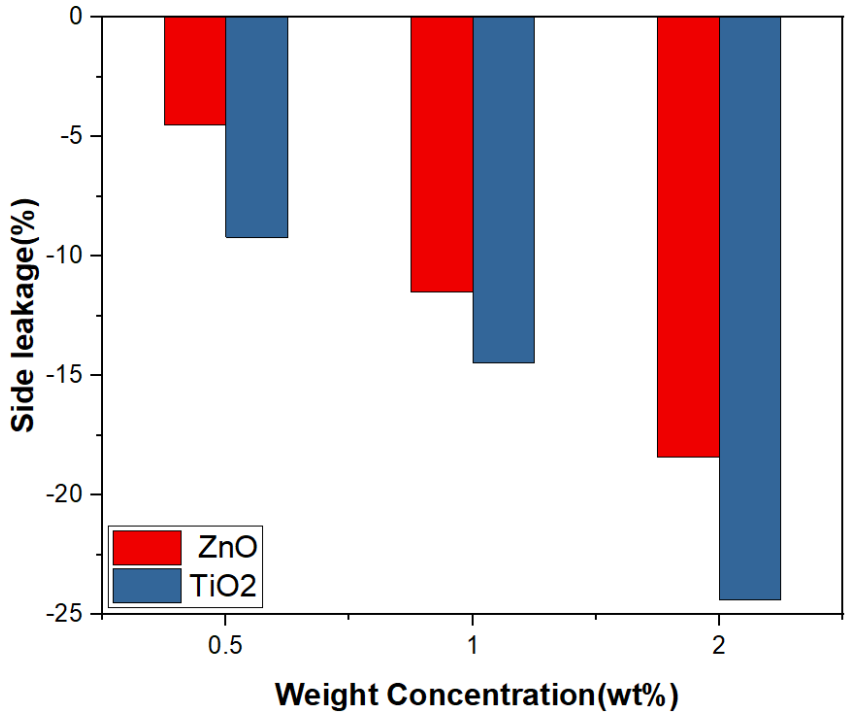

Fig(5.38) Percentage decrease in side leakage flow with a different weight percentage of nanoparticles

The combined effect of the eccentricity ratio and nanoparticle concentrations of ZnO and TiO_2 on the power loss of EJB is shown in Figure (5.39). It appears that the power loss slightly increases as the bearing works at higher eccentricity ratios as a result of the slight increase in friction force discussed above. It also appears that the power loss slightly increases with the increase in nanoparticle concentrations dispersed in the base oil, which is associated with the higher lubricant viscosity.

The percentage increase in power loss is calculated at an eccentricity ratio of 0.5 and presented in figure (5.40). This figure demonstrates that the maximum percentage increase in the bearing power loss becomes 1.29% when it is lubricated with 0.5 wt% TiO_2 nano-lubricant, while it increases to 5.7% when the bearing is lubricated with 2 wt% of such lubricant. It was

observed that the percentage increase becomes 0.17% to 4.18% when the base oil is dispersed with the same weight concentrations of ZnO.

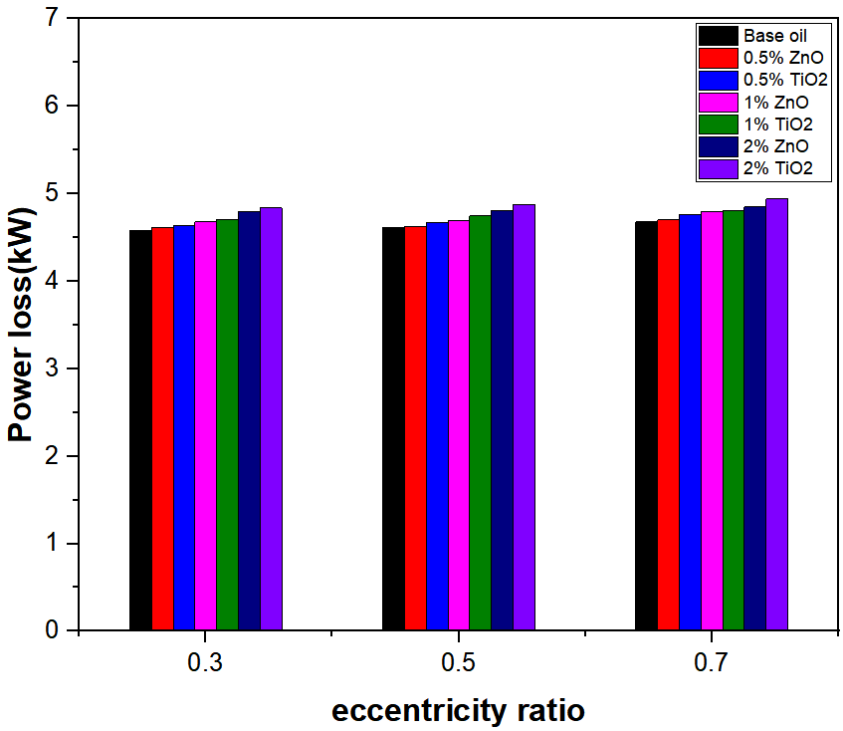

Fig(5.39) Effect of weight concentration and eccentricity ratio on the power loss of bearing

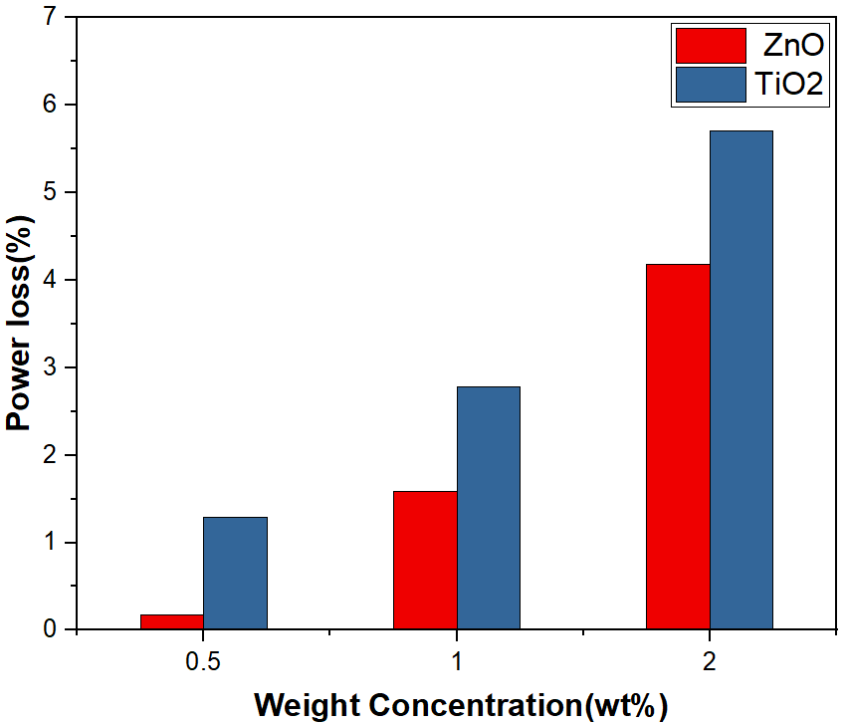

Fig(5.40) Percentage increase in power loss with a different weight percentage of nanoparticles

Figures 5.41(a-c) show the effect of increasing nanoparticle concentration of TiO_2 more than 2 wt% on the oil film pressure, temperature, and load carrying capacity of EJB with an ellipticity ratio of 0.6 when it works at different eccentricity ratios and journal speed of 5000 rpm. For the bearing working at an eccentricity ratio of 0.7, it was found that the pressure, temperature, and load-carrying capacity increases about 5.86%, 10.35%, and 8.61%, respectively, when the bearing is lubricated with 5 wt% of TiO_2 in comparison with that lubricated with 2 wt% of TiO_2.

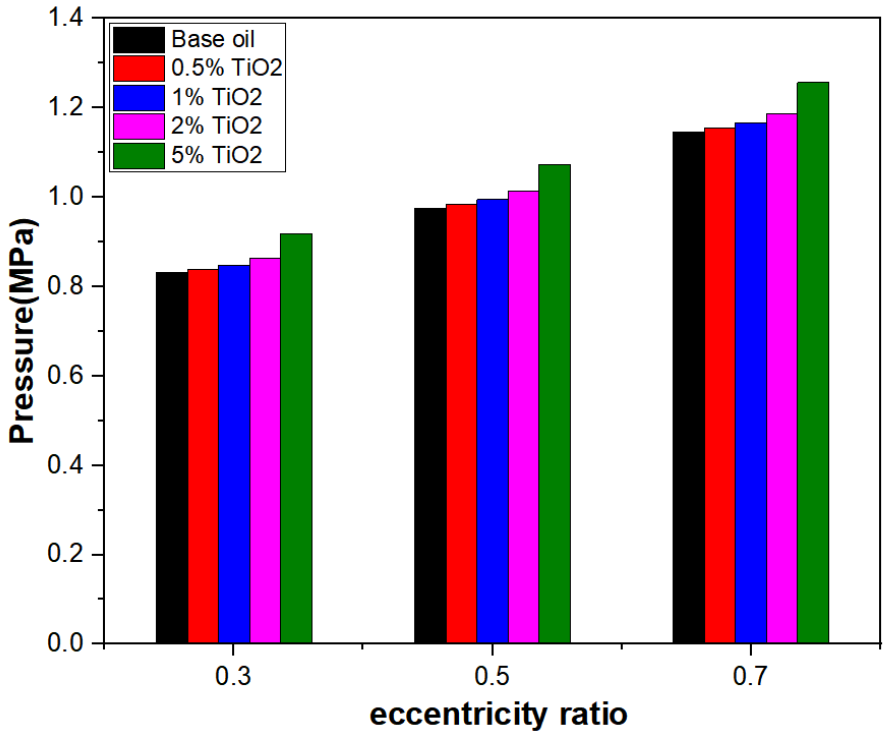

(a)

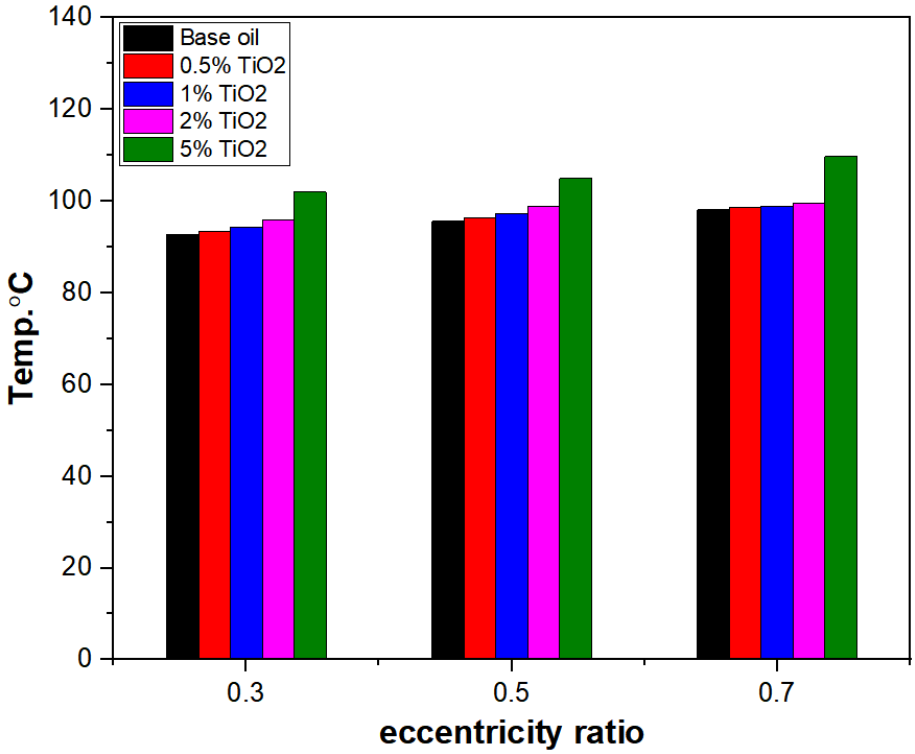

(b)

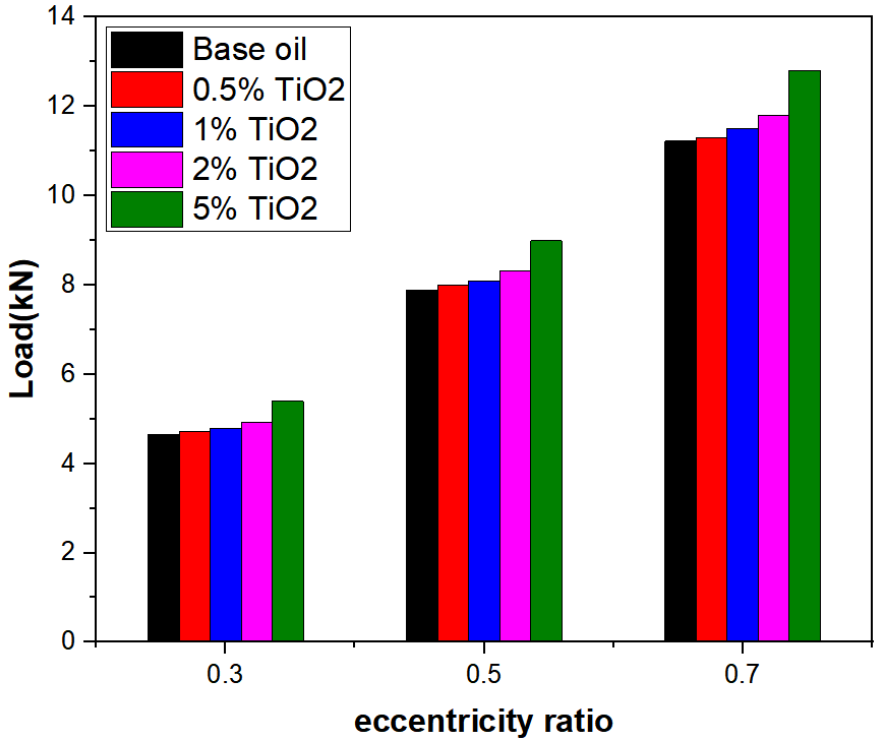

(c)

Fig(5.41) Effect of weight concentration and eccentricity ratio on the (a) oil film pressure, (b) oil film temperature, (c)load carrying capacity

5.4 Performance of Circular Journal Bearing

The effects of different parameters, such as eccentricity ratio, journal speed, and particle concentrations on the performance of a circular journal bearing lubricated with nano-lubricant are presented and investigated in this section according to the following articles:

5.4.1 Effect of Eccentricity Ratio

The results presented in this article are those for a circular journal bearing working at different eccentricity ratios with a journal speed fixed at 5000 rpm.

The variation of the oil film pressure for a bearing working at different eccentricity ratios and lubricated with nano-lubricants based on TiO_2 and ZnO that have different nanoparticle concentrations can be shown in figure (5.42). It can be seen from this figure that the maximum oil film pressure increases with increasing eccentricity ratios due to the closeness between the journal surface and bearing, which results in a thinner oil film and hence a higher film pressure. It can also be noticed from this figure that the maximum oil film pressure increases when the bearing is lubricated with nano-lubricants that have increase particle concentrations as a result of the higher viscosity of the lubricant in this case.

Figure (5.43) represents the variation of the maximum oil film temperature for a bearing working at different eccentricity ratios and lubricated with different weight concentrations of TiO_2 and ZnO. This figure shows the higher maximum oil film temperature when the bearing operates at a higher eccentricity ratio due to the increase in shear rate of lubricant in this situation. However, it has been noticed that the oil film temperature increases slightly because of dispersing of such nanoparticles in the base oil, which can be attributed to the enhancement of the lubricant's thermal

conductivity of the lubricant and its effect on the conduction term of the energy equation.

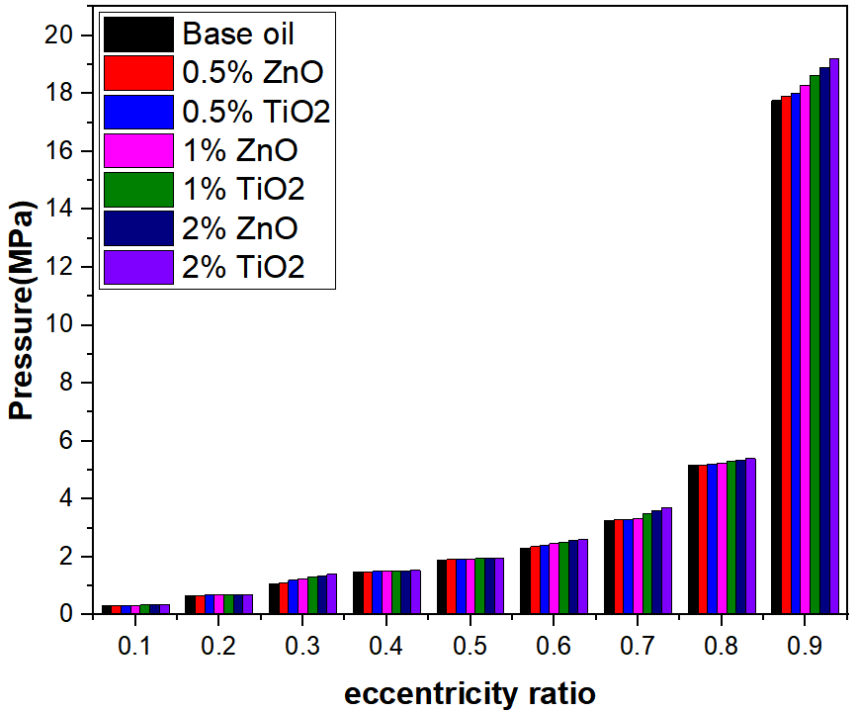

Fig(5.42) Effect of weight concentration and eccentricity ratio on maximum oil film pressure

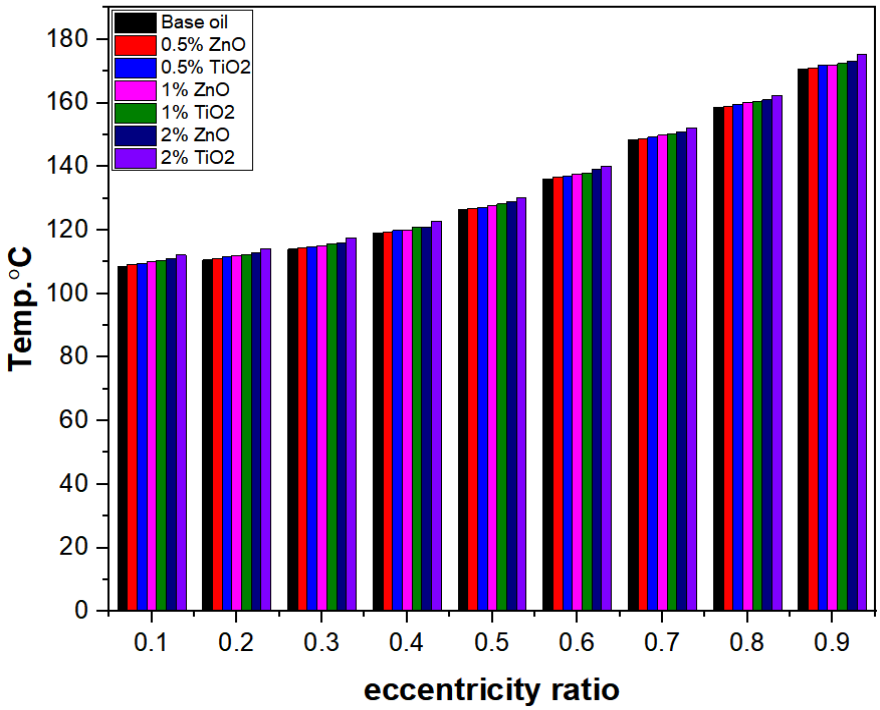

Fig(5.43) Effect of weight concentration and eccentricity ratio on maximum oil film temperature

Figure (5.44) shows the increase in load-carrying capacity with increasing eccentricity ratios due to the increase in oil film pressure in this case. A further increase in the load carried by the bearing is obtained when the bearing is lubricated with a nano-lubricant that has an increase concentration of TiO_2 and ZnO nanoparticles because of the higher oil viscosity. The little increase in the load-carrying capacity can be explained by the small amounts of nanoparticles added to the base oil due to the experimental limitation related to the preparation of the nano-lubricant itself, which is supported by the results obtained by **Shenoy et al. (2012)**.

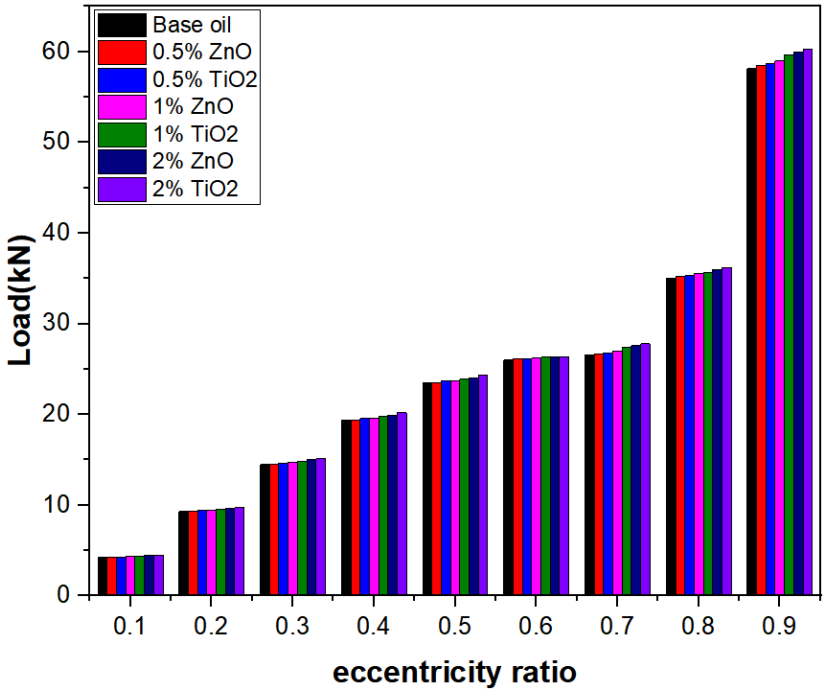

Fig(5.44) Effect of weight concentration and eccentricity ratio on the load carrying capacity

Figure (5.45) indicates the increase in friction force with the increasing eccentricity ratios due to the higher shear rate of the lubricant as a result of the close contact surfaces of the bearing and journal. The increase is higher when the bearing is lubricated with nano-lubricants that have higher nanoparticle concentrations as a result of the higher viscosity of the lubricant.

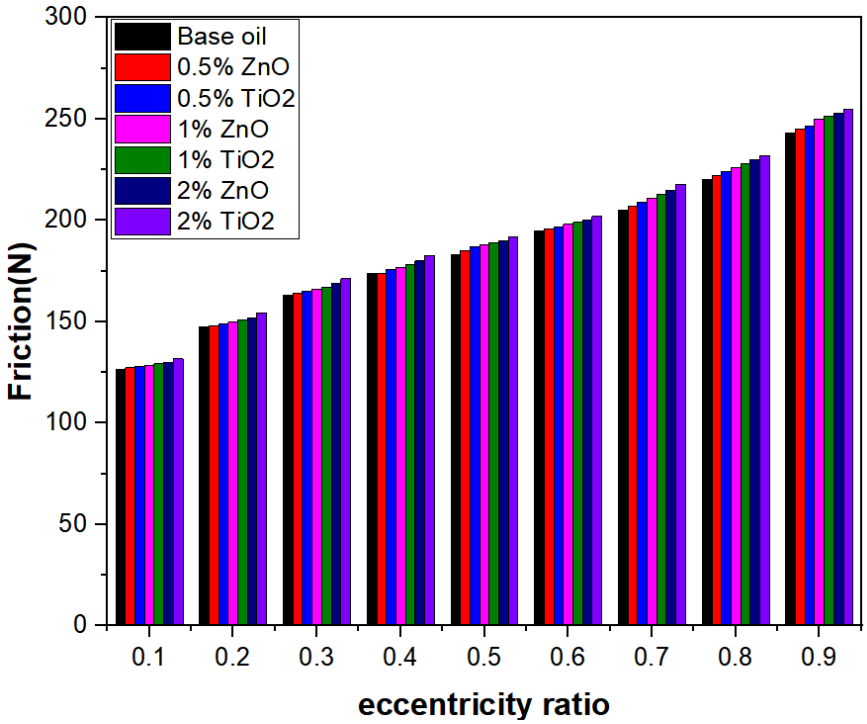

Fig(5.45) Effect of weight concentration and eccentricity ratio on the friction force

Figure (5.46) shows a decrease in the attitude angle with an increase in eccentricity ratio of the journal bearing operating at a journal speed of 5000 rpm due to increase oil film pressure with increase eccentricity ratio. It can also be seen from this figure that the attitude angle drops for the bearing lubricated with higher concentrations of nanoparticles cause of increasing viscosity.

Figure (5.47) shows that the side leakage of the flow from the ends of the bearing increases when the bearing works at higher eccentricity ratios, while the side leakage flow decreases when it is operated with nano-lubricant in comparison with pure oil due to an increase of oil viscosity, which reduces the velocity of the lubricant flow.

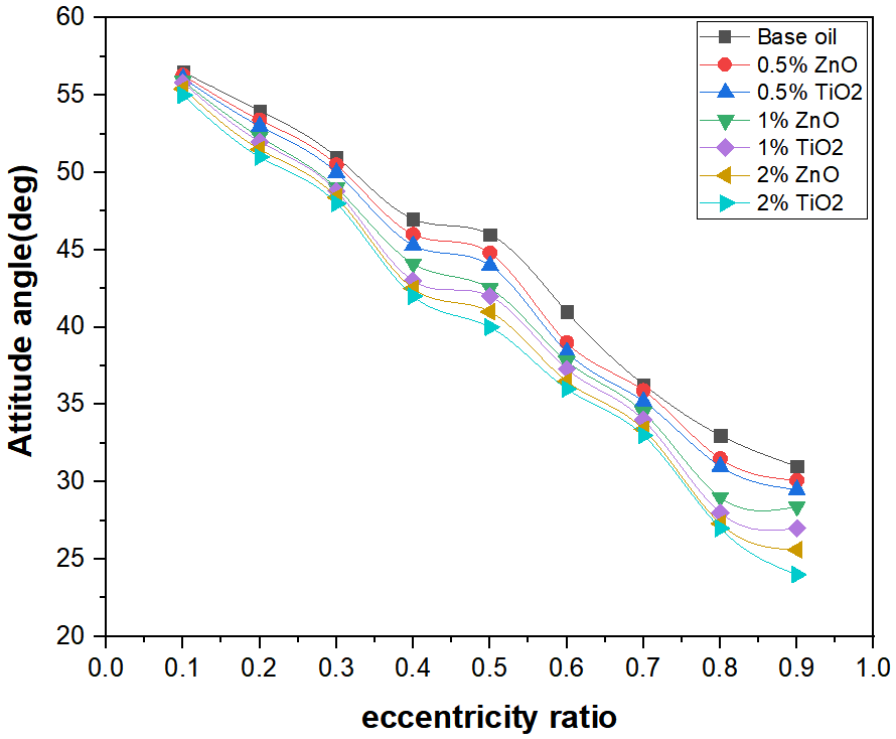

Fig(5.46) Effect of weight concentration and eccentricity ratio on attitude angle

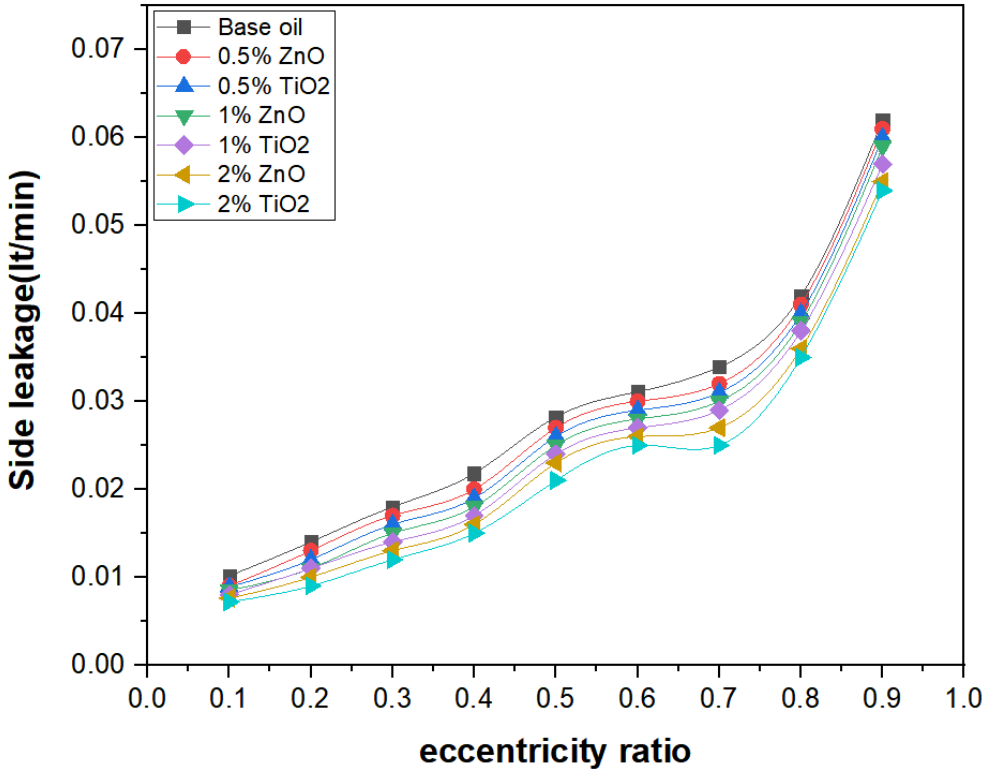

Fig(5.47) Effect of weight concentration and eccentricity ratio on side leakage flow

Figure (5.48) illustrates that the power loss increases for a bearing working at higher eccentricity ratios as a consequence of increased friction force when the bearing working under this circumstance. The increase becomes higher when the bearing is lubricated with different weight concentrations of TiO_2 and ZnO because of the higher oil viscosity, which leads to a higher friction force.

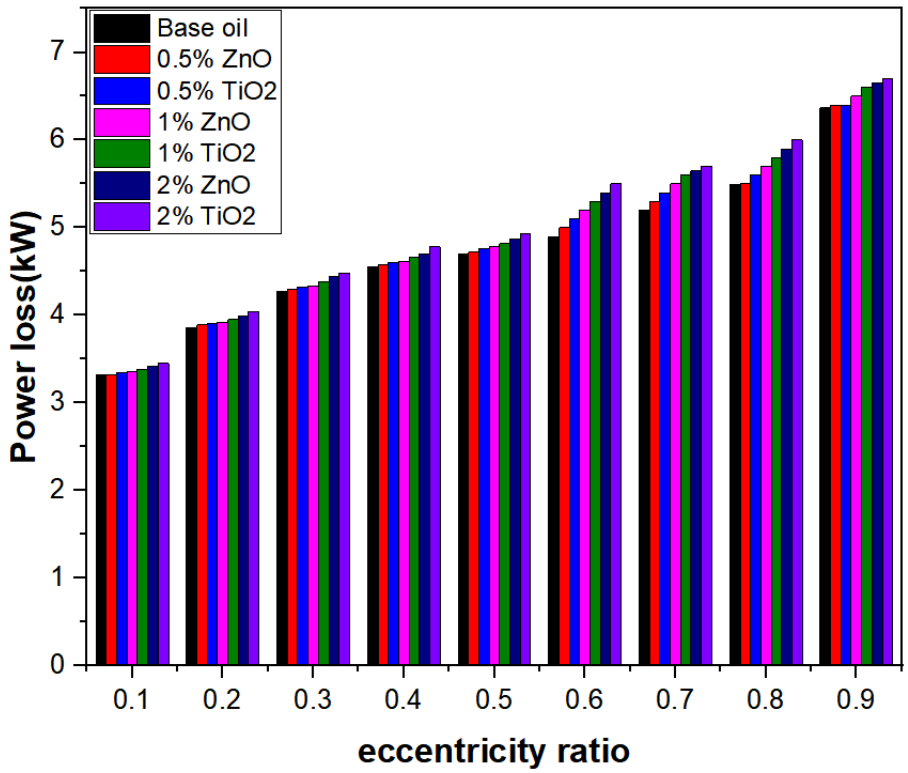

Fig(5.48) Effect of weight concentration and eccentricity ratio on power loss at 5000 RPM

5.4.2 Effect of Journal Speed

The oil film pressure distribution was observed when the bearing operated with an eccentricity ratio of 0.7 and various journal speeds of 3000, 4000, and 5000 rpm lubricated with pure oil as shown in figure (5.49). It can be seen from the figure that oil film pressure has a high magnitude at high journal speeds due to the formation of a larger wedge action in this situation. The percentage increase has been calculated and found to be 16.67% when

the journal speed increases from 3000 to 4000 rpm, while it becomes 15.92% at increasing the journal speed from 4000 to 5000 rpm.

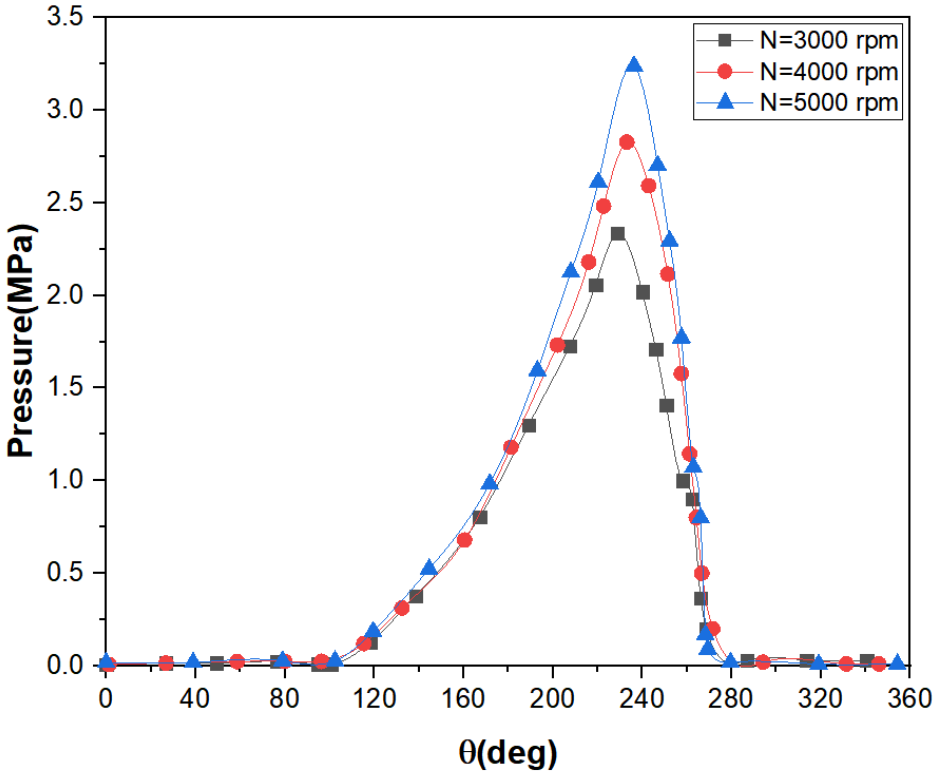

Fig(5.49) Oil film pressure affected by journal speed

Figure (5.50) illustrates the variation in maximum pressure attained when the bearing working under the above-mentioned circumstances lubricated with nano-lubricants that have different nanoparticle concentrations. It was noticed that when the bearing is lubricated with these types of lubricants, the maximum oil film pressure rises due to the increasing oil viscosity. This figure also reveals that the maximum oil film pressure of the bearing operating with nano-lubricants based on TiO_2 increases more than that of the nano-lubricant of ZnO because of the higher aggregate ratio of TiO_2 nanoparticles in comparison with that of ZnO. The maximum oil film pressure increases by about 4.16% and 3.33% at 3000 RPM and the bearing is lubricated with nano-lubricant that has 2 wt% of TiO_2 and ZnO nanoparticles, respectively.

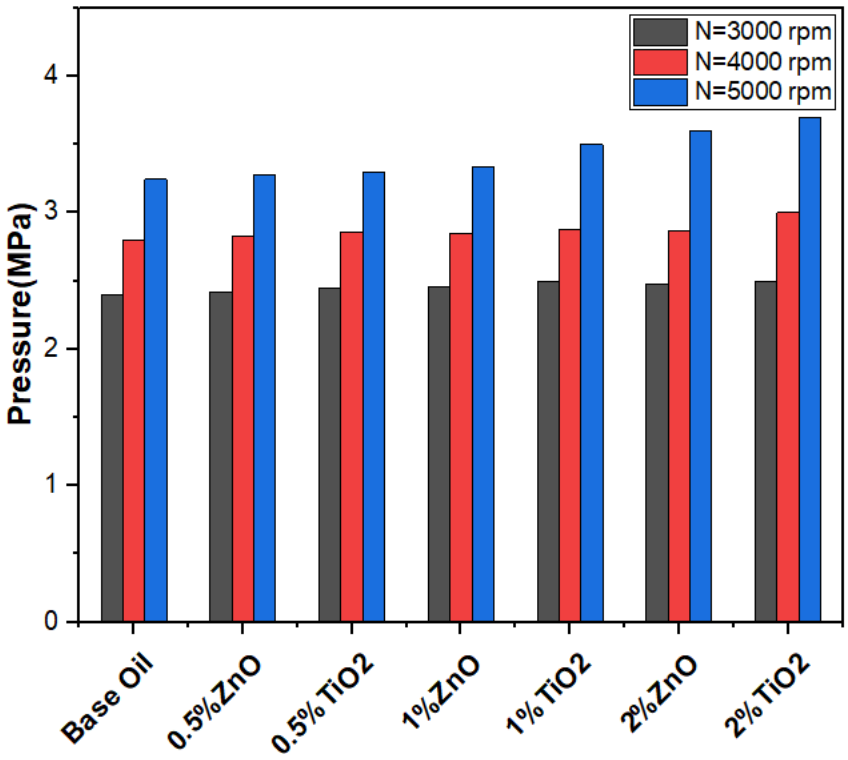

Fig(5.50) Combined effect of nanoparticles weight percentage and journal speed on oil film pressure

Figure (5.51) shows a slight increase in the maximum oil film temperature with increase journal speed. This figure demonstrates the maximum oil film temperature of the bearing at a journal speed of 3000 RPM increases by 0.72% and 0.5% in the cases of 2 wt% of TiO_2 and ZnO, respectively. This can be attributed to the thermal conductivity improvement as a result of dispersing the nanoparticles.

Figure (5.52) illustrates that the oil film temperature distribution is affected by the journal speed. This figure illustrates that the oil film temperature increases as the bearing works at higher journal speeds as a consequence of the increase in oil shear rate with the journal speed.

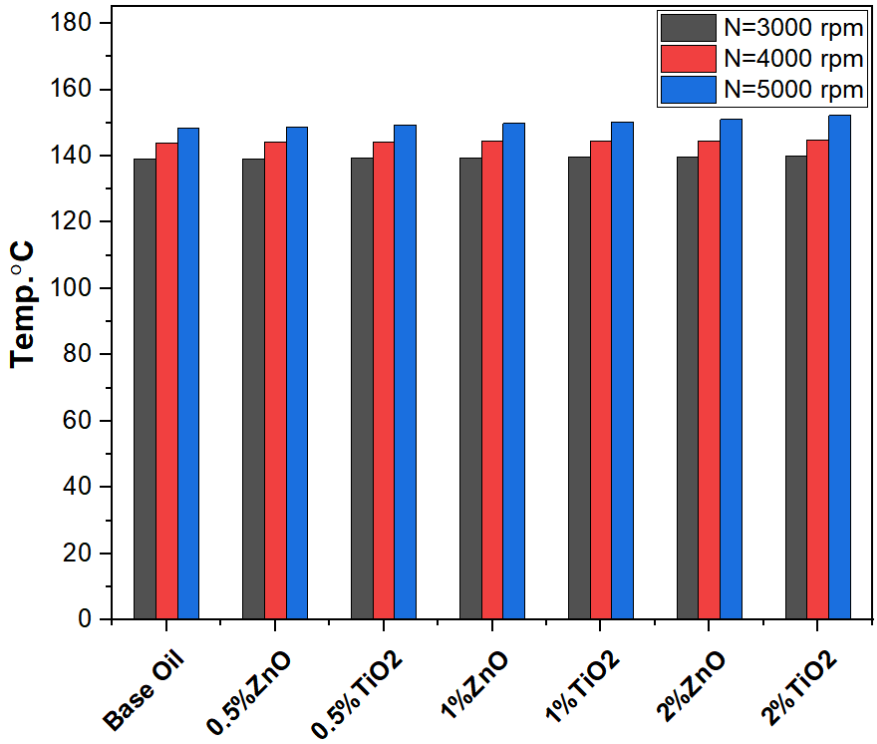

Fig(5.51) Combined effect of nanoparticles weight percentage and journal speed on maximum oil film temperature

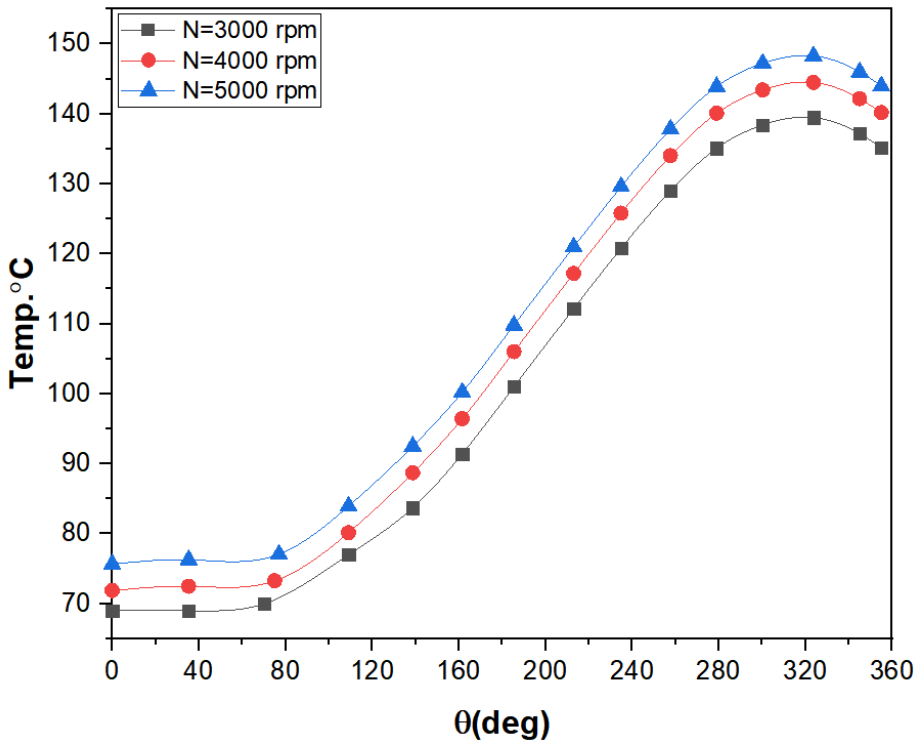

Fig(5.52) Effect of journal speed on the oil film temperature

Figure (5.53) shows the variation in the load-carrying capacity of the bearing when it works at different journal speeds and varying weight concentrations of TiO_2 and ZnO. It has been found that load carrying capacity increases by 3.7% and 2.88% when the bearing is lubricated with 2 wt% of TiO_2 and ZnO, respectively, and works at an eccentricity ratio of 0.7 and a journal speed of 3000 rpm.

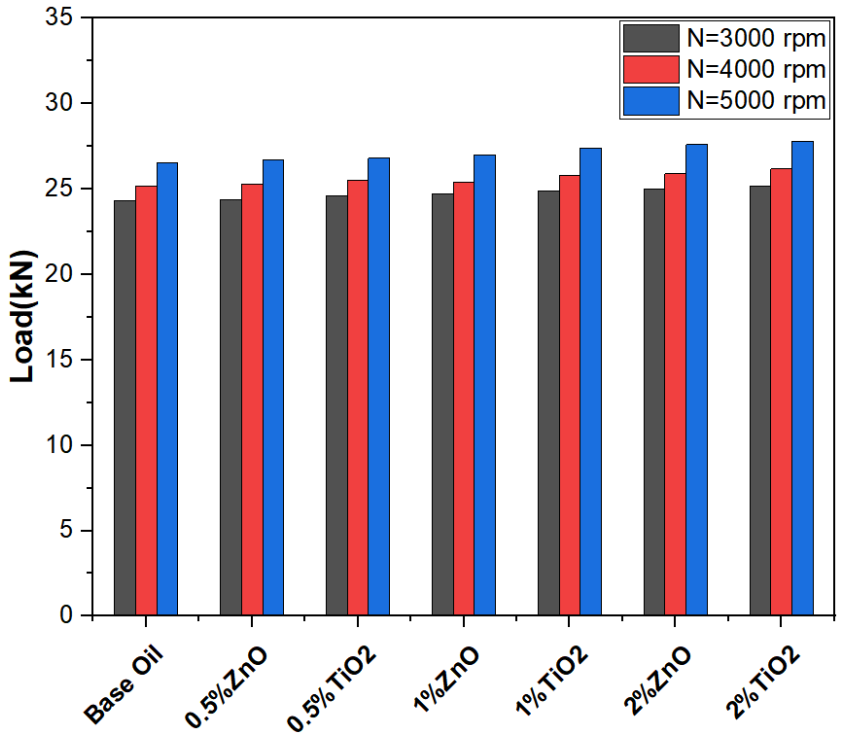

Fig(5.53) Combined effect of nanoparticles weight percentage and journal speed on the load carrying capacity

5.4.3 Effect of Nanoparticle Concentration

The results presented in this section are related to a journal bearing lubricated with nano-lubricants based on TiO_2 and ZnO that have different nanoparticle concentrations (0.5%, 1%, and 2 wt%) at an eccentricity ratio of 0.7 and 5000 rpm of journal speed.

Figures (5.54) and (5.55) show the circumferential pressure distribution for a journal bearing operating under the above conditions. These figures show that the oil film pressure of the bearing improves due to the presence

of the nanoparticles in the base oil and the resulting increase in the viscosity of the oil. This result is supported by that published by **Binu et al. (2014a).**

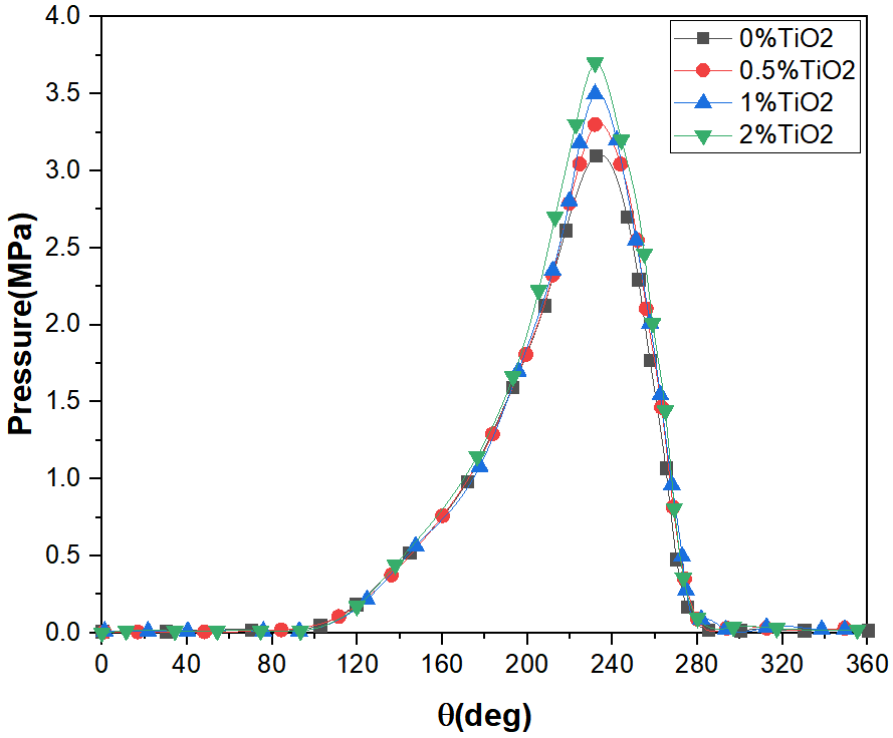

Fig(5.54) Effect of TiO_2 concentration on the circumferential pressure

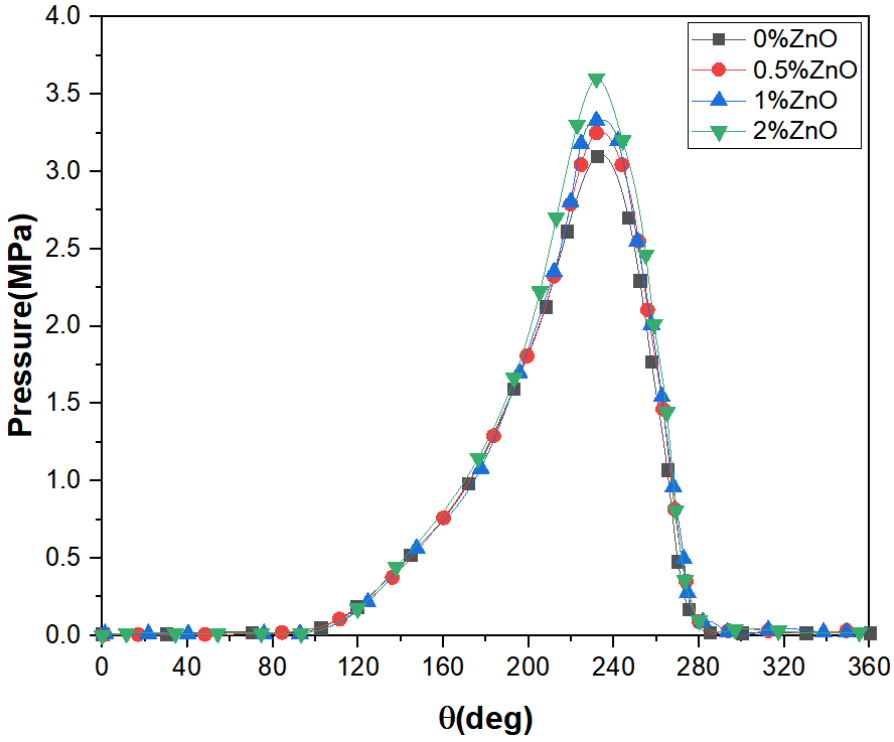

Fig(5.55) Effect of ZnO concentration on the circumferential pressure

Figure (5.56) shows that the maximum percentage increase in oil film pressure ranges between 1.6% and 13.9% when the bearing is lubricated with nano-lubricant that has 0.5 wt% and 2 wt% TiO_2 nanoparticles, respectively, while it becomes 1.05% to 10.9% when the base oil is dispersed with the same weight concentration of ZnO.

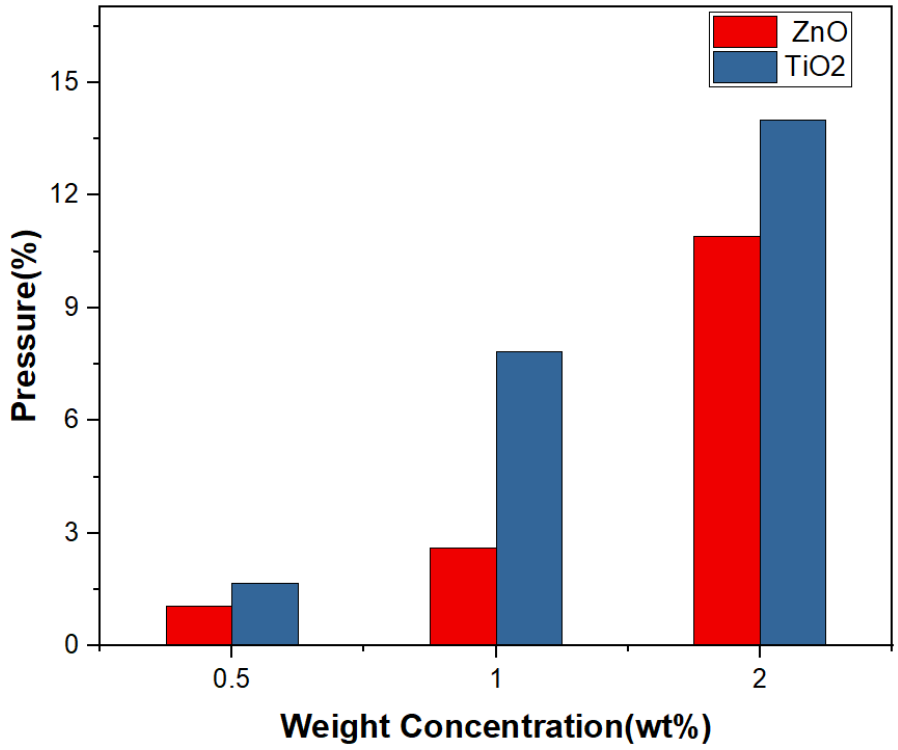

Fig(5.56) Percentage increase in oil film pressure with a weight percentage of different nanoparticles

Figure (5.57) shows the percentage increase in bearing oil film temperature ranging from 0.67% to 2.62% when the bearing is lubricated with base oil blended with 0.5 wt% and 2 wt% of TiO_2 nanoparticles in comparison with that lubricated with the base oil, while the increasing rate becomes 0.2% to 1.82% when the base oil is dispersed with the same weight concentration of ZnO.

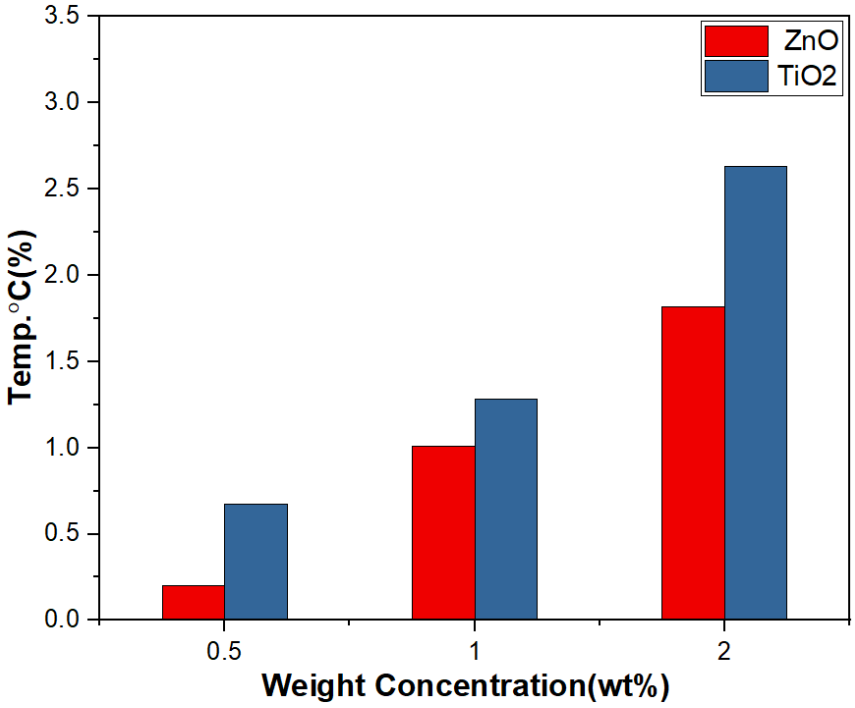

Fig(5.57) Percentage increase in maximum oil film temperature with a weight percentage of different nanoparticles

The percentage increase in load-carrying capacity of the bearing lubricated with different nano-lubricants was calculated and presented in figure (5.58). It can be observed from the figure that the load carried by the bearing increases by 0.92% to 4.68% when it is lubricated with 0.5 wt% and 2 wt% TiO_2 nano-lubricant in comparison to when it is lubricated with base oil. The increasing rate becomes 0.54% to 3.93% when the base oil is dispersed with the same weight concentration of ZnO because of the increasing viscosity of the oil.

Figure (5.59) show the percentage increase in induced friction force at the bearing surfaces for the journal bearing working under the above-mentioned circumstances. This figure depicts that the bearing friction force increases by 1.95% and 6.34% when it is lubricated with 0.5 and 2 wt% of TiO_2, while it becomes 0.97% and 4.87% for a bearing operated with a nano-lubricant based on ZnO with the same concentrations of a nanoparticle. This

can be described by the increase in oil viscosity as a result of the nanoparticles' existence.

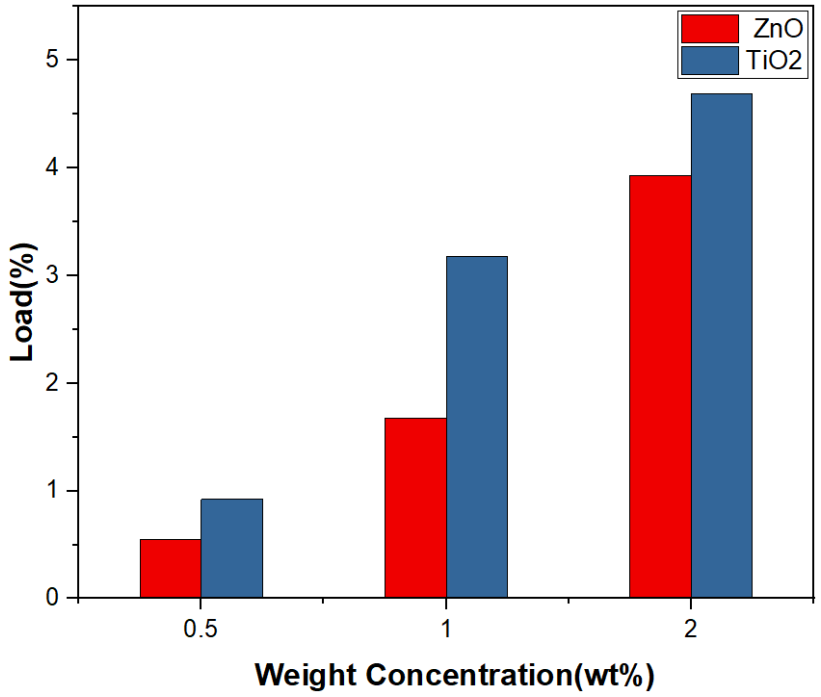

Fig(5.58) Percentage increase in the load with a weight percentage of different nanoparticles

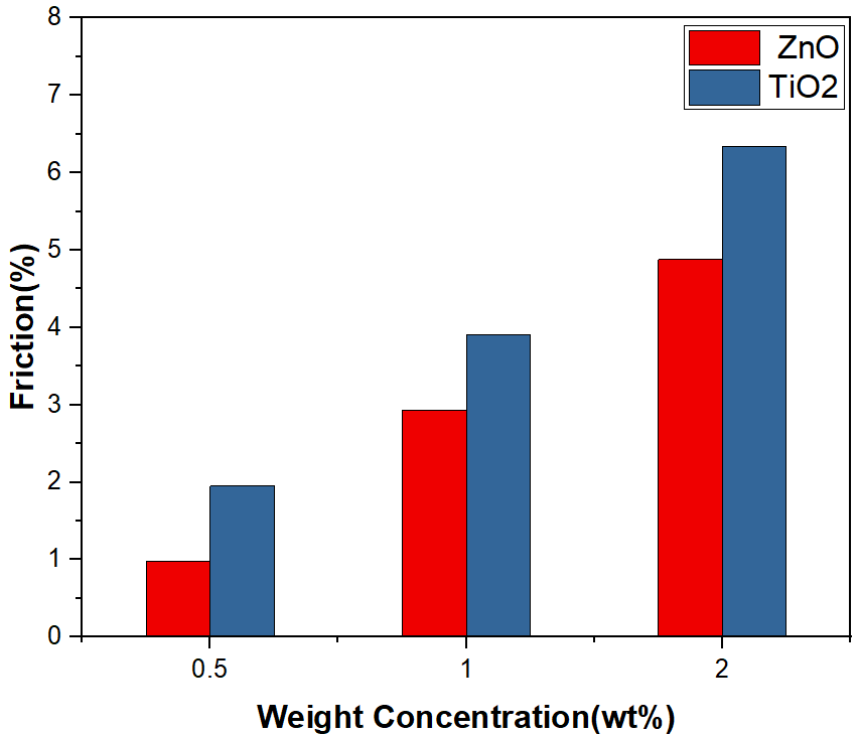

Fig(5.59) Percentage increase in bearing friction force with weight percentage of different nanoparticles

Figure (5.60) illustrates the percentage increase in the coefficient of friction of such a bearing with increase concentrations of a nanoparticle due to the increase in friction force as discussed above.

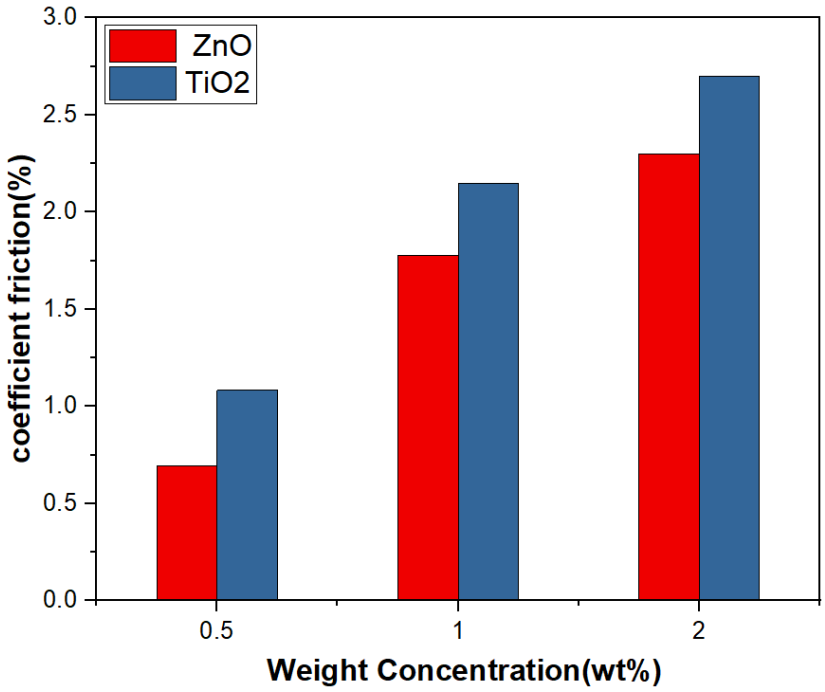

Fig(5.60) Percentage increase in coefficient of friction with weight percentage of different nanoparticles

Figure (5.61) shows that the attitude angle decreases by 3% and 8.5% when the bearing is lubricated with 0.5 and 2 wt% TiO_2 while it decreases by 1.5% and 8% when it is operated with ZnO that has the same concentrations of a nanoparticle. This can be explained by the increase in load components when the bearing is lubricated with this type of lubricant.

The percentage variation of the side leakage flow of the journal bearing under the aforementioned circumstances can be shown in figure (5.62). It has been clearly demonstrated from the figure that the oil leakage from the ends of the bearing decreased by 9% to 26% when the bearing was lubricated with 0.5 and 2 wt% of TiO_2 nanoparticles, respectively, while it became 5.6% and 20.35% when it was operated with a nano-lubricant based on ZnO with the same concentrations of a nanoparticle. This can be explained by the

decreased lubricant velocity as a result of the increased resistance to the flow of the lubricant blended with such nanoparticles. The nano-lubricant based on ZnO shows lower resistance to the flow in comparison with TiO_2 due to the lower aggregate ratio of ZnO.

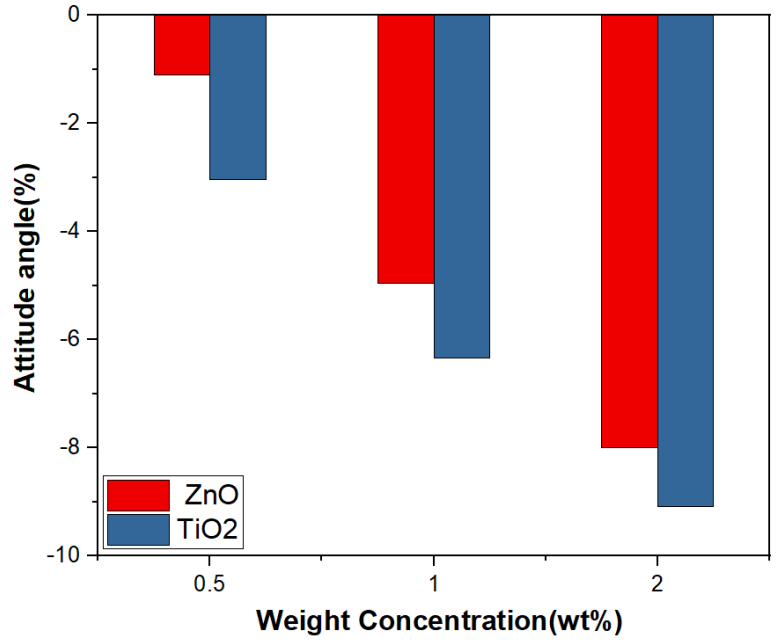

Fig(5.61) Percentage decrease in attitude angle with weight percentage of different nanoparticles

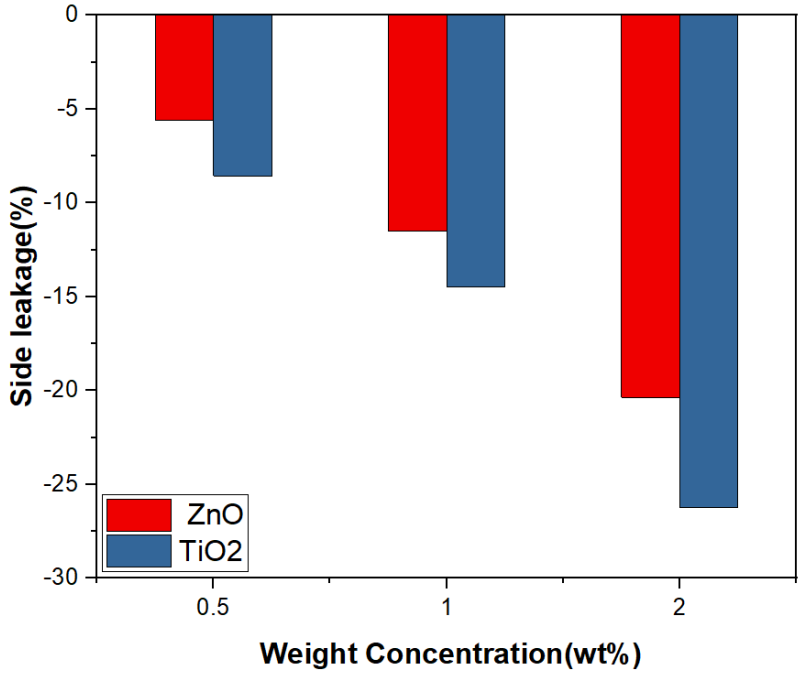

Fig(5.62) Percentage decrease in side leakage flow with weight percentage of different nanoparticles

Figure (5.63) shows that the percentage variation of power loss of journal bearings increased by 3.84% to 9.61% when lubricated with 0.5 and 2 wt% of TiO_2, and by 1.92% to 8.65% when operated with a nano-lubricant based on ZnO, compared to when lubricated with pure oil.

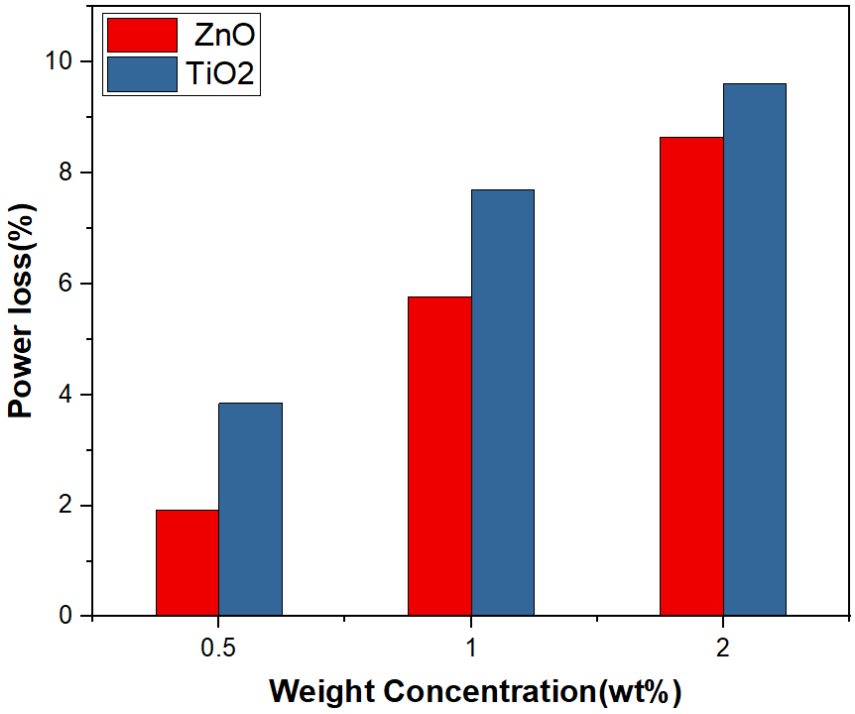

Fig(5.63) Percentage increase in power loss with weight percentage of different nanoparticles

Figures 5.64(a-c) show the effect of an increased nanoparticle concentration of TiO_2 of more than 2 wt% on oil film pressure, temperature, and load-carrying capacity for a bearing working at different eccentricity ratios and a journal speed of 5000 rpm. It has been found that the percentage increase of pressure, temperature, and load-carrying capacity of the bearing at an eccentricity ratio of 0.7 becomes 16.21%, 4.63%, and 7.91%, respectively, when the bearing is lubricated with 5 wt% of TiO_2, compared to the oil blended with 2 wt% of the same type of the nanoparticles as a result of the higher viscosity of the lubricant in this case.

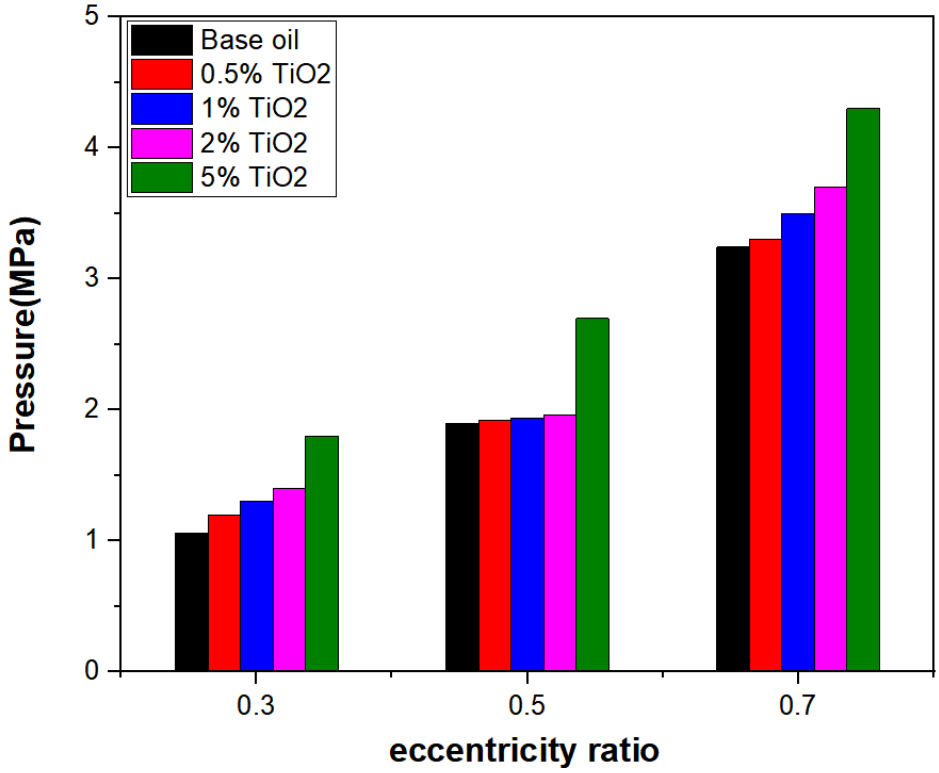
Base oil
0.5% TiO2
1% TiO2
2% TiO2
5% TiO2
Pressure(MPa)
0
1
2
3
4
5
0.3
0.5
0.7
eccentricity ratio

(a)

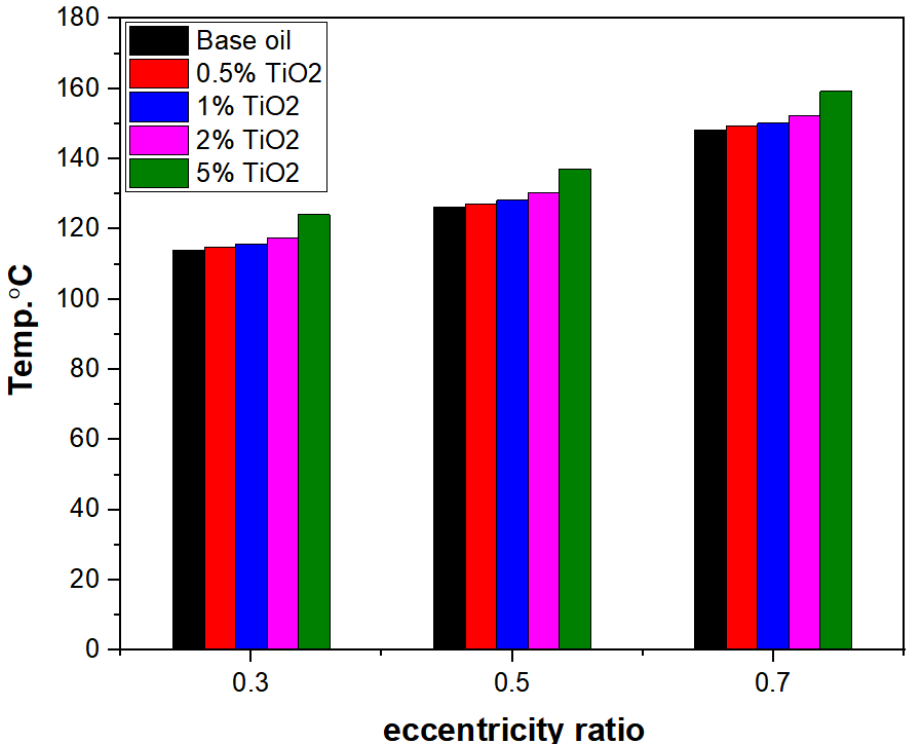
Base oil
0.5% TiO2
1% TiO2
2% TiO2
5% TiO2
Temp.°C
0
20
40
60
80
100
120
140
160
180
0.3
0.5
0.7
eccentricity ratio

(b)

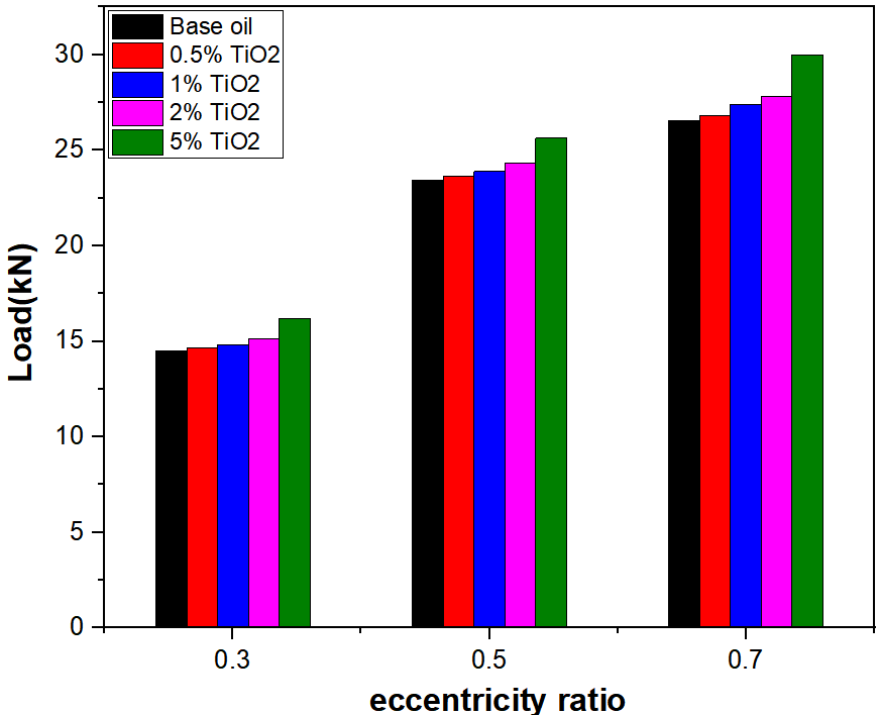

(c)

Fig(5.64) effect of weight concentration and eccentricity ratio on (a) Oil film pressure, (b) oil film temperature, (c) load carrying capacity

5.5 Comparison between Performance of Circular and Elliptical Journal Bearings

A comparative study of the oil film pressure and temperature distributions, load carrying capacity, friction, and power loss for circular and elliptical journal bearings lubricated with pure oil and nano-lubricants was performed and presented in this section. The effects of different values of ellipticity ratios (0 – 1) and nanoparticle concentrations of 2 wt% on the above-mentioned bearing parameters were considered. The comparative study was achieved for a bearing with an eccentricity ratio of 0.7 and a journal speed of 5000 rpm.

Figure (5.65) represents a comparison between the thermal circumferential pressure distribution for the circular and elliptical journal bearings lubricated with pure oil. It can be seen that there are two peaks of

pressure at E_p=1, and only one peak of pressure is observed when the ellipticity ratio is taken as less than 1. This figure indicates that oil film pressure decreased as the bearing has a higher ellipticity ratio. It has been observed that a percentage decrease to 56.21%, 64.3%, and 66% in the oil film pressure of an elliptical bearing can be accomplished when it has ellipticity ratios of 0.3, 0.6, and 1, respectively, compared with that obtained with the circular journal bearing (E_p= 0). This can be accounted to higher clearance (spatially, the horizontal clearance) of such bearings at higher ellipticity ratios, as published by **Huang et al. (2014)**. However, the maximum oil film pressure for the lower lobe of the bearing increases as a result of smaller vertical clearance and, hence, smaller oil film thickness.

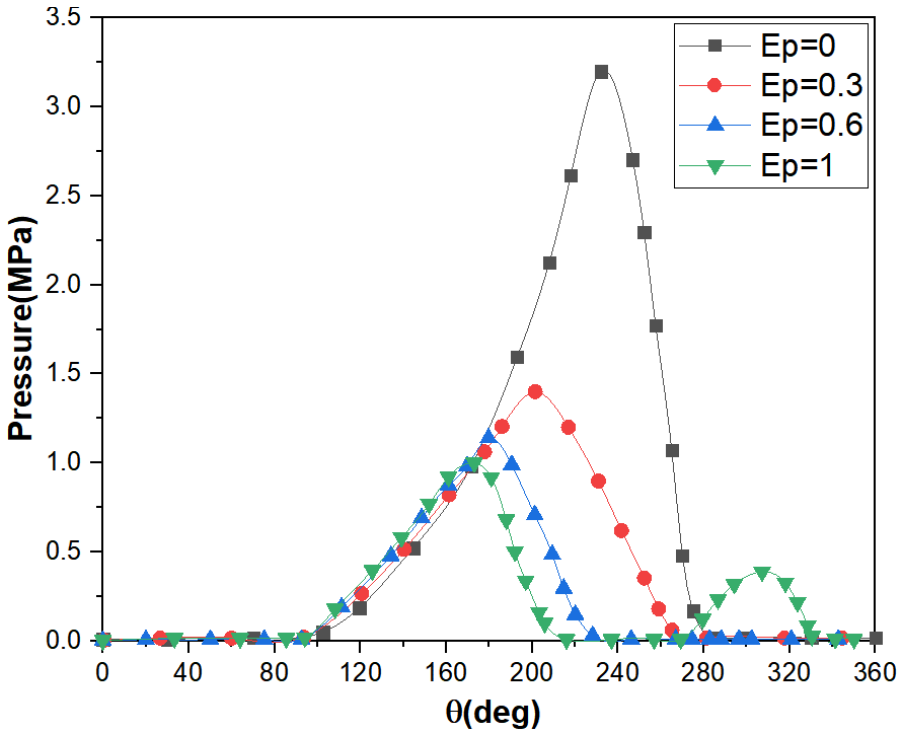

Fig(5.65) Comparison between the circumferential thermal pressure distribution generated in circular and elliptical journal bearing

Figure (5.66) displays a comparison between the maximum oil film pressure obtained in circular and elliptical journal bearings when lubricated with pure oil and 2 wt% of TiO_2 and ZnO. This figure also depicts that the effect of nanoparticles blended in pure oil on the maximum oil film pressure

is more obvious in circular journal bearings than in elliptical journal bearings. This is due to the lower clearance of the circular journal bearing in comparison with that of the elliptical one. It can also be noticed that circular journal bearings operated with nano-lubricant based on TiO_2 give higher oil film pressure than those lubricated with ZnO as a result of a higher aggregate ratio of TiO_2.

The percentage decrease in maximum oil film pressure obtained in an elliptical journal bearing is 60.2%, 67.9%, and 69.3% at ellipticity ratios of 0.3, 0.6, and 1, respectively, in comparison with that of a circular journal bearing (E_p=0) for bearing lubricated with 2 wt% of TiO_2. The maximum oil film pressure appears to be significantly affected by the addition of nanoparticles in pure oil.

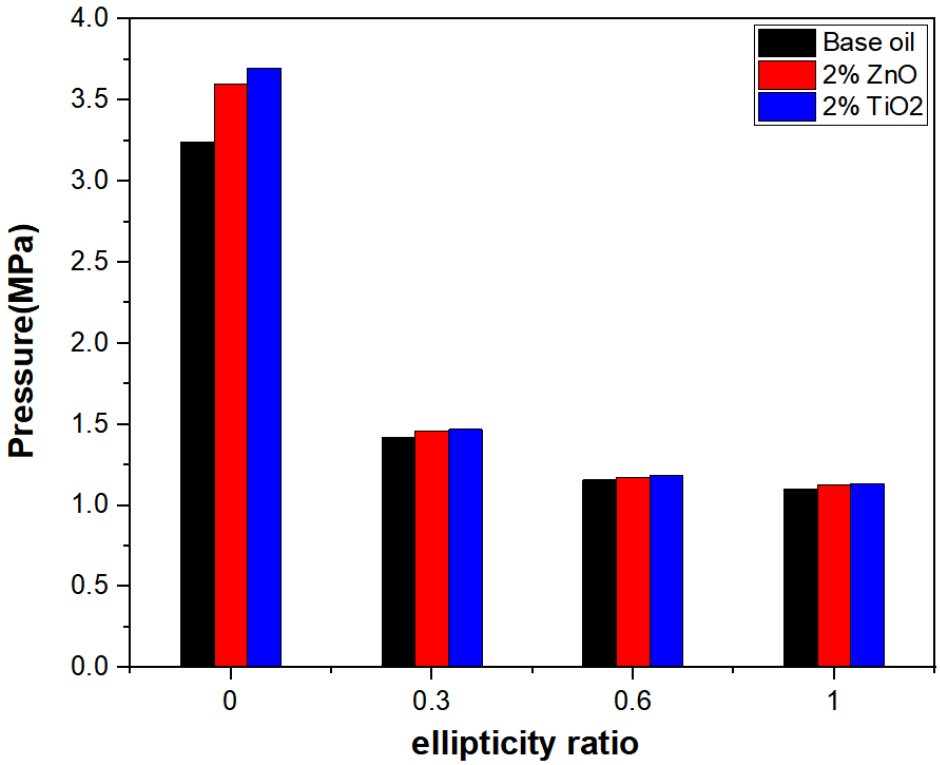

Fig(5.66) Comparison between the maximum pressure generated in circular and elliptical bearings at varying ellipticity ratios

Figure (5.67) shows a comparison between the circumferential temperature distribution for a circular and elliptical journal bearing working at different ellipticity ratios and lubricated with pure oil. It is readily apparent from this figure that a circular journal bearing has a higher magnitude of the oil film temperature in comparison with the elliptical journal bearing due to the smaller oil film thickness in the circular journal bearing compared to the elliptical one. However, the elliptical journal bearing provides superior heat dissipation because of its greater horizontal clearance than the circular journal bearing. It has been found that the percentage decrease in temperature of elliptical bearings was 32.5%, 33.7%, and 35% for the bearings with ellipticity ratios of 0.3, 0.6, and 1, respectively, in comparison with that of a circular bearing (E_p=0) when it worked under the same aforementioned conditions.

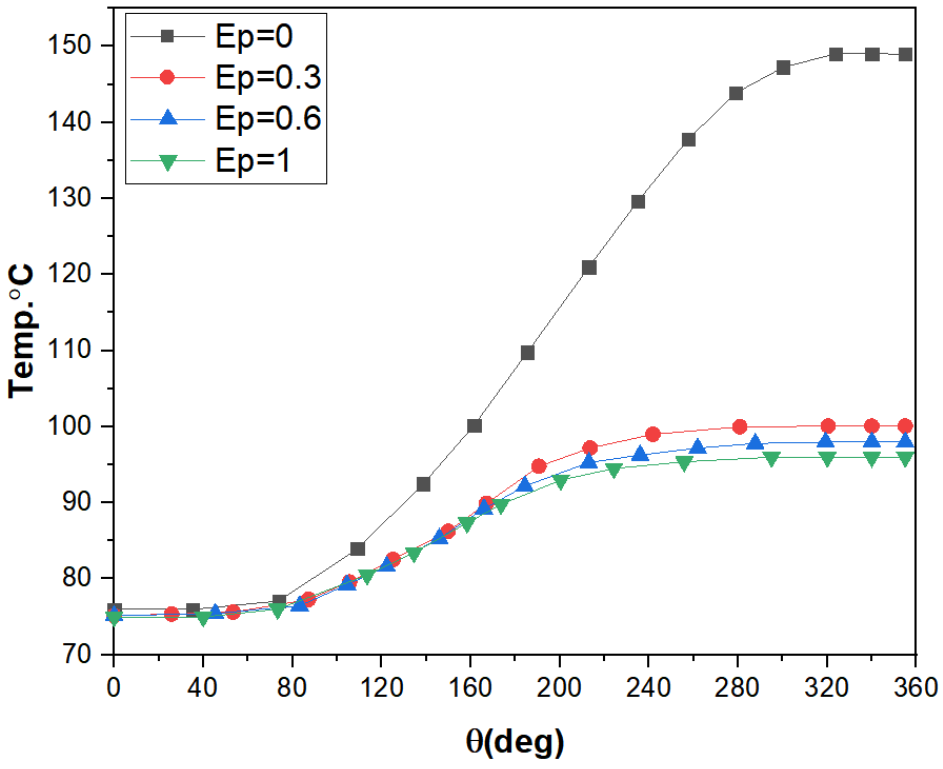

Fig(5.67) Comparison between temperature distribution in circular and elliptical journal bearing

Figure (5.68) illustrates the effect of lubricating such bearings with 2 wt% of TiO_2 and ZnO on the maximum temperature of the oil film. This figure shows that the maximum oil film temperature of the bearings increases slightly when they are lubricated with the above-mentioned nano-lubricants. The percentage decrease in maximum oil film temperature obtained in an elliptical journal bearing is 33.64%, 34.62%, and 35.61% at ellipticity ratios of 0.3, 0.6, and 1, respectively, in comparison with that of a circular journal bearing (E_p=0) for bearing lubricated with 2 wt% of TiO_2.

On the other hand, it can be seen from this figure that the nano-lubricant significantly affects the maximum oil film temperature of the circular journal bearing compared to the elliptical bearing.

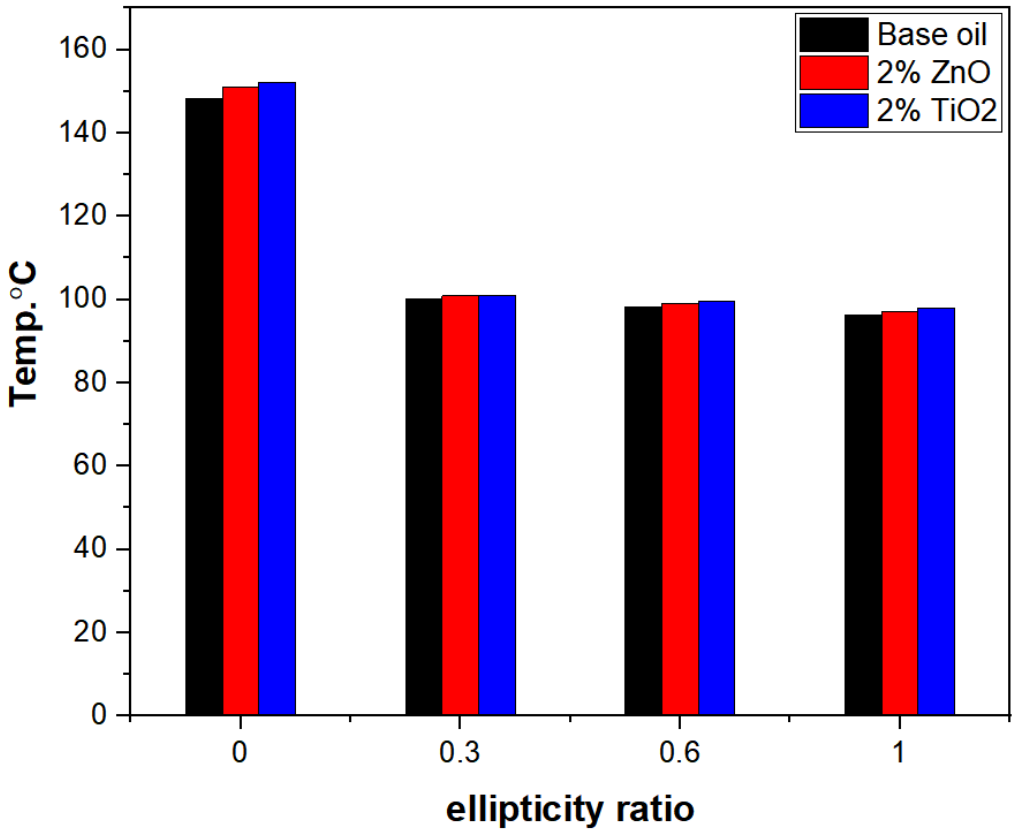

Fig(5.68) Comparison between maximum oil film temperature in circular and elliptical journal bearing

Figure (5.69) shows the variation in the load-carrying capacity with the ellipticity ratio when it was lubricated with a base oil and nano-lubricant that has 2 wt% of nanoparticles. This figure reveals that the load-carrying capacity of a circular bearing is higher than that of an elliptical bearing as a result of the larger oil film thickness of the elliptical bearing in comparison with the circular one. It is also apparent that the load carried by both types of bearings is positively affected by the blending of nanoparticles in the base oil. However, the load-carrying capacity of the elliptical bearing decreases more with higher ellipticity ratios.

The percentage decrease in load capacity has been calculated and found to be approximately 37.4%, 57.5%, and 70% for a bearing with ellipticity ratios of 0.3, 0.6, and 1, respectively, lubricated with 2 wt% of TiO_2 in comparison with a circular bearing.

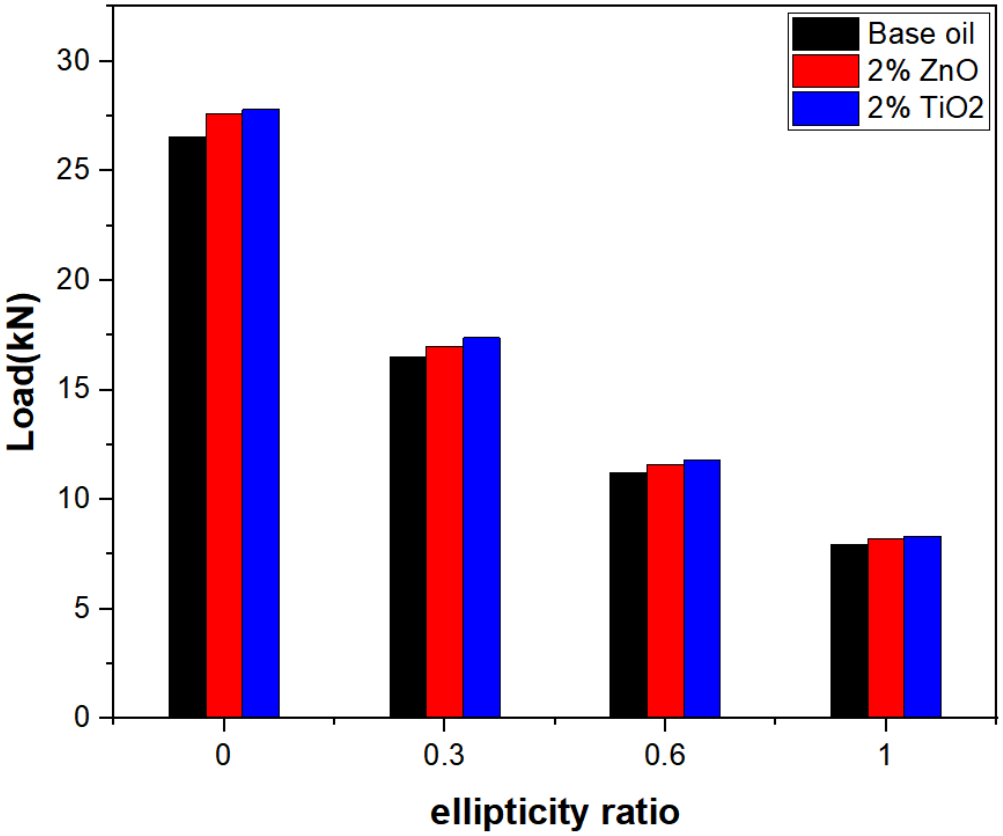

Fig(5.69) Comparison between the load carried by circular journal bearing and elliptical journal bearing

The variation of the induced friction force in the circular and elliptical journal bearing with the ellipticity ratios when lubricated with pure and 2 wt% of TiO_2 and ZnO is illustrated in figure (5.70). This figure clearly shows that the bearing lubricated with different nano-lubricants gives a high friction force based on the higher oil viscosity. In addition, the value of friction force decreases for a bearing with a higher ellipticity ratio due to an increase in oil film thickness that causes a drop in the shear rate of the oil and hence reduces the shear stress at the bearing surfaces.

It has been found that the friction force decreases by 0.61%, 13.4%, and 16.56% for the elliptical bearing with an ellipticity ratio of 0.3, 0.6, and 1, respectively, when it is operated with 2 wt% of TiO_2, in comparison with that of the circular bearing, while this percentage become 1.72%, 14.4%, and 16.7% for the bearing operated with 2 wt% of ZnO.

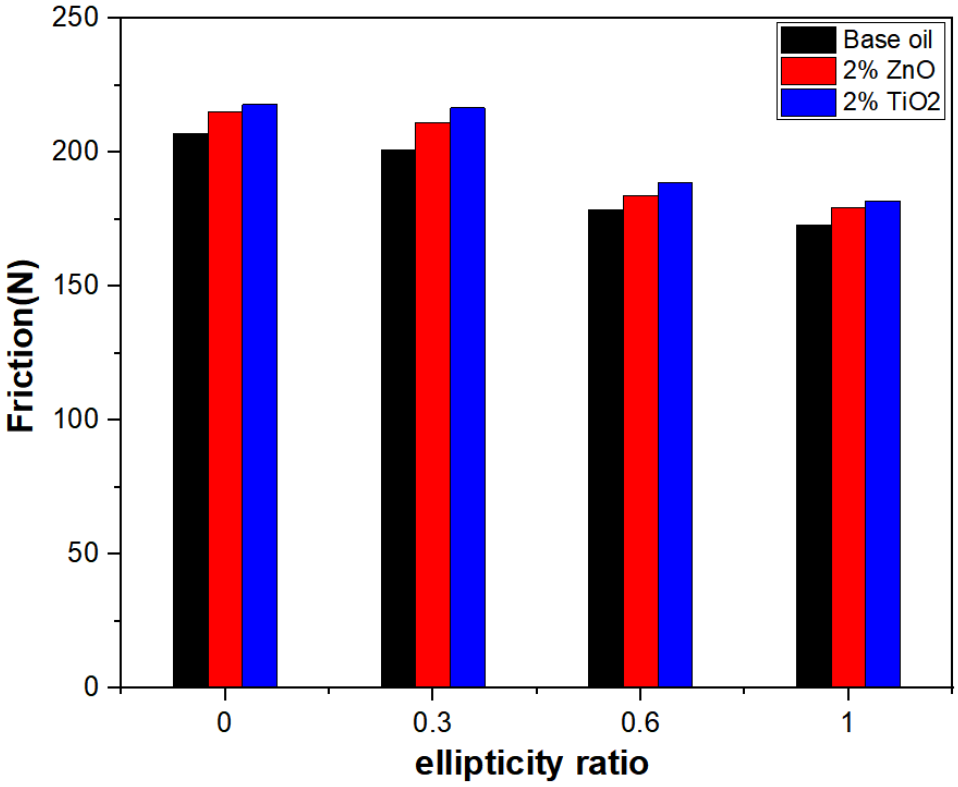

Fig(5.70) Comparison between the friction force in circular and elliptical journal bearings

The behavior of the power loss of the bearing follows the behavior of the induced friction force, as can be shown in figure (5.71). Hence, the power loss predicted to increase at different concentrations of nano-lubricants. The power loss decreases for the elliptical journal bearing with higher ellipticity ratios due to the lower induced friction in this case.

It has been found that percentage decreases in power loss are 0.48%, 13.35%, and 16.46% for the elliptical bearing with ellipticity ratios of 0.3, 0.6, and 1, respectively, in comparison with the value of the circular bearing when it is operated with 2 wt% of TiO_2, while these percentages become 0.88%, 14.15%, and 16.81% when it is operated with 2 wt% of ZnO.

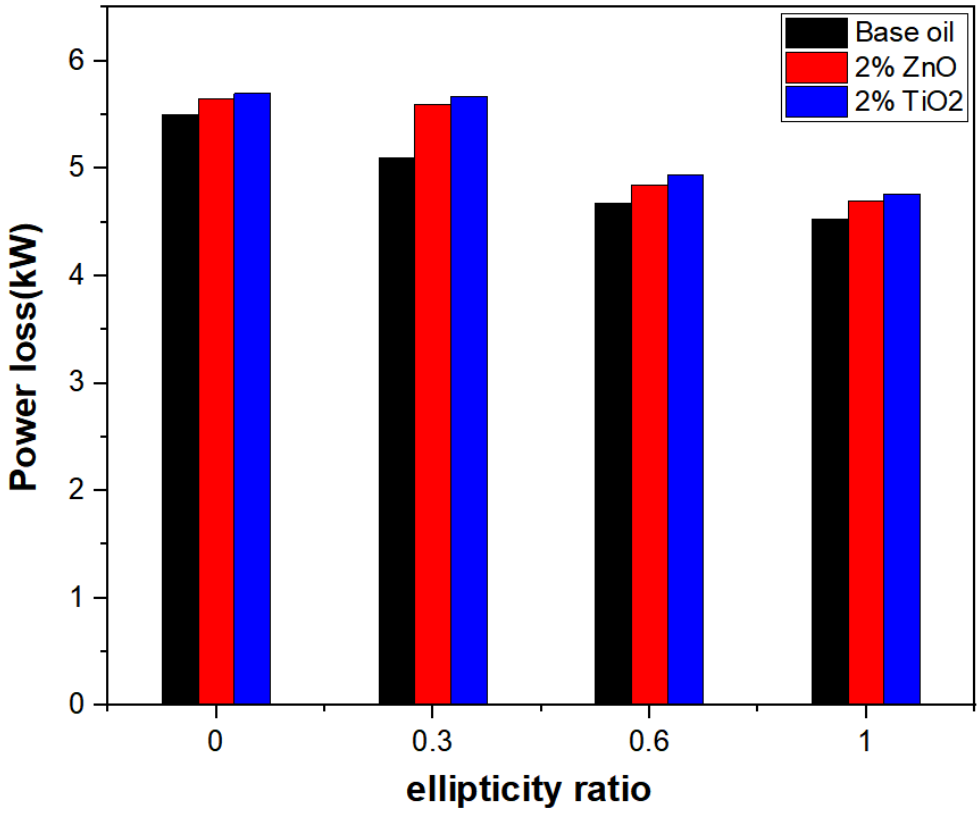

Fig(5.71) Comparison between the power loss in circular and elliptical journal bearings

Chapter 6

Conclusions and Recommendations

CHAPTER SIX

CONCLUSIONS AND RECOMMENDATIONS

6.1 Conclusions

A comparative study of the steady-state performance of circular and elliptical journal bearings lubricated with experimentally characterized TiO_2 and ZnO nano-lubricants has been extensively performed in the current work using the CFD technique.

The following are the main conclusion that can be drawn:

1. The modified Krieger-Dougherty viscosity model was confirmed to be used in calculating the lubricant shear viscosity caused by nanoparticle additives by validating the viscosity of nano-lubricants that was measured experimentally with that calculated by this model.
2. The oil film pressure, temperature distribution, load carrying capacity, friction, and power loss increased with the increasing eccentricity ratios, weight concentration of nanoparticles, and journal speed.
3. The side leakage and attitude angle of journal bearings decreased with an increase in the weight concentration of nanoparticles.
4. Oil film thickness increased with an increase in ellipticity ratio for elliptical journal bearings.
5. The increase in the ellipticity ratio at a constant eccentricity ratio caused a decrease in oil film pressure, temperature distribution, load-carrying capacity, power loss, and friction by 66%, 35%, 70%, 18.2%, 16.5%, respectively.

6.2 Recommendations for Future Works

The following are some recommendations for future work related to the nano-lubrication of hydrodynamic bearings:

1. A comparative study of the dynamic characteristics of different types of journal bearings lubricated with nano-lubricants.
2. An investigation of the static characteristics of different types of bearings considering non-Newtonian and cavitation effects
3. Using PTFE and molybdenum disulfide nanoparticles as an additive to the engine oil
4. Studying the characteristics of magneto-rheological bearings using the CFD technique.
5. Studying the oil film temperature and the elastic deformation effects on the performance of a nano-lubricated elliptical journal bearing under turbulent flow.

References

Azmi, W. H., Sharma, K. V., Sarma, P. K., Mamat, R., Anuar, S., & Dharma Rao, V. (2013). Experimental determination of turbulent forced convection heat transfer and friction factor with SiO_2 nanofluid. *Experimental Thermal and Fluid Science*, *51*, 103–111. https://doi.org/10.1016/j.expthermflusci.2013.07.006

Anoop, K., Sadr, R., Al-Jubouri, M., & Amani, M. (2014). Rheology of mineral oil-SiO_2 nanofluids at high pressure and high temperatures. *International Journal of Thermal Sciences*, *77*, 108–115. https://doi.org/10.1016/j.ijthermalsci.2013.10.016

Ali, M. K. A., Xianjun, H., Mai, L., Qingping, C., Turkson, R. F., & Bicheng, C. (2016). Improving the tribological characteristics of piston ring assembly in automotive engines using Al_2O_3 and TiO_2 nanomaterials as nano-lubricant additives. *Tribology International*, *103*, 540–554. https://doi.org/10.1016/j.triboint.2016.08.011

Ahmed, S. Y., Abass, B. A., & Kadhim, Z. H. (2021). CFD Analysis Of Thermohydrodynamic Behavior of Nanolubricated Journal Bearings Considering Cavitation Effect. *Journal of the Serbian Society for Computational Mechanics*, *15*(1), 110–130. https://doi.org/10.24874/jsscm.2021.15.01.08

Babu, K. S., Nair, K. P., & Rajendrakumar, P. (2014). Computational analysis of journal bearing operating under lubricant containing Al_2O_3 and ZnO nanoparticles. *International Journal of Engineering, Science and Technology*, *6*(1), 34–42. https://doi.org/10.4314/ijest.v6i1.4

Binu, K. G., Shenoy, B. S., Rao, D. S., & Pai, R. (2014a). A Variable Viscosity Approach for the Evaluation of Load Carrying Capacity of Oil Lubricated Journal Bearing with TiO_2 Nanoparticles as Lubricant Additives. *Procedia Materials Science*, *6*, 1051–1067.

https://doi.org/10.1016/j.mspro.2014.07.176

Binu, K. G., Shenoy, B. S., Rao, D. S., & Pai, R. (2014b). Static characteristics of a fluid film bearing with TiO_2 based nanolubricant using the modified Krieger-Dougherty viscosity model and couple stress model. *Tribology International*, *75*, 69–79. https://doi.org/10.1016/j.triboint.2014.03.013

Chen, C. C., Liu, P., & Lu, C. H. (2008). Synthesis and characterization of nano-sized ZnO powders by direct precipitation method. Chemical Engineering Journal, 144(3), 509–513. https://doi.org/10.1016/j.cej.2008.07.047

Chauhan, A., Sehgal, R., & Sharma, R. K. (2010). Thermohydrodynamic analysis of elliptical journal bearing with different grade oils. *Tribology International*, *43*(11), 1970–1977. https://doi.org/10.1016/j.triboint.2010.03.017

Chauhan, A. (2014). *Circular Bearing Performance Parameters with Isothermal and Thermo-Hydrodynamic Approach Using Computational Fluid Dynamics*. *2*(7), 46–52.

Chauhan, A., Singla, A., Panwar, N., & Jindal, P. (2014). CFD based thermo-hydrodynamic analysis of circular journal bearing. *International Journal of Advanced Mechanical Engineering*, *4*(5), 475–482.

Dang, R. K., Chauhan, A., & Dhami, S. S. (2020). Static thermal performance evaluation of elliptical journal bearings with nanolubricants. *Proceedings of the Institution of Mechanical Engineers, Part J: Journal of Engineering Tribology*, *235*(8), 1627–1640. https://doi.org/10.1177/1350650120970742

Dang, R. K., Dhami, S. S., Goyal, D., & Chauhan, A. (2021). Effect of TiO_2 and CuO Based Nanolubricants on the Static Thermal Performance of Circular Journal Bearings. *Tribology in Industry*, *43*(3), 420–433. https://doi.org/10.24874/ti.995.10.20.02

Ebrahimi, A., Akbarzadeh, S., & Moosavi, H. (2020). Geometrical analysis of elliptical journal bearings and its effects on friction and load capacity. *Proceedings of the Institution of Mechanical Engineers, Part J: Journal of Engineering Tribology*, *234*(5), 743–750. https://doi.org/10.1177/1350650119868090

Ferron, J., Frene, J., & Boncompain, R. (1983). A study of the thermohydrodynamic performance of a plain journal bearing comparison between theory and experiments. *Journal of Tribology*, *105*(3), 422–428. https://doi.org/10.1115/1.3254632

Gertzos, K. P., Nikolakopoulos, P. G., & Papadopoulos, C. A. (2008). CFD analysis of journal bearing hydrodynamic lubrication by Bingham lubricant. *Tribology International*, *41*(12), 1190–1204. https://doi.org/10.1016/j.triboint.2008.03.002

Gundarneeya, T. P., & Vakharia, D. P. (2021). Performance analysis of journal bearing operating on nanolubricants with TiO_2, CuO and Al_2O_3 nanoparticles as lubricant additives. *Materials Today: Proceedings*, *45*, 5624–5630. https://doi.org/10.1016/j.matpr.2021.02.350

Gupta, H., Rai, S. K., Kuchhal, P., & Anand, G. (2021). Characterization and experimental investigation of rheological behavior of oxide nanolubricants. *Particulate Science and Technology*, *39*(6), 651–656. https://doi.org/10.1080/02726351.2020.1792018

Hussain, A., Mistry, K., Biswas, S., & Athre, K. (1996). Thermal Analysis of Noncircular Bearings. *Journal of Tribology*, *118*(1), 246–254. https://doi.org/10.1115/1.2837086

H K Versteeg and W Malalasekera. (2007). An Introduction to Computational Fluid Dynamics. In *IEEE Concurrency* (Vol. 6, Issue 4). https://doi.org/10.1109/mcc.1998.736434

Huang, B., Wang, L. Q., & Guo, J. (2014). Performance comparison of circular, two-lobe and elliptical journal bearings based on TEHD analysis. *Industrial Lubrication and Tribology*, *66*(2), 184–193. https://doi.org/10.1108/ILT-11-2011-0086

J.C. Maxwell. (2010). A treatise on electricity and magnetism. *Syria Studies*, *7*(1), 37–72.

Jamalabadi, M. Y. A., Alamian, R., Yan, W. M., Li, L. K. B., Leveneur, S., & Shadloo, M. S. (2019). Effects of nanoparticle enhanced lubricant films in thermal design of plain journal bearings at high reynolds numbers. *Symmetry*, *11*(11), 1–18. https://doi.org/10.3390/sym11111353

Krieger, I. M., & Dougherty, T. J. (1959). A Mechanism for Non-Newtonian Flow in Suspensions of Rigid Spheres. *Transactions of the Society of Rheology*, *3*(1), 137–152. https://doi.org/10.1122/1.548848

Kole, M., & Dey, T. K. (2011). Effect of aggregation on the viscosity of copper oxide-gear oil nanofluids. *International Journal of Thermal Sciences*, *50*(9), 1741–1747. https://doi.org/10.1016/j.ijthermalsci.2011.03.027

Kumar, M., Chandravanshi, M. L., & Mishra, P. C. (2021). Geometrical analysis of elliptical journal bearing lubricated

with Newtonian fluid. *AIP Conference Proceedings*, *2341*(May). https://doi.org/10.1063/5.0050234

Lourtioz, J. M., Lahmani, M., Dupas-Haeberlin, C., & Hesto, P. (2016). Nanosciences and nanotechnology: Evolution or revolution? *Nanosciences and Nanotechnology*, 1–438. https://doi.org/10.1007/978-3-319-19360-1

Li, Q., Zhang, S., Wang, Y., Xu, W. W., & Wang, Z. (2019). Investigations of the three-dimensional temperature field of journal bearings considering conjugate heat transfer and cavitation. *Industrial Lubrication and Tribology*, *71*(1), 109–118. https://doi.org/10.1108/ILT-03-2018-0113

Mishra, P. C. (2007). Thermal analysis of elliptic bore journal bearing. *Tribology Transactions*, *50*(1), 137–143. https://doi.org/10.1080/10402000601105573

Mishra, P. C., Pandey, R. K., & Athre, K. (2007). Temperature profile of an elliptic bore journal bearing. *Tribology International*, *40*(3), 453–458. https://doi.org/10.1016/j.triboint.2006.04.009

Murshed, S. M. S., Leong, K. C., & Yang, C. (2008). Investigations of thermal conductivity and viscosity of nanofluids. *International Journal of Thermal Sciences*, *47*(5), 560–568. https://doi.org/10.1016/j.ijthermalsci.2007.05.004

Maneshian, B., & Nassab, S. A. G. (2009). Thermohydrodynamic analysis of turbulent flow in journal bearings running under different steady conditions. *Proceedings of the Institution of Mechanical Engineers, Part J: Journal of Engineering Tribology*, *223*(8), 1115–1127. https://doi.org/10.1243/13506501JET575

Mousavi, S. B., Heris, S. Z., & Estellé, P. (2020). Experimental comparison between ZnO and MoS_2 nanoparticles as additives on performance of diesel oil-based nano lubricant. *Scientific Reports*, *10*(1). https://doi.org/10.1038/s41598-020-62830-1

Nicoletti, R. (2014). The importance of the heat capacity of lubricants with nanoparticles in the static behavior of journal bearings. *Journal of Tribology*, *136*(4). https://doi.org/10.1115/1.4027861

Prabhakaran Nair, K., Rajendra Kumar, P. K., & Sreedhar Babu, K. (2011). Thermohydrodynamic analysis of journal bearing operating under nanolubricants. *American Society of Mechanical Engineers, Tribology Division, TRIB*, 17–21. https://doi.org/10.1115/IJTC2011-61244

Pawar, S. M., Jadhav, S. G., & Phalle, V. M. (2014). CFD analysis of two lobe hydrodynamic journal bearing. *International Journal of Engineering Development and Research (IJEDR)*, *2*(3), 2974–2979.

Patil, R. D. R. J., & Deshmukh, R. (2016). A review paper on performance investigation of journal bearing with hybrid nano-additives in lubricating oil. *International Journal for Scientific Research & Development*, *3*(11), 139–142.

Parvar, M., Saedodin, S., & Rostamian, S. H. (2020). Journal of Heat and Mass Transfer Research Experimental Study on the Thermal Conductivity and Viscosity of a Transformer Oil- based Nanofluid Containing ZnO Nanoparticles. *Journal of Heat and Mass Transfer Research*, *7*, 77–84. https://doi.org/10.22075/jhmtr.2020.19303.1267

Ramaganesh, R., Baskar, S., Sriram, G., Arumugam, S., & Ramachandran, M. (2020). Finite element analysis of a journal bearing lubricated with nano lubricants. *FME Transactions*, *48*(2), 476–481. https://doi.org/10.5937/FME2002476R

Sehgal, R. (2010). Experimental Measurement of Oil Film Temperatures of Elliptical Journal Bearing Profile Using Different Grade Oils. *Tribology Online*, *5*(6), 291–299. https://doi.org/10.2474/trol.5.291

Shenoy, B. S., Binu, K. G., Pai, R., Rao, D. S., & Pai, R. S. (2012). Effect of nanoparticles additives on the performance of an externally adjustable fluid film bearing. *Tribology International*, *45*(1), 38–42. https://doi.org/10.1016/j.triboint.2011.10.004

Solghar, A. A. (2015). Investigation of nanoparticle additive impacts on thermohydrodynamic characteristics of journal bearings. *Proceedings of the Institution of Mechanical Engineers, Part J: Journal of Engineering Tribology*, *229*(10), 1176–1186. https://doi.org/10.1177/1350650115574734

Singla, A., & Chauhan, A. (2016). Evaluation of oil film pressure and temperature of an elliptical journal bearing - An experimental study. *Tribology in Industry*, *38*(1), 74–82.

Susilowati, Tauviqirrahman, M., Jamari, J., Bayuseno, A. P., & Muchammad. (2016). A comparative study of finite journal bearing in laminar and turbulent regimes using CFD (computational fluid dynamic). *MATEC Web of Conferences*, *58*. https://doi.org/10.1051/matecconf/20165804001

Sepyani, K., Afrand, M., & Hemmat Esfe, M. (2017). An experimental evaluation of the effect of ZnO nanoparticles on the rheological behavior of engine oil. In *Journal of Molecular Liquids* (Vol. 236, pp. 198–204). Kamran Sepyani, Masoud Afrand, Mohammad Hemmat Esfe. https://doi.org/10.1016/j.molliq.2017.04.016

Suryawanshi, S. R., & Pattiwar, J. T. (2018). Effect of TiO_2 nanoparticles blended with lubricating oil on the tribological performance of the

journal bearing. *Tribology in Industry*, *40*(3), 370–391. https://doi.org/10.24874/ti.2018.40.03.04

Suryawanshi, S. R., & Pattiwar, J. T. (2019). Tribological performance of commercial Mobil grade lubricants operating with titanium dioxide nanoparticle additives. *Industrial Lubrication and Tribology*, *71*(2), 188–198. https://doi.org/10.1108/ILT-04-2018-0147

Susilowati, S., Hilmy, F., Arfiandani, D., Muchammad, Tauviqirrahman, M., & Jamari, J. (2019). Effect of eccentricity ratio on the hydrodynamic performance of journal bearing considering cavitation. *AIP Conference Proceedings*, *2097*(April). https://doi.org/10.1063/1.5098243

Sadabadi, H., & Nezhad, A. S. (2020). Nanofluids for performance improvement of heavy machinery journal bearings: A simulation study. *Nanomaterials*, *10*(11), 1–13. https://doi.org/10.3390/nano10112120

Singh, A., Verma, N., Chaurasia, A., & Kumar, A. (2020). Effect of TiO_2 additive volume fraction in lubricant oil on the performance of hydrodynamic journal bearing. *IOP Conference Series: Materials Science and Engineering*, *802*(1). https://doi.org/10.1088/1757-899X/802/1/012005

Thamaphat, K., Limsuwan, P., & Ngotawornchai, B. (2008). Phase Characterization of TiO_2 Powder by XRD and TEM. In *Kasetsart J. (Nat. Sci.)* (Vol. 42, pp. 357–361).

Wan, Q., Jin, Y., Sun, P., & Ding, Y. (2015). Tribological behaviour of a lubricant oil containing boron nitride nanoparticles. *Procedia Engineering*, *102*, 1038–1045. https://doi.org/10.1016/j.proeng.2015.01.226

Wang, L., Geng, H., Zhang, W., Ge, X., & He, M. (2021). Effect of Ellipticity on Cavitation Mechanism and Thermal Effect of Elliptical Journal Bearings. *Tribology Online*, *16*(4), 279–285. https://doi.org/10.2474/trol.16.279

Appendixes

Appendix (A): User-Defined Function (UDF) for specifying a temperature-dependent viscosity

```
include "udf.h"
#define BETA 0.034
#define Tin 313
#define muin 0.0985
DEFINE_PROPERTY(cell_viscosity, cell, thread)
{
real mu_lam;
real temp=C_T(cell, thread);
mu_lam=muin*exp(-BETA*(temp-Tin));
return mu_lam;
}
```

Appendix (B): Nanoparticles Specification

Maximize your productivity through
Skyspring nanomaterials

Titanium Oxide Nanoparticles/ Nanopowder (TiO2, 99.5%, 30nm)

Product #: 7910DL
TiO2, Anatase, 99.5%, 30 nm
Appearance : White Powder
CAS Number: 1317-70-0
Empirical Formula: TiO_2

Specifications

Purity: 99.5+%
APS: 30 nm
SSA: > 50m^2/g
Morphology: nearly spherical
Typical Impurities (Max ppm):

Ca	100	Pb	0.5
Mg	100		
Nb	150		
Hg	0.5		

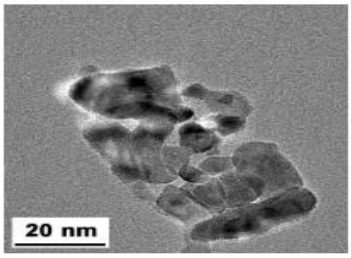

Maximize your productivity through
Skyspring nanomaterials

Zinc Oxide Nanoparticles/ Nanopowder (ZnO, 99.8%, 30nm)

Product Name: Zinc Oxide Powder
Product Number: 8410DL
Form: Powder
CAS Number: 1314-13-2
Empirical Formula: ZnO

Specifications

APS: 30 nm
Purity: 99.8%
Color: white to light yellow
Typical Impurities (Max ppm):

Cu:	25
Cd:	25
Mn:	25
Pb:	20
As:	20

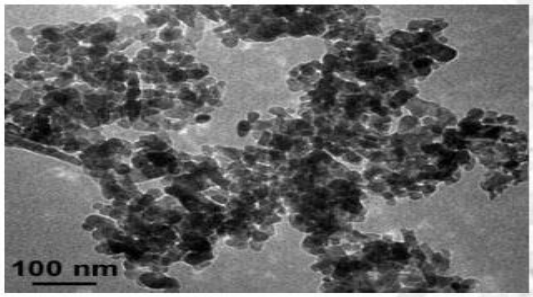

Appendix (C): Published Research

Arabian Journal for Science and Engineering
https://doi.org/10.1007/s13369-022-07219-0

RESEARCH ARTICLE-MECHANICAL ENGINEERING

Performance Analysis of Experimentally Characterized Titanium Dioxide and Zinc Oxide Nano-Lubricated Journal Bearing Considering Thermal and Cavitation Effects

Mohammed O. Yasir[1] · Saba Y. Ahmed[1] · Basim A. Abass[1]

Received: 2 June 2022 / Accepted: 22 August 2022

Abstract
This study is concerned with steady-state thermo-hydrodynamic performance analysis of journal bearing lubricated with experimentally characterized titanium dioxide and zinc oxide nano-lubricants using the computational fluid dynamics technique. For this purpose, nano-lubricants have been prepared by blending different weight fractions of the nanoparticles in SAE15W40 base oil. The prepared nano-lubricants are characterized by performing different experimental tests such as the X-ray diffraction, dynamic light scattering and the scanning electron microscopy. The nano-lubricants viscosities are measured by using suitable rheometer and then compared with that calculated by Krieger–Dougherty equation. The effect of aggregated nanoparticles in the prepared nano-lubricants on the nano-lubricants viscosities has been considered by evaluating the aggregate ratio which was found to be 2.4 and 2.1 for titanium dioxide and zinc oxide nano-lubricants, respectively. A three-dimensional computational fluid dynamic model has been built to analyze the thermal performance of the journal bearing using ANSYS FLUENT software. The effects of the particle weight fraction, the journal speed, bearing eccentricity ratio, and the cavitation on the thermo-hydrodynamic behavior of such bearing have been extensively studied. The obtained results show that dispersing small weight fractions of the nanoparticles in the base oil increases the load-carrying capacity by about 9–23% with a negligible increase in oil film temperature.

Keywords Journal bearing · Nano-lubricants · Cavitation · CFD analysis

Arabian Journal for Science and Engineering

COUNTRY	SUBJECT AREA AND CATEGORY	PUBLISHER	H-INDEX
Germany Universities and research institutions in Germany	Multidisciplinary Multidisciplinary	Springer Berlin	50

PUBLICATION TYPE	ISSN	COVERAGE	Arabian Journal for Science and Engineering
Journals	21914281, 2193567X	1984, 1986, 1996-2021	Q1 Multidisciplinary best quartile SJR 2021 0.47 powered by scimagojr.com

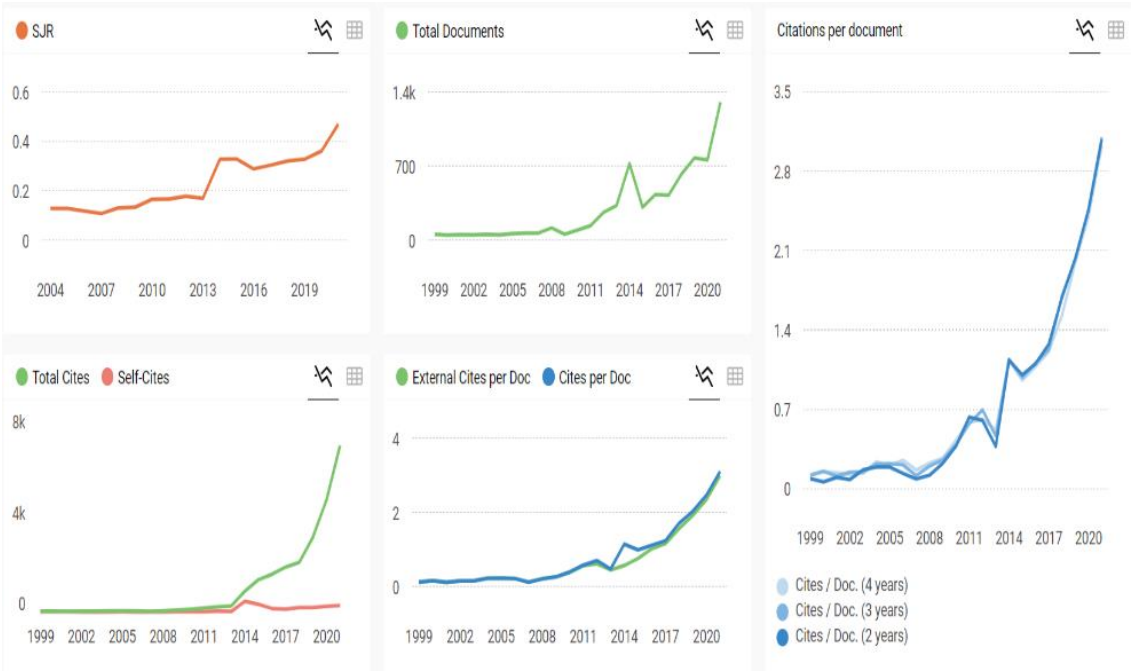
SJR
0.6
0.4
0.2
0
2004 2007 2010 2013 2016 2019
Total Documents
1.4k
700
0
1999 2002 2005 2008 2011 2014 2017 2020
Citations per document
3.5
2.8
2.1
1.4
0.7
0
1999 2002 2005 2008 2011 2014 2017 2020
Cites / Doc. (4 years)
Cites / Doc. (3 years)
Cites / Doc. (2 years)
Total Cites
Self-Cites
8k
4k
0
1999 2002 2005 2008 2011 2014 2017 2020
External Cites per Doc
Cites per Doc
4
2
0
1999 2002 2005 2008 2011 2014 2017 2020

الخلاصة

تهدف الدراسة الحالية إلى إجراء دراسة مقارنة لأداء المساند المقعدية الدائرية والبيضوية المزيتة بالزيت النقي SAE 15W40 والزيت النانوي المحضر عمليا والحاوي على مواد نانوية مثل اوكسيد التيتانيوم(TiO_2) واوكسيد الزنك(ZnO) بتراكيز وزنية مختلفة (0.5%,1%,2wt%).

تم استخدام نموذج ثلاثي الابعاد لطبقة الزيت باستخدام تقنية ديناميك الموائع الحسابية CFD عن طريق برنامج ANSYS FLUENT 19.تم حل معادلات الاستمرارية والجريان والطاقة خلال التدفق الطباقي للمساند الصلبة والناعمة الاسطح عند ظروف حدية مناسبة لتحديد ضغط ودرجة حرارة طبقة الزيت ، مما يسمح بتقييم معاملات أداء المحمل الرئيسية مثل تحمل المسند للأحمال ،كمية الزيت المتسربة من اطراف المسند ، قوة الاحتكاك ، فقدان الطاقة وزاوية الوضع. تمت دراسة هذه المعاملات مع الأخذ في الاعتبار تأثير سرعات المسند المختلفة (3000-5000 دورة في الدقيقة) ، التراكيز الوزنية للجسيمات النانوية المختلفة، نسب لاتمركز تراوحت من 0.1 الى 0.9 ونسب البيضوي من 0 الى 1. حيث تم دراسة تأثير درجة حرارة طبقة الزيت وكذلك تركيز الجسيمات النانوية على لزوجة مادة التشحيم النانوية باستخدام نموذج لزوجة كرايكر-ديكارتي.

تم عمل دراسة تحقق للتأكد من دقة النموذج العددي وذلك من خلال مقارنة النتائج المتحصلة في العمل الحالي مع تلك العددية والعملية المنشورة من قبل باحثين مختلفين في الادبيات العلمية الرصينة.

أظهرت النتائج المتحصل عليها أن ضغط ودرجة حرارة طبقة الزيت، تحمل المسند للأحمال، كمية الزيت المتسربة ، الاحتكاك، وفقدان الطاقة ازدادت عندما عمل المسند بنسب لاتمركز أعلى وسرعات دورية عالية لكل من المساند الدائرية والبيضوية. لوحظ ان هذه المعلمات تزداد مع زيادة تركيز الجزيئات النانوية,ماعدا كمية الزيت المتسربة وزاوية الوضع حيث تقل مع زيادة تركيز الجزيئات النانوية عند اي نسبة لاتمركز.

كذلك اظهرت النتائج المتحصل عليها للمساند الدائرية والبيضوية ان الضغط ودرجة حرارة الزيت وقدرة تحمل الأحمال وقوة احتكاك وفقدان طاقة كانت اعلى بالمسند الدائري بالمقارنة مع البيضوي.

جمهورية العراق
وزارة التعليم العالي والبحث العلمي
جامعة بابل / كلية الهندسة
قسم الهندسة الميكانيكية

دراسة مقارنة للمساند المقعدية الدائرية والبيضوية المزيتة بزيوت نانوية

رسالة
مقدمة إلى كلية الهندسة/جامعة بابل
كجزء من متطلبات نيل درجة ماجستير
في الهندسة/الهندسة الميكانيكية/ميكانيك تطبيقي
من قبل

محمد عدي ياسر علي

بأشراف

أ.د.باسم عجيل عباس
أ.د.صبا يعسوب احمد

٢٠٢٣ م
١٤٤٤ هـ